

FINAL TECHNICAL REPORT

CONTRACT N° : G4RD-CT-2001-00504

PROJECT N° : GRD1-2000-26800

ACRONYM : TBC PLUS

**TITLE : NEW INCREASED TEMPERATURE CAPABILITY
THERMAL BARRIER COATINGS**

PROJECT CO-ORDINATOR :

Alstom Power Generation, Mannheim, APOWGEN

PARTNERS : - Forschungszentrum Jülich GmbH, FOJU.IWVE
- Commission of the European Communities, COMC.IAMI
- Deutsches Zentrum fuer Luft- und Raumfahrt e.V., DLR.IMR
- Office National d'Etudes et de Recherches Aéropatiales, ONERA.MMP
- Chromalloy United Kingdom Ltd, CUK.CE
- Lufthansa Technik AG, LHT.MPEP
- Avio SpA, AVIO
- MTU Motoren- und Turbinen-Union München GmbH, MTU.MPD
- Snecma S.A., SNECMAMO

REPORTING PERIOD : FROM 1.4.2001 TO 31.05.2006

PROJECT START DATE : 1.4.2001 DURATION : 62 months

Date of issue of this report : 31.07.2006



**Project funded by the European Community
under the 'Competitive and Sustainable
Growth' Programme (1998-2002)**

1. Table of contents	page
2. Executive Publishable Summary.....	3
3. Objectives of the project.....	4
4. Scientific and technical description of results.....	5
WP1...SPECIFICATIONS AND PATENTS.....	5
1.2+1.3 Specifications	5
1.4 Procurement of substrate materials.....	5
1.5 Bondcoat application.....	6
WP2...DEVELOPMENT OF SPRAY POWDERS AND INGOTS.....	7
2.1 Procurement of raw material.....	7
2.2 Powder (ingot) preparation.....	7
2.3 Spray and evaporation tests.....	..8
WP3...DEVELOPMENT OF COATING PROCESS AND MANUFACTURE OF TEST SAMPLES.....	..9
3.1 Optimisation of EB-PVD coating process.....	..9
3.2 Optimisation of APS coating process.....	..9
3.3 Manufacture of coated specimens for tests.....	11
3.4 Feasibility study on EB-PVD LaMn-Hexaaluminate coating process	11
WP4...SCREENING OF KEY PROPERTIES AND PROCESS PARAMETERS	16
4.1 Ageing.....	16
4.2 Phase stability.....	16
4.3 Sintering behaviour.....	17
4.5 Thermal properties.....	18
4.6 Microstructural investigations.....	21
4.4 Downselection.....	22
WP5...INDUSTRIAL PROCESSING OF SELECTED COATING SYSTEMS	24
5.1 Technology transfer.....	24
5.2 Procurement of spray powders and ingots.....	24
5.3 Processing trials using industrial equipment.....	25
5.4 Coating of test pieces.....	27
WP6...FULL CHARACTERISATION OF SELECTED COATINGS.....	28
6.1 Ageing and microstructural features.....	28
6.2 Microstructural stability under high temperature.....	28
6.3 Thermophysical properties.....	32
6.4 Mechanical characteristics.....	36
6.5 Durability and ranking tests.....	38
6.6 Modelling.....	47
WP7...PRODUCTION OF COATED INDUSTRIAL SCALE COMPONENTS	50
7.1 Process developm. and coating appl. for burner rig test vane.....	50
7.2 Process developm. and coating appl. for stationary GT	50
7.3 Process development and coating application for aero-engine....	52
WP8...RIG AND ENGINE TESTS.....	55
8.1 High temperature burner rig test.....	55
8.2 Component test in stationary gas turbine.....	57
8.3 Field test on wing.....	58
5. List of deliverables.....	60
6. Comparison of initially planned activities and work actually accomplished.....	61
7. Management and co-ordination aspects.....	62
7.1 Performance of the consortium.....	62
7.2 Name and contact details of follow-up persons.....	64
8. Results and Conclusions	65

2. Executive Publishable Summary

Objectives

This project was directed towards the implementation of efficient and environmental friendly technologies for gas turbines (aero-engines and land-based gas turbines). The goal was to increase the efficiency and to reduce the harmful emissions. This was intended by the development of advanced thermal barrier coatings (TBC), which should allow to increase the entry working temperature by at least 50°C.

Results

The goal of the project was to find new suitable TBC top coating candidates for industrial application in gas turbines produced by the APS as well as by the EB-PVD process. The way to reach this goal comprised mainly two steps:

- Development and investigation of the various TBC candidates with regard to their main physical properties and microstructure produced under laboratory conditions as basis for the subsequent down-selection of the most suitable coatings.
- Production of the down-selected TBCs under industrial conditions with subsequent investigation of the material properties and intensive testing with regard to their structural, mechanical, fatigue, corrosion and erosion properties.

In the first step zirconia based TBCs as pentavalent doped zirconia as well as new material compositions like pyrochlore and magnetoplumbite were developed for EB-PVD and APS coating methods and their physical properties were determined and investigated (thermal conductivity, thermal expansion, density, sintering behaviour and of the development of the microstructural and phase stability). The down-selection was based on the screening of the key properties for higher temperature application. All investigation results were compared to the conventional 8% yttria partially stabilised zirconia (YPSZ) as reference. During the investigations it turned out that the new compositions were only applicable by using a double layer structure with conventional TBC as intermediate layer.

In the second step the down-selected coating systems were intensively investigated and tested as double layer coatings produced by APS and EB-PVD. As in the first step the results were compared to the reference YPSZ coating.

- Zirconia based coating system: YPSZ plus full stabilised zirconia
- New coating system: YPSZ plus metal oxide doped hexaaluminate

The APS zirconia based coating system showed equal to or better results than the reference YPSZ. The new coating system revealed an amorphous-crystalline transition in the hexaaluminate at about 1000°C resulting in unsatisfactory fatigue behaviour compared to the reference coating. This effect could be eliminated by an additional stabilisation heat treatment. Moreover, it was found that a better powder quality for this composition had a decisive impact on achievement of improved fatigue properties of the coating system.

The EB-PVD produced zirconia based coating system also showed equal to or better results than the reference YPSZ. Difficulties related to industrial scale manufacture of EB-PVD coating of doped hexaaluminate were overcome in the framework of a feasibility study, which was carried out by the partner DLR. A sophisticated process could be developed using double source and jumping beam evaporation processes. Samples produced by this process showed promising results with regard to their coating homogeneity and fatigue properties.

Application

Component tests on all down selected coating systems in a burner rig facility were started and showed first promising results, but they couldn't be completed until the project end and were still on-going. It is planned that after passing all required tests and approvals selected coating systems produced by EB-PVD (YPSZ plus full stabilised zirconia) and APS (YPSZ plus metal oxide doped hexaaluminate) will be subjected to a component test in the aircraft industry as well as in the gas turbine industry.

3. Objectives of the project

This project is directed towards the implementation of efficient and environmental friendly technologies for gas turbines (aero-engines and land-based engines).

It is widely accepted that the evolution of gas turbines can be mapped in terms of the turbine entry temperature (TET) and as such, any new developments require TETs to increase even further than the present state-of-the-art levels. This continuous need has been addressed by turbine materials (superalloys) developments, new cooling concepts, novel combustor designs and by the gradual introduction of TBCs in the engine hot sections. The latter option, undertaken in the last couple of decades has shown to be the most beneficial one not only for the present but also for the near future. However, to reach the targets demanded by the new class of clean, lean, safe and affordable gas turbines, new TBCs are ultimately required with much better properties and with a capacity to function in a "prime reliant" mode.

The development of an advanced TBC system in this project is in full compliance with the EC targets of reducing fuel consumption by 20% and reducing NO_x and CO₂ emissions by 80% and 20%, respectively. It is the aim of the project to allow for a significant increase in the turbine entry (working) temperature which, in conjunction with new design principles and cooling schemes, will enable the environmentally harmful emissions to be reduced significantly.

The TBCPLUS project will provide thermal barrier systems for hot section components of gas turbines with a 50°C minimum increase in maximum operating temperature (keeping all other properties unchanged) over the current industry-standard coating (7-8% Y₂O₃ partially stabilised ZrO₂) which is limited to a maximum operating temperature of around 1200°C (time dependent, see table 1).

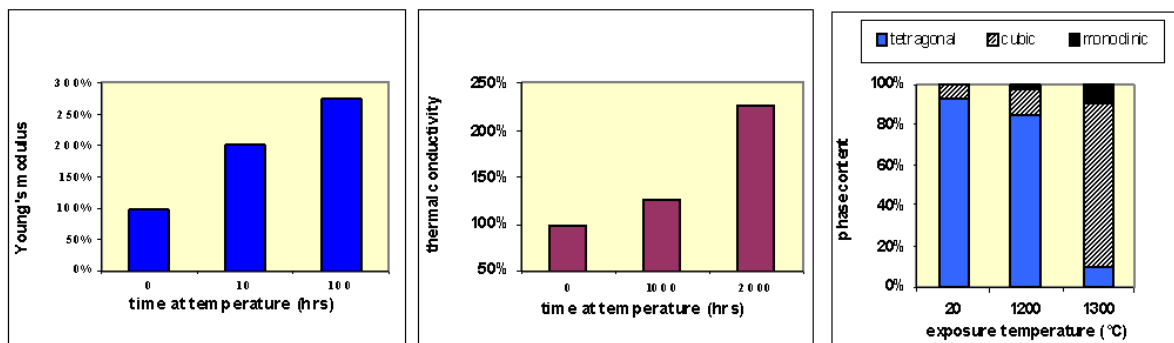


Fig. 1: Changes of Young's modulus, thermal conductivity and phase content of conventional TBC with time and temperature

Increasing the temperature capability by at least 50°C will result in a 2-4% increase in efficiency which would amount to a total cost saving on fuel of around 120 MEuro per annum and a reduction in harmful CO₂ and NO_x emissions by ¾ million tons and 3,000 tons, respectively, if these improvements were transferred across the engines of all the industrial partners involved in the project.

The expected deliverables will help the European GT industry to close technology gaps and remain competitive to meet the increasing global market requirements. The targeted efficiency increase by 2-4% due to the project results can be translated in a reduction of approximately 300,000 tons of kerosene (worth 100 MEuros) at Europe's sky and about 1 million tons of CO₂, anticipated that all aero-engines utilise the critical material technology delivered by this project. Specifically, the project will develop new advanced TBCs, with unheralded performance capabilities by today's norms and standards, exploiting new materials structures and compositions. It will characterise test and model the life of these

coatings, thus making sure that their industrial exploitation will be eminent upon conclusion of the project.

In the first half of the project, a broad investigation of the new systems had to be performed. This allowed to select 2 systems which were most promising for APS and EB-PVD coatings. In the second part of the project a detailed characterisation and the transfer to industrial scale manufacturing of the selected coatings had to be performed. The exploitation of the processing aspects of the research was an important point which was also addressed in this report. All activities should result in component tests performed by burner rig and field testing.

4. Scientific and technical description of results

The relevant results of the project are presented in a condensed form. Detailed information was given in the annual progress reports and in the midterm report. Additionally the final reports of the partners are delivered jointly with this final report for deeper information.

WP1 Specifications and patents

1.2+1.3 Specifications

The systems to be investigated were defined as shown in table 1:

Material type		System	Material
Standard	S	reference	7-8 YSZ Metco 204NS
Zirconia based	A	duplex YSZ	7-8 YSZ + 13-14 YSZ on top
	B	Ta-zirconate	TaYO ₄ doped ZrO ₂
New compositions	C	Magnetoplumbite	LaMg(Mn)Al ₁₁ O ₁₉
	D	(duplex) Pyrochlore	7-8YSZ + (La,Nd) ₂ Zr ₂ O ₇ on top

Table 1: Coating systems

Technical specifications were worked out and the properties were defined, which were to be determined during the development work. Procurement of substrate and bond coat materials was allocated for each test. It was agreed that C-UK would supply PtAl bond coatings for all EB-PVD thermal barrier coatings and MTU NiCoCrAlY bond coatings for APS.

The sample plan from MTU was revised and the following was decided:

- BET: all ageing and tests done at FZJ
- XRD: all ageing and tests done at JRC
- Dilatometry, thermodiffusion and density: all tests done at ONERA
- Cp: done at SNECMA

1.4 Procurement of substrate materials

In advance substrates were supplied and machined for the full characterisation of the selected systems in WP6:

- Hastelloy X: supplied by SNECMA and C-UK
- IN617: supplied by Alstom
- Single crystal CMSX4: supplied by Avio

The substrates were machined according to the needs for the special work packages. In turn, they were sent to the bond coating manufacturers (MTU and SNECMA for CoNiCrAlY's and C-UK for Pt-Aluminides). After the bond coating was applied, the samples were coated with the top coatings according to table 1 by APS (SNECMA) and EB-PVD (C-UK).

1.5 Bondcoat application

The bond coatings were applied by C-UK, MTU and SNECMA according to the detailed plan.

Manufacture of the plasma sprayed industrial reference coating by SNECMA

The Sulzer Metco $ZrO_2 - 8 Y_2O_3$ powder 204NS was sprayed on plate-shaped substrates. The spraying was performed at Snecma Moteurs, Corbeil plant, by a Sulzer Metco F4 gun using the Snecma specification DMP 14-044. No bond coating was applied since the coating evaluation performed in WP 4 was focussed entirely on the ceramic top coating.

Special efforts were undertaken for the machining of samples for TMF and tensile tests: for the TMF experiments hollow rods of single crystals (CMSX4) were needed. The material was delivered by Avio and machining took place at (former) Alstom Sweden. The IN617-specimens for the tensile tests (critical strain to crack) were supplied by Alstom and machined to the required dimensions.

Patents

A patent survey was carried out by MTU und described in detail in the 6-month report. An assessment of the patent situation and the status of the patent filings of the new system by the consortium was as follows:

Double layer system 7-8%YSZ + 14%YSZ

This system uses state-of-the-art TBC materials in multi-layer coatings. To increase the bonding strength of TBC, 7%-YSZ can be used as the first layer on the bond coating. As the second layer applied on top, fully stabilised 14%-YSZ can be used since this material is high-temperature resistant and shows no phase transformation. Since no patent has yet been filed by a third party for this specific combination, FZJ filed a patent application on 25.2. 2000 and the patent has in the meantime been published under the reference number DE 10008861. The PCT was filed on 6.2.2001 under WO 01/63006.

La-Mg-Mn-Hexaaluminate (single and duplex)

A patent application covering the single system was filed by G. Schäfer and R. Gadow on 20.2.1998 and the pertinent patent is now listed under reference numbers EP 1060281, DE 19807163 C1, WO 9942630 A1. The patent was assigned to MTU Aero Engines.

A further patent application concerning this material was filed by DLR. It deals with the magnetoplumbitic structure LaMn-Hexaaluminate, especially for EB-PVD coatings. The german patent was filed on 9.5.2001 under DP 10122545.8, the european patent on 25.4.2002 under EP 02009402.5, the US patent on 9.5.2002 under US 141341. It was offered to the partners as option contract (license agreement).

A patent was filed by MTU for a multilayer system, consisting of an inner layer of 7-8%YSZ and an outer layer of La-Mg(Mn)-Hexaaluminate (patent document P804546/DE/1, patent No. 102004025798.1 applied at 24.05.2004).

As summary, a patent survey is given in table 2:

<i>System</i>	<i>Patent filed by</i>	<i>Owner of patent applic.</i>	<i>Date of appl.</i>	<i>Before start of project</i>	<i>During current project</i>	<i>Potential use for TBCplus-consortium</i>
LaMg-Hexaalumin. single	Gadow	MTU	1998	X		Licenses (reasonable fee)
LaMnMg-Hexaal. single	DLR	DLR	2001	X		Licenses (reasonable fee)**)
LaMnMg-Hexaal. Duplex	MTU	MTU	24.05. 2004		X	To be determined
7-8%YSZ/14%YSZ duplex	FZJ	FZJ	2000	X		Licenses (reasonable fee)
**) <i>This patent is based on work before the project was started, although the date of filing falls within the TBC project.</i>						

Table 2: Patent survey

The consortium had enough freedom of work through the patents of DLR, FZJ, and MTU on materials with magnetoplumbite structure especially Lanthanum-hexaaluminate. TBC-materials with pyrochlore-structure were blocked by patents of United Technologies.

WP2 Development of spray powders and ingots

2.1 Procurement of raw material

EB-PVD coatings (DLR + C-UK)

The ingot fabrication for compositions A, B and D was carried out by powder routes, for composition C by chemical and powder routes (see table 1). Chemical route powders for fabrication of ingots of composition C, D was produced by DLR using alkoxide based starting materials. Detailed description for chemical powder production was given in the semi-annual progress reports.

APS coatings (FZJ)

The commercially not available powders B, C, D were prepared by FZJ. The synthesis route for all three powder was optimised to lower the content of impurities (unreacted oxides and other phase compositions). Detail descriptions of preparation and characterisation were given in the 6- and 12 month reports.

2.2 Powder (ingot) preparation

EB-PVD coatings (DLR)

Powder route was applied for production of ingots for all four systems by Co. HTM Reetz. DLR produced ingots for compositions A and B by using a technique which was patented previously by Leusahake et al. DLR produced also ingots from chemically produced powders for composition C in various compositions differing from that of the stoichiometry. As a supplement, chemically produced ingots of LaMn-Hexaaluminate composition were also delivered by Co. HTM Reetz. Optimised ingots were used for evaporation tests and manufacture of samples in WP3 (D17).

APS coatings (FZJ)

The powders were spray-dried to get a particle size and quality, which was useable for plasma-spraying. The X-ray characterisation obtained for all powders showed nearly no impurities. Details were given in the 12-month report.

2.3 Spray and evaporation tests

These tests must be regarded as first trials. Details were described in the midterm report.

APS-Coatings (FZJ)

- System A
 - This system was a variation of a state-of-the-art TBC material in a double layer structure. The industrially produced powder made difficulties with regard to some impurities (for example of zirconium nitrate), which increased the sintering activity.
- System B
 - This powder was produced by coprecipitation. The composition was 10% Ta₂O₅, 10% Y₂O₃, 80% ZrO₂. The handling of this material was nearly in the same way as for standard YSZ. Thus for spray-drying and plasma-spraying comparable parameters were used. However, the level of Ta₂O₅ impurities in the material had to be optimised.
- System C
 - This powder was prepared by a solid state reaction. The spray-drying process was optimised in three runs to get a powder, which was suitable to prepare reproducible plasma-sprayed coatings.
- System D
 - This powder was prepared by a solid state reaction, too. The spray-drying process was performed according to parameter optimised for standard zirconia. A statistical design plan was used to optimise the parameters for plasma-spraying.

EB-PVD-Coatings (DLR)

- System S (reference)
 - The evaporation conditions for standard composition (7YSZ) were approx. 70 kW and 30 minutes for a coating of approx. 200 µm thickness. Under these conditions a substrate temperature of about 970-1000°C was achieved.
- System A
 - The evaporation tests showed that 14YSZ composition required a slightly lower power level (65-70 kW) than that for the standard ZrO₂ composition (70 kW). Substrate temperatures (920-950°C) were similar to those of the standard composition.
- System B
 - The evaporation tests with these ingots showed similar evaporation behaviour and conditions as those of standard composition and composition of the system D. Under a base voltage of 39.5 kV, an EB-Power of 65 kW and a coating time of 30 minutes were required to achieve 200 µm coating thickness.
- System C
 - Early sublimation of MgO caused non-uniform evaporation and unpredictable spit formation in several shapes and appearances. Several attempts have been made to overcome this difficulty (see midterm report). However, it was not possible to solve the problems. Therefore, the composition LaMgAl₁₁O₁₉ had been replaced by LaMnAl₁₁O₁₉.
 - Evaporation tests showed that a MnO-content of 5 to 6 % was achievable and the coatings yielded a stoichiometrical composition of LaMnAl₁₁O₁₉, despite of the poor quality of the coating and many spitting during evaporation. Optimisation runs were carried out.
- System D
 - The evaporation tests of this ingot showed a smooth evaporation behaviour at the conditions near to that of standard composition. An EB power of 60 kW and a coating time of 30 minutes were typical for this composition.

WP3 Development of coating process and manufacture of test specimens

3.1 Optimisation of EB-PVD coating processes

System A

The coating in this system was carried out with the ingots from Co. HTM Reetz. Samples having double layers of YPSZ and 14YSZ were also manufactured and used for testing in WP4.

System B

XRD-analysis of the coating showed formation of fully stabilised ZrO₂-phase. Observations by SEM of the coating showed a narrower columnar morphology, compared to that of the standard composition.

System C

A double-source evaporation was applied. XRF analysis showed 5-6 wt. % MnO in the LaMnAl₁₁O₁₉ coatings. SEM observations of the as-coated coating displayed a featureless morphology being different from that of the standard composition (7YPSZ). Although the columnar structure was visible, no defined feather-arm structure at the column edges was observed. EDX analysis of the as-received coating indicated that the elements, La, Al, Mn were distributed in a relatively high homogeneity along the coating. XRD analysis of the LaMnAl₁₁O₁₉ coatings after a 2 hours of heat treatment at 1000°C showed that this coating crystallised directly to lanthanum hexaluminate yielding an interlocking needle-like morphology within the columns of heat-treated sample on viewing in BSE-mode of SEM.

System D

XRD analysis of the coating showed a weakly crystalline pyrochlore structure. This coating displayed a more spread and less denser morphology, compared to that of the standard composition 7YPSZ.

Conclusions for EB-PVD coatings

All compositions were successfully EB-PVD-coated and with these results milestone M2 was fulfilled. The process optimisation for zirconia based systems had been finished by February 2002. The process optimisation for non-zirconia based new compositions for composition D on time for composition C were delayed due to the change in this composition.

The test specimens were delivered for composition C at end of August 2002 and for all other compositions at end of February 2002 to the partners ONERA, JRC and FZJ for WP4. The task was finished on time, apart from the composition C.

3.2 Optimisation of APS coating processes

For all systems coatings were produced by atmospheric plasma-spraying. The project objective was to have two different microstructures for each material, which was realised by a different porosity level.

System A

The plasma-spraying process for system A was performed according to parameters, which were used for the reference YSZ material. The optimisation of the plasma-spraying process was finished by a factorial design plan, which covered a large area of different parameters (fig. 2a).

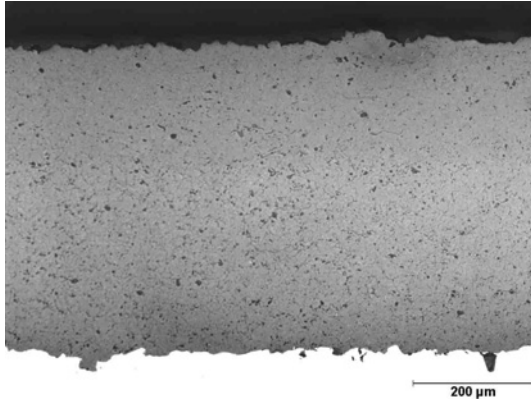


Fig. 2a: APS-coating of the fully stabilised system

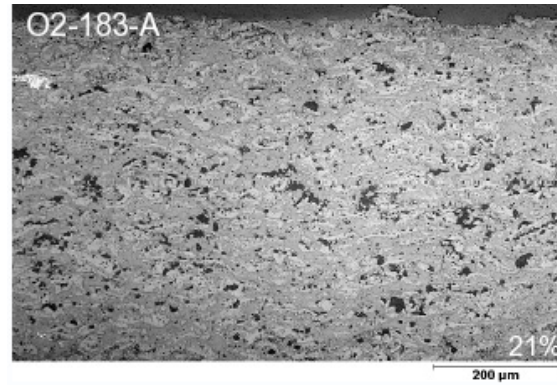


Fig. 2b: APS-coating of LaMg-Hexaaluminate

System B

The coatings had only a small amount of Ta_2O_5 in the as-sprayed condition, which disappeared after heat treatment. The delivered material revealed a chemical pure composition.

System C

It turned out that in the plasma-sprayed coatings the amount of amorphous phases was high (50 –70%). The microstructure of plasma-sprayed $LaMgAl_{11}O_{19}$ (fig. 2b) was very different to other zirconia based materials. Especially the porosity level was very high (> 20%). So the investigations in the plasma-spraying process and in the characterisation of the coatings required an extended work-programme to find significant values to lower the amount of amorphous phases. This was not possible in the course of this work package. Partially optimised coatings were delivered for characterisation right in time and the additional optimisation of the parameters for plasma-spraying continued during the WP4 and the down selection. Meanwhile significant parameters had been found to lower the amount of amorphous phases. The know how was transferred to the industrial partners, so that they could optimise the coating properties within the industrial work package WP5. The negative influence of the amount of amorphous phases on the coating properties was confirmed by the dilatometer measurements of ONERA.

System D

Because of the Neodymium inside, the material and the coatings showed a light blue appearance. There were no problems with impurities and phase changes after plasma-spraying. This material was only better than YSZ in a double layer system with YSZ near the bond coating.

Conclusions for APS coatings

For all materials it was possible to produce the powders and the coatings in a reproducible way and all coatings showed no principle disadvantage for an application as TBC. With these results milestones M1 and M2 were fulfilled.

Thus these materials were used for further investigations in the project (WP4). The process optimisation for the systems had been finished up to April 2002. The test specimen were delivered to the partners ONERA, JRC and FZJ for WP4. The whole work was finished right in schedule. The only exception were some coatings of 14 YSZ, which had been prepared after down selection. For this task powder was taken, which was ordered for WP5.

3.3 Manufacture of coated specimens for screening tests

It was possible to produce coatings for all four compositions and for the reference material in a reproducible way by the EB-PVD process as well as by the APS process. The manufacture of the samples was partly described in the chapters 3.1 and 3.2 and the further use will be documented in chapter 4.

3.4 Feasibility study on EB-PVD LaMn-Hexaaluminate coating process

After several vane trials to transfer the EB-PVD LaMn-Hexaaluminate coating process to industrial scale, it was decided in the consortium to make a step back to the laboratory level and to carry out a feasibility study at the partner DLR. The main objective of this study was to establish a stable process which can produce samples with correct coating composition and structure and a suitable efficiency.

The study consisted of two parts. In Part I (optimisation), the process parameters were determined to yield compositionally homogeneous, reproducible and good quality $\text{LaMnAl}_{11}\text{O}_{18}$ -coatings (i.e. less to none-spitting and compositional fluctuations). The target of Part II (reproducibility) was to determine the substrate temperature effect on microstructure and on deposition of crystalline coatings for reproducible coatings.

In order to avoid spitting and bath stability problems caused by early evaporation of MnO during single source processing, the double source and jumping beam evaporation of $\text{LaAl}_{11}\text{O}_{18}$ and MnO at separate sources had been applied throughout the feasibility study.

Within Part I, the following steps were taken to determine the parameters:

Step 1: Two trials were carried out to test single source evaporation of MnO.

Step 2: Ten trials to test single source evaporation of $\text{LaAl}_{11}\text{O}_{18}$.

Step 3: Six trials to test and optimise double source evaporation by means of jumping beam technique.

Step 4: Deposition of a limited number of samples with $\text{LaMnAl}_{11}\text{O}_{19}$ using jumping beam technique evaporation.

In order to reach substrate temperatures up to 1000°C in Part II, an over-source heater was planned to apply. However, a cost-effective construction of such a heater was not possible within a foreseeable time. Therefore, the substrate temperature was increased up to 950°C by applying higher electron beam power and using a steel construction in the chamber.

Step 5: Reproducibility tests

Step 6: Substrate Temperature 800-950°C

Step 7: Delivery trials on flat and cylindrical substrates

Step 1: Evaporation of MnO occurred by sublimation and required no addition of oxygen during deposition. The MnO-vapour cloud had large diameter and was distributed flatly in the chamber. In order to avoid oxidation of Mn^{2+} to Mn^{3+} in the MnO-ingots, it was advisable not to heat-treat them in air prior to evaporation.

Step 2: The optimum evaporation parameters for $\text{LaAl}_{11}\text{O}_{18}$ were determined in 10 runs. Some trials were listed in table 3. On the contrary to MnO, smoother evaporation of $\text{LaAl}_{11}\text{O}_{18}$ required some oxygen. Without oxygen release, that means, under relatively low chamber pressures (1.5×10^{-3} mbar, see trial Nr. 57), a higher deposition rate (as high as 20 $\mu\text{m}/\text{min}$) was possible. However, the coating quality was extremely low, due to heavy spitting (table 3). In the presence of high amount of oxygen and with higher chamber pressure (8×10^{-3} mbar), the deposition rate was in turn very low (trial Nr. 58). A reduction of chamber pressure under similar conditions resulted in an increase of the deposition rate (trial Nr. 59).

Trial Nr.	Evaporation Behaviour	Feed rate mm/min	Gas	Gas Flow rate l/min	Ch. Press.	Power kW	Coating (μm)	Subs T°C
56	spitting	0,10	none	-	$3 \cdot 10^{-3}$	44	84	810
57	Heavy spitting	0,10	none	-	$1,5 \cdot 10^{-3}$	45	200	825
58	spitting	0,06	O ₂	10,8	$8 \cdot 10^{-3}$	45	19	900
59	spitting	0,09	O ₂	10,8	$5 \cdot 10^{-3}$	40	59	900

Table 3: Summary of process parameters for the single source LaAl₁₁O₁₈ trials (Step 2)

La- and Al-oxide distribution showed different vapour cloud distributions (i.e. more La over the pool, less La away from the crucible). More Al was observed at the farer end of the chamber, indicating a larger Al-cloud diameter than that of La.

Step 3: Double source evaporation were carried out in six optimisation runs in which the dwell time and jumping frequencies of jumping beam deposition were varied. The parameters from five runs showed that longer dwell times on both ingots favored the compositional homogeneity (table 4). The maximum applicable power with the present ingots was app. 50 kW, 12.5 kW being on MnO ingot. Lower chamber pressure and presence of some oxygen during evaporation yielded to reasonable deposition rates (app. 2 $\mu\text{m}/\text{min}$). Substrate temperature in these trials was below 900°C.

Optimised conditions yielded to constant hold of parameters resulting in relatively homogeneous coating compositions. The amount of MnO varied between 3 to 23 wt.% over the deposition length of 200 mm. Coatings deposited under optimised conditions without rotation were dense and showed no defined columnar morphology development, probably due to the lack of rotation.

Trial No.	Feed rate mm/min	Gas	Gas Flow rate (l/min)	Pressure (mbar)	Dwell (ms)	Time (min)	Power kW	Coating (μm)	Sub T°C
65	0,09 0,075 (MnO)	none	-	$7 \cdot 10^{-4}$	46/10	10	43	70-90	800
66	0,085 0,064 (MnO)	O ₂	1,44	$2,4 \cdot 10^{-3}$	23/5	10	48,8	60	870
69	0,085 0,078 (MnO)	O ₂	1,44	$6 \cdot 10^{-3}$	46/15	10	49,8	33	710
70	0,83 0,76 (MnO)	O ₂	1,44	$1,7 \cdot 10^{-3}$	46/15	10	49,5	50-58	740
72	0,8 0,5 (MnO)	O ₂	1,20	$2 \cdot 10^{-3}$	46/15	60	49,5	110	810

Table 4: Evaporation and deposition parameters for the optimisation trials of the jumping beam technique coatings. Trials 65-70 were carried out without rotating the substrates, trial 72 with rotation (steps 3 and 4); example for trial 70 in fig. 3.

Step 4: Trial Nr. 72 was carried out with a rotation speed of 12 min⁻¹ for 60 minutes and by employing jumping beam technique (table 4). MnO-content of the coatings was in the range of 5 and 10 % deposited on the substrates positioned at both ends of the LaAl₁₁O₁₈-ingot, having a distance of 75 mm from each other.

Step 5: Reproducibility trials showed that the coatings achieved the same composition and quality as in Part I optimised conditions (trial Nr. 37 and 48 in table 5, fig. 4).

Step 6: Variation of substrate temperature between 850 and 950°C showed that the MnO-content in the coating composition was almost near to zero if the substrate temperature exceeded 920°C (table 5). Evaporation tests with MnO-ingot showed that MnO-evaporation occurred without the formation of a melt by sublimation. Under the chamber pressure

conditions present during the EB-PVD-processing, the evaporation of MnO occurred at rather low temperatures. Non-presence of MnO in the coating composition, despite evaporation of MnO from the ingot, indicated that this sublimation temperature was as low as 920°C. Therefore, as the substrate temperature exceeded 920°C, the condensation (deposition) of MnO in the coatings was not possible.

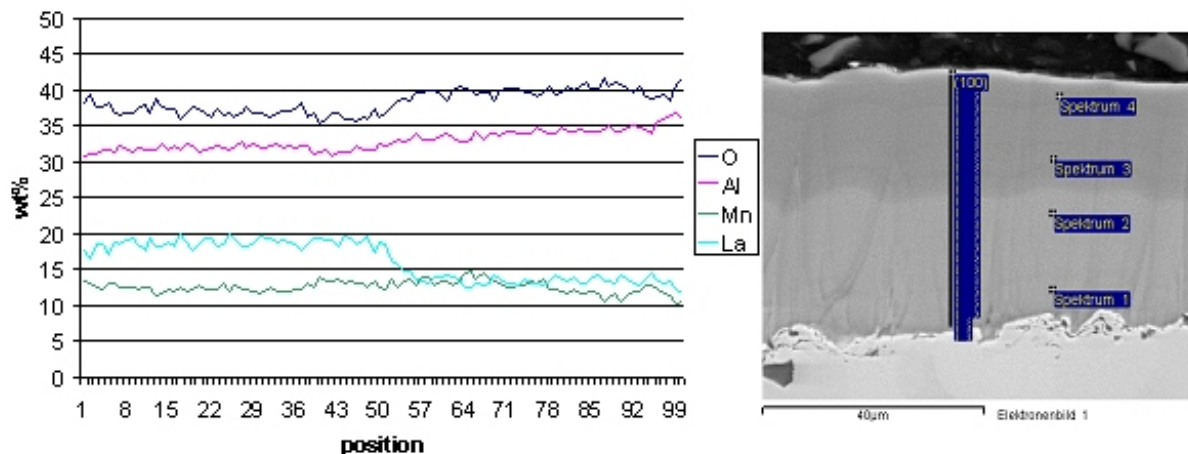


Fig. 3: EDX-Analysis of O, Al, La, Mn along the thickness at coating trial 70 (deposition conditions see table 4) and microsection of coating.

Step 7: After determination of process conditions, EB-PVD deposition of LaMn-Hexaluminat had been carried out on a set of flat substrates of IN 617 and alumina at trials 47 and 48 and a set of cylindrical substrates of CMSX-4 at trial 49 (not in table 5). All metallic substrates were previously Pt/Al bond-coated by C-UK. These samples were delivered to ALSTOM, SNECMA and ONERA for further thermal shock and cyclic testing and conductivity characterisation, respectively.

Trial Nr.	Feed rate mm/min	Rotat. Speed rpm	Gas	Gas Flow rate (l/min)	Pressure (mbar)	Beam Focus	Dwell (ms)	Time (min)	Power kW	Thick (µm)	Sub T°C
37	0,66 0,5 (MnO)	-	O ²	1,20	1,4 · 10 ⁻³	110/110 1377	46/15	10	54,0	30-40	850
40	0,66 0,5 (MnO)	12	O ²	1,20	1,4 · 10 ⁻³	110/110 1373	46/15	10	55,0	20-60	950
46	0,66 0,4 (MnO)	12	O ²	1,20	1,3-1,5 · 10 ⁻³	115/115 1300	46/15	30	52,4	30-70	910
47	0,66 0,4 (MnO)	12	O ²	1,20	1,7 · 10 ⁻³	115/115 1300	46/15	90	52,4	100-170	910
48	0,66 0,4 (MnO)	12	O ²	1,20	2,2-1,6 · 10 ⁻³	115/115 1300	46/15	45	52,4	90	850

Table 5: EB-PVD-Process parameters for reproducibility and substrate temperature variation trials (steps 5 and 6).

An X-ray analysis showed that the coatings were weakly crystalline but predominantly amorphous in the as coated condition (table 6). Heat treatments at temperatures between 900 to 1100°C were carried out and showed the crystallisation of LaMn-Hexaaluminat for the rotated sample of trial 72 by 1100°C, while the non rotated sample of trial 65 only developed perovskite as crystalline phase.

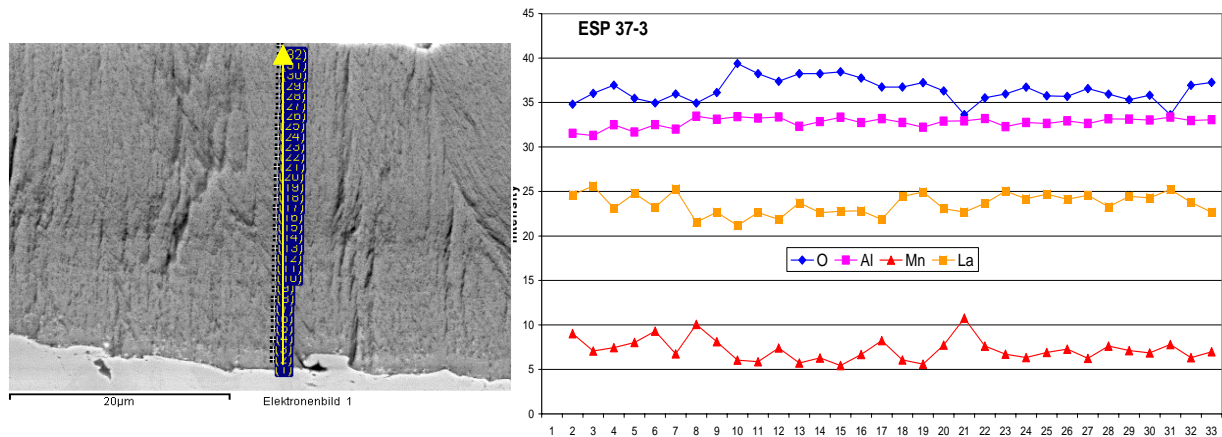


Fig. 4: EDX-analysis of the coating 37 showing the distribution of O, Al, Mn and La

Coating Nr	As-coated	900°C/6h	1000°C/1h	1100°C/1h
ESP 65-3	γ -alumina (semi crystalline)	-	γ -alumina	LaAlO_3
ESP 72	γ -alumina	γ -alumina	γ -alumina	$\text{LaMnAl}_{11}\text{O}_{18} + \text{LaAlO}_3(\text{w})$

Table 6: Phase sequences of trials 65 and 72 in as coated condition and after heat treatment at different temperatures

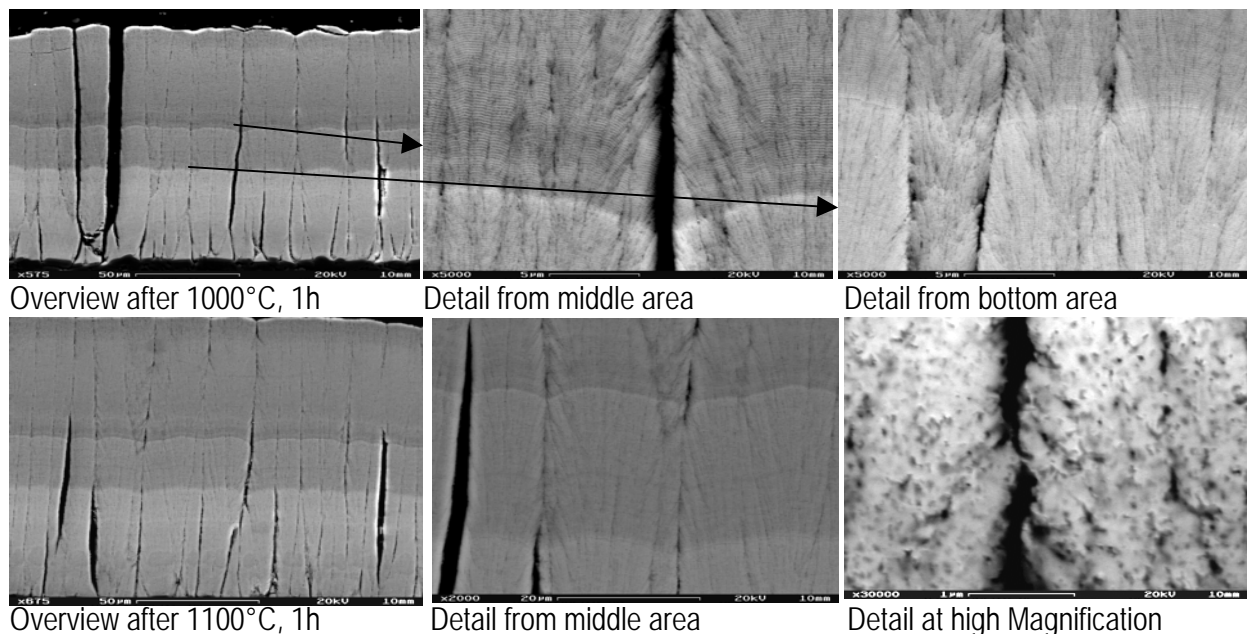


Fig. 5: SE micrographs of the heat-treated coatings from trial 72, showing columnar morphology and feather-arm formations. After crystallisation, the needle-like crystals of $\text{LaMnAl}_{11}\text{O}_{18}$ become apparent in the columns and on the column edges.

Heat-treatment of the coatings on substrates displayed that the crystallisation which probably occurred between 1000-1100°C resulted in formation of cracks as indicated by DSC-measurements of coatings from trial 72 which showed that the crystallisation occurred around 1000°C at a heating rate of 2K. Those became deeper and larger at higher temperatures or after longer holding times and with higher heating rates. After heat-treatment and crystallisation, $\text{LaMnAl}_{11}\text{O}_{19}$ formed in terms of needle-like crystals which were homogeneously distributed in the coating. Despite the compositional variation along the

coating as visible with colour differences, no morphology and phase differences in the coatings were observed (fig. 5).

Conclusions:

In summary, the achievement of good quality and homogeneous $\text{LaMnAl}_{11}\text{O}_{19}$ coatings with a reasonable deposition rate ($2 \mu\text{m}/\text{min}$ under rotation) is possible by means of double source evaporation. Coatings with reproducible composition and quality can be deposited by application of the following parameters:

- Chamber pressure should be kept $1\text{-}2 \times 10^{-3}$ mbar.
- Some oxygen release into the chamber during deposition is necessary (app. 1,2 l/min).
- Maximum applicable power is 55 kW. Using a dwell time of 46/15, a power of 10-12kW is applicable on MnO-ingot.
- Ingot diameters can be adjusted as 62,5/30 mm for $\text{LaAl}_{11}\text{O}_{18}$ and MnO, respectively to obtain the desired composition.
- Constant pool level should be maintained to avoid melt overflow (very important to avoid compositional fluctuations).
- A rotation speed of 12 rpm produces the columnar structure typical to EB-PVD-coatings.
- A substrate temperature up to 920°C yields the desired composition under the given preconditions. Above this temperature, MnO-depletion in the coatings has been observed.
- Homogeneous coatings with similar composition are achievable at a length of 125 mm in the substrate plane. This yields approximately 40% reduction in coating amount (considering a total available length of 200 mm in the chamber).
- Despite the increase of substrate temperature up to 910°C , all the deposited coatings were weakly crystalline, crystalline phase being γ -alumina. On heat-treatment of the coatings from trial 72 at 1100°C , the crystallisation of $\text{LaMnAl}_{11}\text{O}_{18}$ was detected, although this resulted in the development of a crack network in the coating.

WP4 Screening of key properties and process parameters

The objective of this workpackage was to characterise the most critical properties of the new coating systems and their evolution with thermal ageing and to compare them with standard systems in order to select the most promising compositions (down-selection) for further exploitation in workpackage 6. Therefore the properties of the new coatings were investigated with respect to their high temperature behaviour. For this purpose ageing experiments were done at 1300 and 1400 °C for 100 hours.

4.1 Ageing (JRC and ONERA)

Ageing at 1300°C and 1400°C for 100 hours was performed on all available systems :

- EBPVD coatings on alumina or sapphire substrates, from DLR (8YPSZ reference, 14YSZ, TaYO₃ZrO₂, LaNdZr₂O₇, LaMnAl₁₁O₁₉) and C-UK (8YPSZ reference),
- free standing APS coatings from FZJ (8YPSZ reference, 14YSZ, TaYO₃ZrO₂, LaNdZr₂O₇, LaMgAl₁₁O₁₉ with two different microstructures, dense and porous, for the last four compositions) and Snecma (8YPSZ reference).

4.2 Phase Stability (JRC)

Qualitative and quantitative phase analyses by means of X-ray diffraction for all the specimens have been performed. Preferential orientations (textures) have also been analysed for EB-PVD coatings.

	Composition	Phase evolution with ageing	
APS	8YPSZ	Development of Cubic phase	Ref.
	14YSZ	Stable	+
	YTaSZ	Stabilise	+
	LaNdZr ₂ O ₇	Stable but occurrence of unexplained reaction with sample holder	0
	LaMgAl ₁₁ O ₁₉	Stable	+
EB-PVD	8YPSZ	Development of Cubic phase	Ref.
	14YSZ	Stable	+
	YTaSZ	Stable	+
	LaNdZr ₂ O ₇	Stable but evidence of La-Nd dissociation	0
	LaMnAl ₁₁ O ₁₉	Stabilise	+
+ means advantages compared to the reference 0 means equal to the reference - means disadvantages compared to the reference			

Table 7: Performance table for phase stability

Conclusions:

All new compositions revealed the expected crystallographic structures which were more stable than the reference. A “performance” table 7 had been drawn, which summarised the phase evolution and had contributed to the final down-selection .

4.3 Sintering behaviour

Specific surface area

For all EB-PVD samples and for all samples of APS coatings the surface before and after heat treatment was measured by gas adsorption (BET). All samples were analysed after spraying and after heat treatment at 1300 °C and 1400 °C for 100 hours.

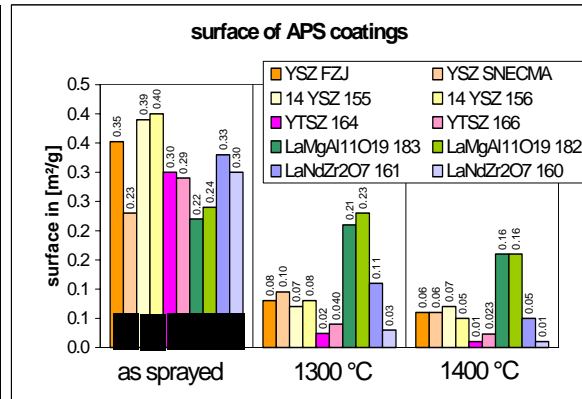
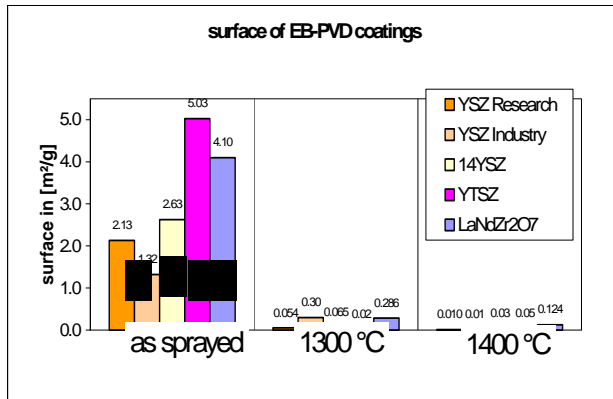


Fig. 6a) Specific surface of EB-PVD coatings

Fig. 6b) Specific surface of APS coatings (two porosities)

It was remarkable that all coatings lost nearly 90% of their surface during heat treatment but solely LaMgAl₁₁O₁₉ lost only about 10% (green bars in fig. 6b).

Conclusions:

The specific area seemed not to be selective enough for ranking the compositions from a sintering point of view. LaMgAl₁₁O₁₉ was the only composition being actually less sensitive to sintering.

Dilatometry of APS free standing coatings

The objective was to follow sintering effects at 1300°C and 1400°C (after 10 hours) from continuous coating shrinkage evaluated by dilatometry. All APS free standing coatings had been tested. The main results were the following (see fig. 7).

- The TaYO₃ZrO₂ composition was very sensitive to sintering which began as early as 1000°C.
- The 14YSZ composition showed at 600°C an important volume increase which had been attributed to the oxidation of zirconium nitride impurities present in the initial powders. This composition preheated in a furnace at 600°C for two hours presented a thermal expansion quite similar to the reference with a smaller propensity to sintering.
- The LaMgAl₁₁O₁₉ composition expanded much less than the reference and showed two important shrinking reactions at 875 and 1130°C corresponding to the crystallisation of amorphous zones present in the as sprayed condition. After a pre-heat treatment at 1130°C for two hours in a furnace the hexaaluminate appeared to be very resistant to sintering.
- The pyrochlore composition LaNdZr₂O₇ had a behaviour quite similar to the reference.

It has to be noted that the dilatometry measurements on EB-PVD coatings had been cancelled due to mostly difficult preparation of free standing coatings. They have been replaced by thermal conductivity determination on all compositions.

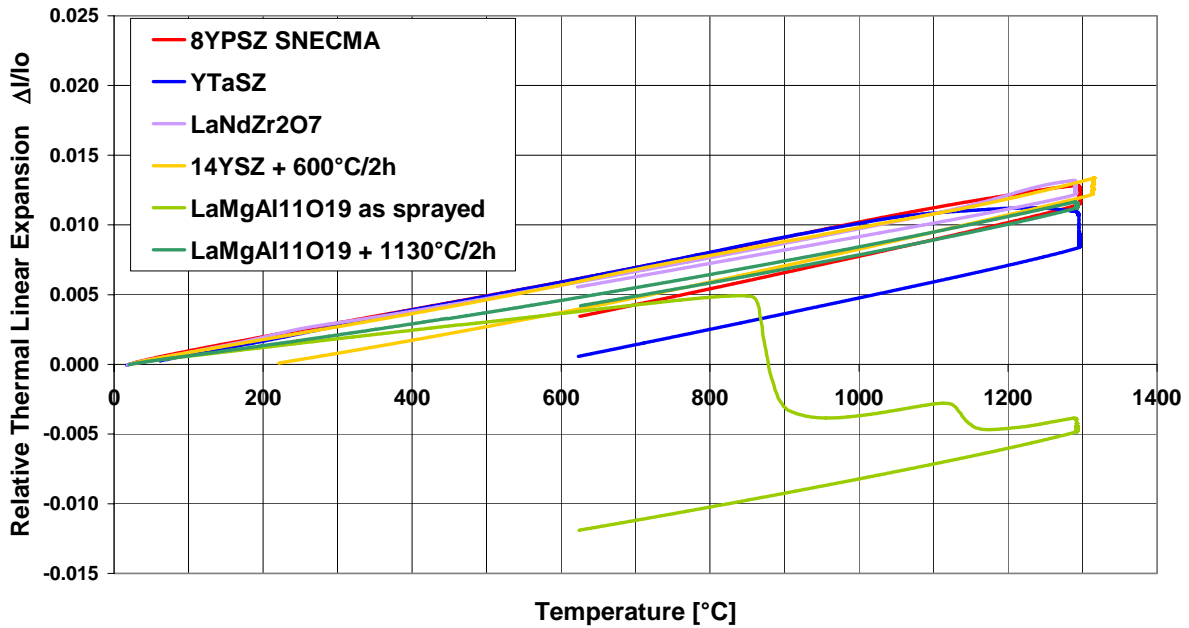


Fig. 7: Dilatometry curves of the APS coatings: relative thermal linear expansion $\Delta l/l_0$ as a function of temperature

Remark : 14YSZ : dilatometry after heat treatment (in furnace) at 600°C/2h

LaMgAl₁₁O₁₉ : dilatometry after heat treatment (in furnace) at 1130°C/2h

	Composition	Sintering behaviour (dilatometry)	
APS	8YPSZ		Ref.
	14YSZ	Attn. Zr-N impurities !	0
	YTaSZ	Sintering as low as 1000°C	-
	LaNdZr ₂ O ₇		0
	LaMgAl ₁₁ O ₁₉	- amorphous to crystalline transition - low thermal expansion coefficient	+ (after HT)

Table 8: Performance table for sintering behaviour

Conclusions:

All new compositions except YTaSZ sintered rather less than the reference 8YPSZ. The thermal expansion coefficient between 400°C and 1000°C was within the normal range of $(9.7 - 10.2) \cdot 10^{-6} [K^{-1}]$ for all compositions, except for LaMgAl₁₁O₁₉ ($8 \cdot 10^{-6} [K^{-1}]$) after heat treatment at 1130°C/2hours). All results were summarised in the "performance" table 8.

Task 4.4 Downselection at the end of chapter 4

4.5 Thermal properties

The general objective of this task was the determination of the thermal conductivity of virgin coatings and its evolution with sample ageing. Thermal conductivity K was determined from diffusivity α according to the equation:

$$K = \alpha \cdot \rho \cdot C_p$$

where ρ is the coating density and C_p is the coating specific heat.

Specific heat (Snecma)

Specific heat of the various compositions (powders) had been measured by differential calorimetry from 100 to 1400°C. Extrapolation to room temperature gave the following values which had been used for thermal conductivity calculation (table 9):

composition	8YPSZ	14YSZ	TaYSZ	LaNdZr ₂ O ₇	LaMgAl ₁₁ O ₁₉	LaMnAl ₁₁ O ₁₉
Cp [J.kg-1.K-1]	470	485	435	420	730	775

Table 9: Thermal conductivity values

Data were transferred to ONERA for calculation of the thermal conductivity.

APS route (ONERA)

Density / porosity of free standing APS coatings (ONERA)

Density had been measured for the following APS coatings, in the virgin state and after heat treatments at 1300 and 1400°C for 100 hours: both 8YPSZ FZJ and Snecma references, 14YSZ, YTaSZ, LaNdZr₂O₇ and LaMgAl₁₁O₁₉ from FZJ.

Density increased to a few percents after ageing at 1400°C for most compositions except for the Mg-hexaaluminate for which the increase reached 10 to 15%.

Thermal conductivity of free standing APS coatings (ONERA) :

Thermal diffusivity of free standing APS coatings had been measured at room temperature under atmospheric pressure, in the as-sprayed as well as in aged condition for the following compositions: both 8YPSZ FZJ and Snecma references, 14YSZ, YTaSZ, LaNdZr₂O₇ and LaMgAl₁₁O₁₉ from FZJ.

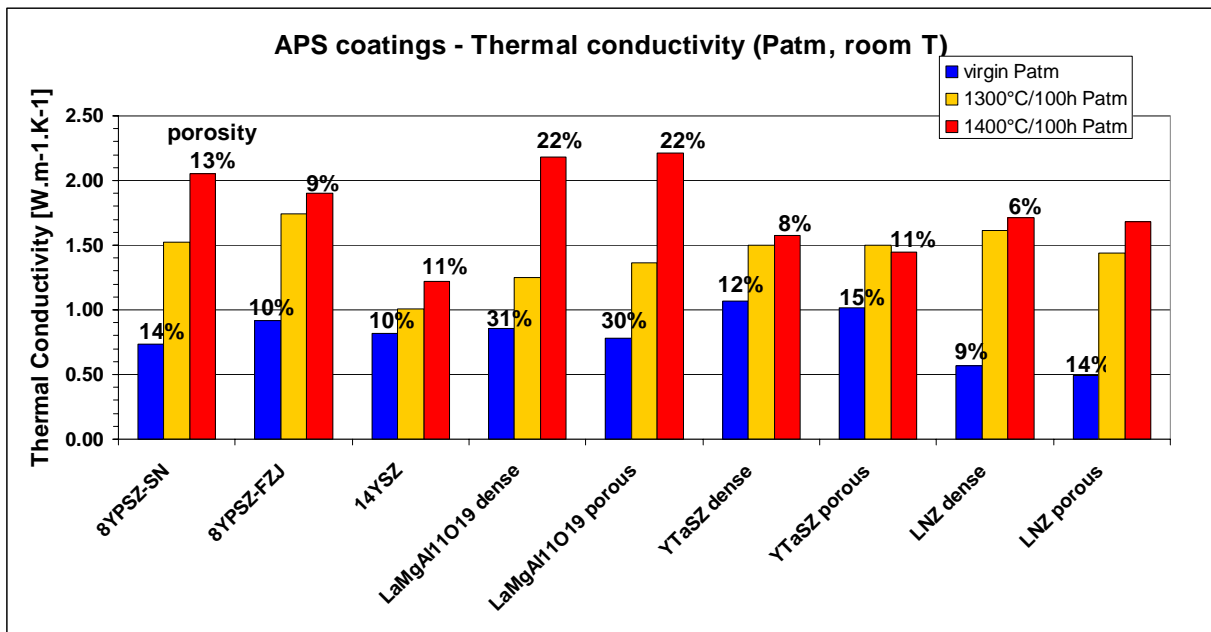


Fig. 8: Thermal conductivity and corresponding total porosity (%) of APS free standing coatings (as-sprayed) at room temperature and vacuum

As a general rule, the thermal conductivity (fig. 8) of plasma sprayed coatings was much more sensitive to morphology than to composition. For quite similar morphologies (porosity range within 10-15%) the new compositions were more insulating than the reference. As already observed with EB-PVD coatings, the thermal conductivity of LNZ strongly increased

with ageing but still remained competitive compared to the reference. $\text{LaMgAl}_{11}\text{O}_{19}$ should have quite a high intrinsic conductivity as hexaaluminate coatings with ~ 30% porosity have similar thermal conductivity as 8YPSZ ones with only ~ 15% porosity.

Conclusions for APS coatings:

Thermal conductivity of APS new compositions was lower than the reference. The increased conductivity after ageing was much more sensitive to morphology - and thus to sintering - than to composition.

EB-PVD route (ONERA)

Density / porosity of EB-PVD coatings on alumina substrates (ONERA)

Density had been measured for the following coatings from DLR, in the virgin state and after heat treatments at 1300 and 1400°C for 100 hours : 8YPSZ (both DLR and C-UK references), 14YSZ, YTaSZ, $\text{LaNdZr}_2\text{O}_7$, $\text{LaMnAl}_{11}\text{O}_{19}$ (including after crystallisation at 1100°C for one hour) and the duplex system 7YPSZ/14YSZ.

The density hardly changed from the virgin state to the 1300°C aged one but it increased up to 10 to 15% after ageing at 1400°C. It has to be noted that the YTaSZ composition had a relatively high density ($> 6000 \text{ [kg.m}^{-3}\text{]}$) whereas LaMn-hexaaluminate had a very low density ($< 3000 \text{ [kg.m}^{-3}\text{]}$) compared to the other compositions ($< 5000 \text{ [kg.m}^{-3}\text{]}$).

For all compositions density increased up to 10 to 15% after ageing at 1400°C. Total porosity decreased from about 15 to 20% in the virgin state down to 5% after 1400°C/100 hours ageing.

Thermal diffusivity / conductivity of EB-PVD coatings on alumina substrates (ONERA)

Thermal diffusivity was measured by a laser flash method for the following coatings from DLR, in the virgin condition and after heat treatments at 1300 and 1400°C for 100 hours : 8YPSZ (both DLR and C-UK references), 14YSZ, $\text{TaYO}_3\text{ZrO}_2$, $\text{LaNdZr}_2\text{O}_7$ and $\text{LaMnAl}_{11}\text{O}_{19}$ (including after crystallisation at 1100°C for one hour).

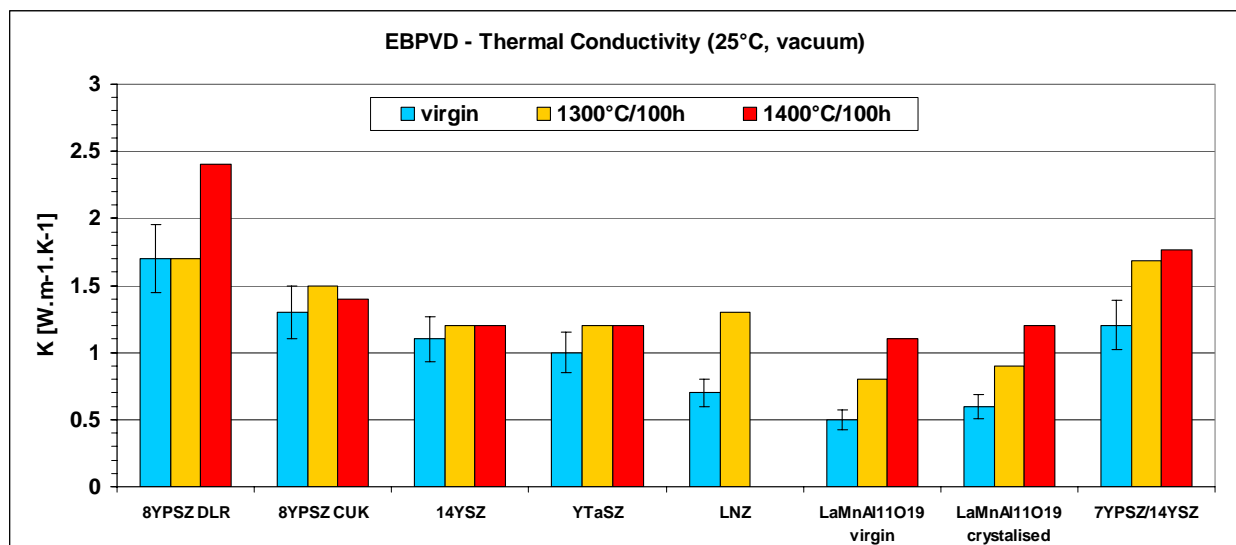


Fig. 9: Thermal conductivity of EB-PVD coatings at room temperature and vacuum as a function of ageing

Thermal conductivity values (fig. 9) of the new compositions were low, about $1 \text{ [W.m}^{-1}\text{.K}^{-1}\text{]}$. As a general rule, thermal conductivity evolution with ageing followed the density one: slight

increase at 1300°C then up to ~15% increase after ageing at 1400°C. This meant that sintering was controlled to a large extent by the porous morphology whereas the matrix chemistry had a minor effect.

The thermal conductivity of the pyrochlore composition strongly increased as low as 1300°C (all pyrochlore coatings aged at 1400°C/100 hours spalled). LaMnAl₁₁O₁₉ composition after ageing also showed an important loss in thermal insulation capacities which, however, still remained comparable to the standard properties. Note that coating quality was not yet optimised. As expected the thermal conductivity of the duplex system (7YPSZ / 14YSZ) was in between the values of partially and fully stabilised zirconia.

Conclusions for EB-PVD coatings:

Thermal conductivity of EB-PVD new compositions was lower than the reference and increased up to 10 to 15% after ageing at 1400°C. The evolution with in service temperature was very slight and quite identical for all compositions.

General conclusions on thermal conductivity:

The increased conductivity after ageing was much more important for APS coatings than for EB-PVD coatings. Actually the thermal conductivity of APS coatings was much more sensitive to morphology - and thus to sintering - than to composition whereas EB-PVD thermal conductivity depended mainly on composition. In all the new compositions had better insulation properties than the reference as documented in the “performance” table 10.

	Composition	Thermal conductivity	
APS	8YPSZ		Ref.
	14YSZ		+
	YTaSZ		+
	LaNdZr ₂ O ₇	strong increase for 1400°C ageing	+
	LaMgAl ₁₁ O ₁₉	strong increase after ageing	0
EB-PVD	8YPSZ		Ref.
	14YSZ		+
	YTaSZ		+
	LaNdZr ₂ O ₇	samples spalled off at 1400°C	+
	LaMnAl ₁₁ O ₁₉	strong increase for 1400°C ageing	+

Table 10: Performance table for thermal conductivity

4.6 Microstructural investigations

The objective was to provide reliable coating microstructures to correlate with macroscopic observations of sintering. Microstructure characterisations were performed by

- JRC in order to better assess the sintering due to ageing by characterisation of coating morphology evolution by means of Scanning Electron Microscopy of the coating surfaces and the (fractured) cross section.
- ONERA on polished cross-sections for quantitative image analysis on APS coatings.

The main results were documented in the “performance” table 11.

- As a general rule the total porosity decreased with ageing which could be correlated with the density evolution.
- The globular porosity increased, specially for the YTaSZ composition, whereas the porosity corresponding to the lamellar pores and fine cracks decreased.
- Thus sintering mainly contributed to a rounding off of pores.
- LaMgAl₁₁O₁₉ virgin APS coatings did not show any lamellar structure but mainly rounded pores and a large amount of glass-like (amorphous) zones. The microstructure did not change after ageing but the initially amorphous zones crystallised.

	Composition	Morphology evolution with ageing	
APS	8YPSZ	Re-crystallisation, original lamellar structure still visible	Ref.
	14YSZ	Intense re-crystallisation and densification; lamellar structure no more visible	-/0
	YTaSZ	Intense densification	-/0
	LaNdZr ₂ O ₇	Melted-like re-crystallisation; densification; lamellar structure no more visible	-
	LaMgAl ₁₁ O ₁₉	No lamellar structure visible; amorphous-like area in the virgin state; crystallisation, typical grain size seems unchanged	0/+
EB-PVD	8YPSZ	Inter- and intra-columnar densification	Ref.
	14YSZ	Inter- and intra-columnar densification, full re-crystallisation at interface	0
	YTaSZ	Full re-crystallisation; very high grain growth	-
	LaNdZr ₂ O ₇	Full re-crystallisation; considerable grain growth	-
	LaMnAl ₁₁ O ₁₉	No columnar structure visible; crystallisation	0

Table 11: Performance table for morphology evolution

4.4 Downselection (see page 17)

The following table 12 summarises the results of all characterisations performed within workpackage 4 with respect to the standard system 8% YPSZ.

	Composition	Phase stability	Sintering behaviour	Thermal conductivity	Morphology evolution
APS	8YPSZ	Ref.	Ref.	Ref.	Ref.
	14YSZ	+	0	+	-/0
	YTaSZ	+	-	+	-/0
	LaNdZr ₂ O ₇	0	0	+	-
	LaMgAl ₁₁ O ₁₉	+	+ (after HT)	0	0
EB-PVD	8YPSZ	Ref.		Ref.	Ref.
	14YSZ	+		+	0
	YTaSZ	+		+	-
	LaNdZr ₂ O ₇	0		+	-
	LaMnAl ₁₁ O ₁₉	+		+	0

Table 12: Downselection due to physical properties

Taking into account the above observations and data, a down-selection of two compositions was made for both APS and EB-PVD: fully stabilised zirconia 14YSZ and hexaaluminates ($\text{LaMgAl}_{11}\text{O}_{19}$ for plasma sprayed coatings and $\text{LaMnAl}_{11}\text{O}_{19}$ for EB-PVD), see table 13. As these compositions, in particular 14YSZ, were known to have a lower toughness as the reference 8YPSZ, they were tested in workpackage 6 with a double layer configuration, the inner layer being the standard 8YPSZ and the outer layer being the new composition. Furthermore only one morphology will be considered as the two porous structures tested in WP4 appeared to be very similar.

	Selected system	Reasons for selection
APS	14YSZ duplex	- high phase stability - low thermal conductivity
	$\text{LaMgAl}_{11}\text{O}_{19}$ single or duplex	- high phase stability - low sintering after previous crystallisation heat treatment
EB-PVD	14YSZ	- high phase stability - low thermal conductivity
	$\text{LaMnAl}_{11}\text{O}_{19}$ single or duplex	- high phase stability - low sintering after previous crystallisation heat treatment - low thermal conductivity

Table 13: Downselected coating compositions

Conclusions of workpackage 4:

The following systems had been characterised with respect to their phase stability, sintering behaviour, thermal properties and microstructure evolution.:

- EBPVD coatings from DLR (8YPSZ reference, 14YSZ, $\text{TaYO}_3\text{ZrO}_2$, $\text{LaNdZr}_2\text{O}_7$, $\text{LaMnAl}_{11}\text{O}_{19}$) and C-UK (8YPSZ reference),
- APS coatings from FZJ (8YPSZ reference, 14YSZ, $\text{TaYO}_3\text{ZrO}_2$, $\text{LaNdZr}_2\text{O}_7$, $\text{LaMgAl}_{11}\text{O}_{19}$ with two different microstructures, dense and porous, for the last four compositions) and Snecma (8YPSZ reference)

It turned out that all new compositions had better phase stability and better thermal insulation properties than the standard 8 wt.% yttria partially stabilised zirconia. Remaining selection criteria were the sintering behaviour (dilatometry) and the morphology evolution, which eliminated the YTaSZ and $\text{LaNdZr}_2\text{O}_7$ compositions. Finally the selected systems were the fully stabilised zirconia 14YSZ and the hexaaluminate (La-Mg for APS and La-Mn for EBPVD coatings).

WP5 Industrial processing of selected coating systems

The objective of this work package was to transfer the processes as developed into industrial equipment and comprised processing trials and the coating of test pieces. The task was started in time but the original time schedule could not be met due to delays of

- APS coating: problems with the powder quality of the new material LaMg-Hexaaluminate,
- EB-PVD coating: coating problems with the new material LaMn-Hexaaluminate using one ingot.

5.1 Technology transfer

The technology transfer of the coating processes of the two down selected coating systems from FZJ to SNECMA (APS) and from DLR to C-UK (EB-PVD) was already started prior to the mid-term meeting and was an ongoing process during 2003.

For the APS powders the technology transfer of 14 YSZ process was without problems. For the LaMg-Hexaaluminate it had been completed after the delivery of the second powder material with better quality in February 2004.

In the case of the EB-PVD process DLR had completed the technology transfer for the composition 14% YSZ. For the new material LaMn-Hexaaluminate the transfer did not succeed and resulted in the feasibility study carried out by DLR (see WP3.4).

5.2 Procurement of spray powders and ingots

APS route (FZJ and SNECMA)

An evaluation of possible industrial powder suppliers to the project was performed taking into account technical, economical and geographical aspects. It was decided to sub-contract the industrial powder production to H.C. Starck, Germany due to their technical capabilities and their company position in Europe. A meeting between H.C. Starck, SNECMA and FZJ was held in order to discuss the powder specifications and to transfer the know-how from FZJ to H.C. Starck. The orders of the down selected powders $ZrO_2 - 14\% Y_2O_3$ and $LaMgAl_{11}O_{19}$ were placed in early 2003.

14% yttrium stabilised zirconia

The experiments performed in WP3 on fully stabilised zirconia have been obtained for fused and crushed powders, but it was decided in the consortium to change the powder to a spray dried one. A lot of 50 kg of the $ZrO_2 - 14\% Y_2O_3$ powder was received and accepted in July 2003. Initial spray trials with the new powder were performed by FZJ and the spray parameters were transferred to Snecma Moteurs in October 2003.

LaMg-Hexaaluminate

The $LaMgAl_{11}O_{19}$ powder was more difficult to produce. The first batches produced by H.C. Starck showed a large and non-acceptable quantity of impurities. By the interaction of FZJ, changes in the manufacturing process were proposed. In particular a longer milling time was applied by H.C. Starck and the results showed a powder with reduced and acceptable impurity level. After a few optimisation trials concerning the spray drying operation, a powder with correct composition and correct flowability was produced by H.C. Starck. A lot of 80 kg of the $LaMgAl_{11}O_{19}$ powder had been received and accepted in February 2004.

The particle shape of the spray-dried powder of H.C. Starck was quite unusual for this type of powder compared to the 14% YSZ powder (fig. 10). The impurity content of the powder was very low and the chemical analysis confirmed a good quality.

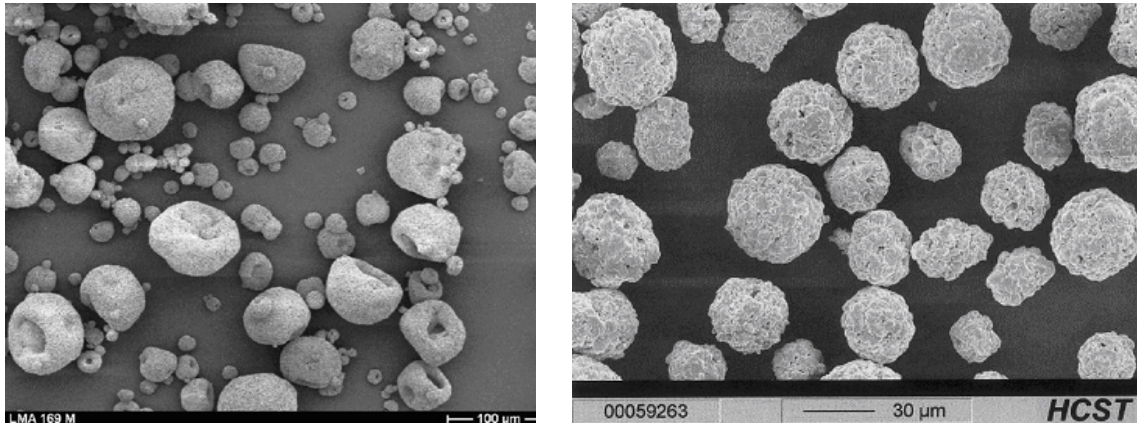


Fig. 10: Spray dried powder of LaMg-Hexaaluminate (left) and of 14% YSZ (right)

EB-PVD route (DLR)

14% yttrium stabilised zirconia

The company HTM Reetz fabricated 14% YSZ-ingots for C-UK following the DLR instructions which were gained during the task of process optimisation for EB-PVD-deposition of new compositions (see WP3.1 and WP3.2).

LaMn-Hexaaluminate

Optimisation trials were carried out at C-UK applying the ingot provided by DLR and the ingot with higher La_2O_3 -content ordered by C-UK at Co. HTM Reetz.

5.3 Processing trials using industrial equipment

APS route (FZJ and SNECMA)

For the industrialisation of the spray processes of the new compositions, standard industrial processing equipment was used at the SNECMA Moteurs processing plant in Corbeil Evry. All spray trials were performed in a booth using a Sulzer Metco F4 gun. A set of different spray parameters was tested for each composition. The choice of spray parameters used in the spray trials was based on earlier experience at SNECMA and the initial spray trials of the powders carried out by FZJ. The choice of an acceptable microstructure was based on the amount and distribution of the porosity as well as the process deposition efficiency.

14% yttrium stabilised zirconia

The experiments performed in WP3 on fully stabilised zirconia had been obtained for fused and crushed powders. As it was decided to change the powder to a spray dried one, FZJ was willing to perform additional experiments as a support of the industrial partners with the finally used powder supplied by the company H.C. Starck. The results of the investigation revealed a slightly higher but not critical yttrium content.

The objective was to find values resembling the standard SNECMA thermal barrier coating, $\text{ZrO}_2 - 8\% \text{Y}_2\text{O}_3$. Among the different parameters tested, it was possible to choose a set of parameters for this material that gave an acceptable microstructure and a homogeneous distribution of the pores (fig. 11 left).

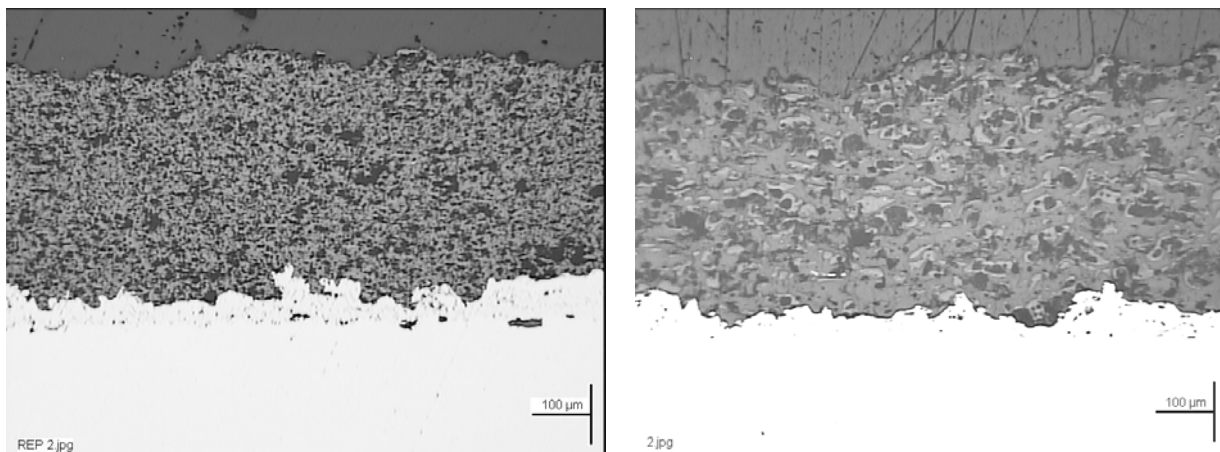


Fig. 11: Acceptable coating microstructure of the ZrO_2 - 14% Y_2O_3 composition (left) and of the $\text{LaMgAl}_{11}\text{O}_{19}$ composition (right)

LaMg-Hexaaluminate

In the same manner the spray parameters were optimised for the $\text{LaMgAl}_{11}\text{O}_{19}$ composition in order to achieve an acceptable coating microstructure (fig. 11 right). The porosity size was slightly larger for this composition compared to the zirconia based compositions and the matrix was divided into two zones (contrast differences within the optical microscopy). This was known due to the preliminary spray trials by FZJ where no composition differences were detected between the zones.

EB-PVD route (DLR and C-UK)

14% yttrium stabilised zirconia

DLR completed the technology transfer for the down-selected composition 14% YSZ to C-UK successfully and carried out process trials.

LaMn-Hexaaluminate

The technology transfer with the second down-selected composition $\text{LaMnAl}_{11}\text{O}_{19}$ was clearly more difficult. After optimisation trials with this composition at C-UK applying the ingot provided by DLR in a 1st trial and the ingot with higher La_2O_3 -content ordered by C-UK at Co. HTM Reetz in a 2nd and 3rd trial, the composition and microstructure of the samples were analysed at DLR (example in fig. 12: trial 3 carried out at C-UK in the period between October 2003 to March 2004).

These results showed that the composition deviated very strongly within the coating and generally either very high MnO- or high Al_2O_3 -contents were detected. In general, La_2O_3 -contents were lower than those given in the allowed range for the composition. These compositions were hardly possible to yield on crystallisation the magnetoplumbite phase which is known under the chemical composition of $\text{LaMnAl}_{11}\text{O}_{19}$.

In order to overcome the coating problems with EB-PVD LaMn-Hexaaluminate a re-evaluation of the coating process was decided by the consortium by carrying out a feasibility study at DLR with the objective to establish a stable process which can produce samples with correct coating composition and structure and a suitable efficiency (see WP 3.4).

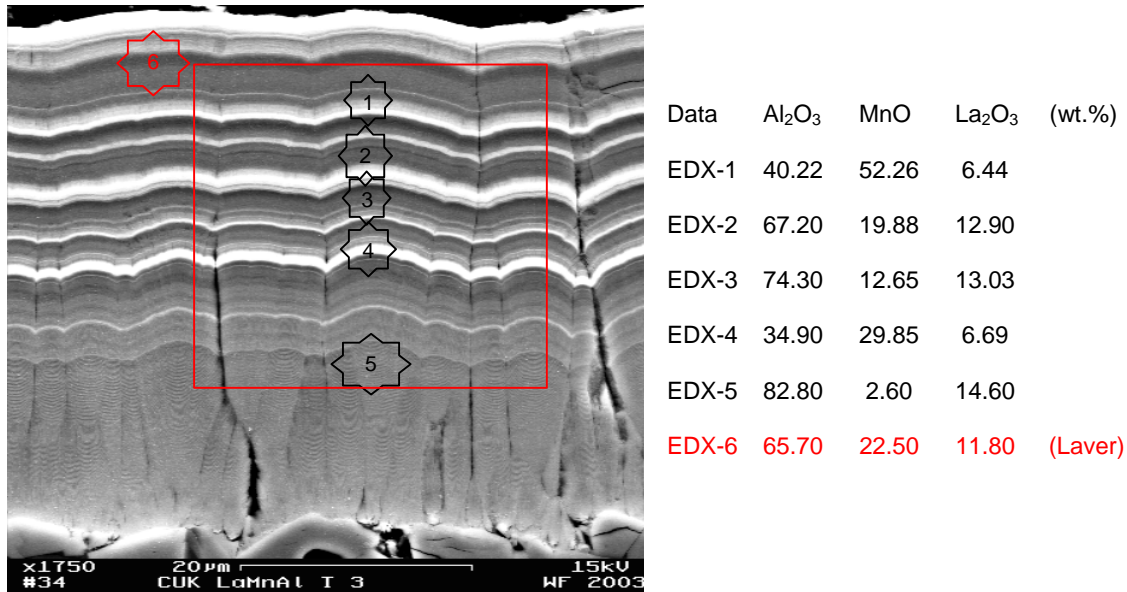


Fig. 12: EDX analysis of LaMn-Hexaaluminate at positions 1 to 6 on trial 3

5.4 Coating of test pieces

A bi-layer configuration of the new thermal barrier coating compositions for APS and EB-PVD process had been selected within the TBC plus programme. On top of the bond coating, a 0.15 mm standard ZrO₂ - 8% Y₂O₃ layer was sprayed and on top of this layer a 0.15 mm thick layer of either ZrO₂ - 14% Y₂O₃ or LaMgAl₁₁O₁₉ was sprayed.

APS route (SNECMA)

The bi-layer configuration was successfully applied onto the technological samples for the mechanical, thermal exposure, corrosion and erosion tests. Single layers of the new compositions were applied for the evaluation of coating properties such as microstructural evolution, sintering, phase stability, creep, thermal conductivity, thermal expansion and density measurements.

A complete set of samples with standard ZrO₂ - 8% Y₂O₃ was also sprayed as a reference to the new compositions. In total, 150 samples were coated for the evaluation in WP6. All samples were delivered to the partners in May 2004.

EB-PVD route (C-UK)

The 14% YSZ duplex coatings for WP6 as well as 8% YSZ reference samples were manufactured by C-UK and shipped to the partners by end of October 2003.

Within the feasibility study (WP3.4) a set of samples for material property investigations and fatigue testing was produced for verification of the established process.

WP6 Full characterisation of selected coatings

The main focus of this work package was the investigation of the down selected APS and EB-PVD coatings with respect to their high temperature behaviour in comparison to the reference systems (standard coatings).

- Investigation of the microstructure of the single coatings
- Determination of the physical properties of the single coatings
- Thermo-mechanical testing of the coating systems
- Corrosion tests of the coating systems
- Modelling by finite element method (FEM)

As the application of the new coatings was done in terms of a double layer structure, single layers coating as well as coating systems were investigated.

- APS single layers coatings: 8% yttrium (partially) stabilised zirconia (8Y(P)SZ), 14% fully yttrium stabilised zirconia (14YSZ) and LaMg-Hexaaluminate ($\text{LaMgAl}_{11}\text{O}_{19}$)
- APS coating systems (duplex layer): 8YPSZ / 14YSZ and 8YPSZ / $\text{LaMgAl}_{11}\text{O}_{19}$
- EB-PVD single layers coatings: 8YPSZ and 14YSZ
- EB-PVD coating systems (duplex layer): 8YPSZ / 14YSZ

The coating system EB-PVD 8YPSZ / $\text{LaMgAl}_{11}\text{O}_{19}$ was not subject of investigation, because this coating was discussed in the feasibility study (see chapter WP3.4).

All coatings were produced under industrial conditions by the following companies:

- APS: MTU (bond coating), SNECMA (TBC) and partly LHT (bond coating and TBC)
- EB-PVD: C-UK for all coatings.

6.1 Ageing and microstructural features (JRC and ONERA)

Ageing at 1200, 1300 and 1400°C for 100 hours was performed on the following coatings:

- EB-PVD coatings on alumina or sapphire substrates from C-UK (duplex 8YPSZ/14YSZ)
- free standing APS coatings from Snecma and partially LHT:
 - single layers 8YPSZ, 14YSZ and $\text{LaMgAl}_{11}\text{O}_{19}$ (thickness 500 μm)
 - duplex 8YPSZ/14YSZ and 8YPSZ/ $\text{LaMgAl}_{11}\text{O}_{19}$ (thickness 150 μm /150 μm)

For trying to understand the transformations occurring within $\text{LaMgAl}_{11}\text{O}_{19}$ coatings (thermal expansion), additional heat treatments had been performed at 1000°C / 2 hour and 1150°C / 2 hours (crystallisation heat treatment).

6.2 Microstructural stability under higher temperature

The microstructural investigations were distributed between ONERA and JRC carried out in close collaboration. The more general investigations and comparison with WP4 was done by JRC and the more detailed investigations by ONERA.

APS free standing coatings (JRC)

Phase and morphology evolutions had been assessed by respectively X-ray diffraction at surface and SEM (top view and fracture surface, in some cases metallographical cross sections). All findings for APS coatings were summarised in table 14 and compared with the results from WP4. In all cases the coatings behaved similarly to those of WP4. Only for the 8YSZ coatings from WP6 the monoclinic phase evolution was greater than in WP4: 20%

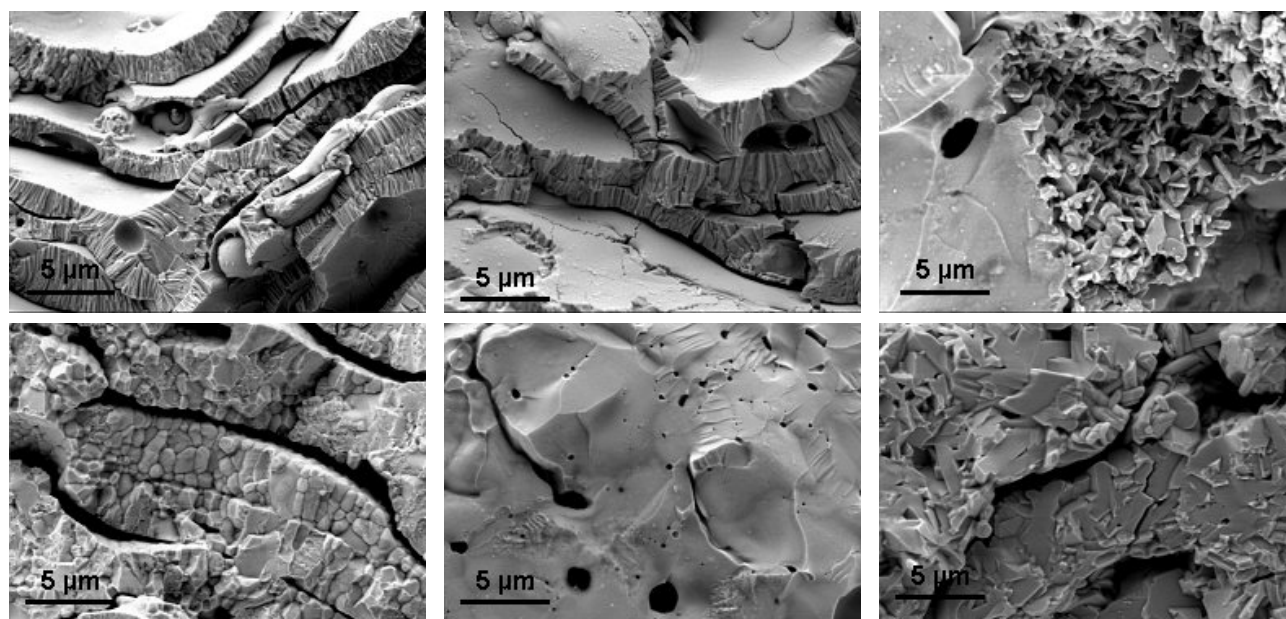
volumetric versus a few percent. However, this amount of monoclinic phase was considered typical of standard 8YSZ and was not considered as a concern.

		APS Coating			
		As received	1200C ageing	1400C ageing	Comparison with WP4
8YSZ	Morphology	Typical APS lamellar structure, inside lamellae columnar grains	Grains rounding-off, less evidence of growth	Massive recrystallisation of equiaxial grains, some lamellae sintering	Comparable
	Phase evolution	Tetragonal <2% monoclinic 0% cubic	Tetragonal < 2% monoclinic < 20% cubic	Cubic ≈ 20% monoclinic ≈ 20% cubic	Higher monoclinic contents after ageing
14YSZ	Morphology	Typical APS lamellar structure, inside lamellae columnar grains	Grain growth, lamellae sintering	Strong recrystallisation, massive lamellae sintering	Comparable
	Phase evolution	Cubic	Cubic	Cubic	Identical
LAMgAl₁₁O₁₉	Morphology	Bimodal microstructure: dense glassy phase and cavities with porous grains (2 μm)	Bimodal microstructure: crystallisation of the dense phase.	Bimodal microstructure: Further crystallisation of the dense phase, grains up to 2 μm.	Comparable
	Phase evolution	LAMgAl ₁₁ O ₁₉ and amorphous phase	Full crystallisation, pure LAMgAl ₁₁ O ₁₉	Further refinement of structure, pure LAMgAl ₁₁ O ₁₉	Comparable

Table 14: Microstructure of aged APS coatings (in air, 100 hours, stand alone coatings)

APS free standing coatings (ONERA)

Fractography (fig. 13) and cross section analysis (fig. 14) had been performed on 8YPSZ single layer, duplex 8YPSZ/14YSZ and 8YPSZ/LaMgAl₁₁O₁₉ in virgin and aged states.

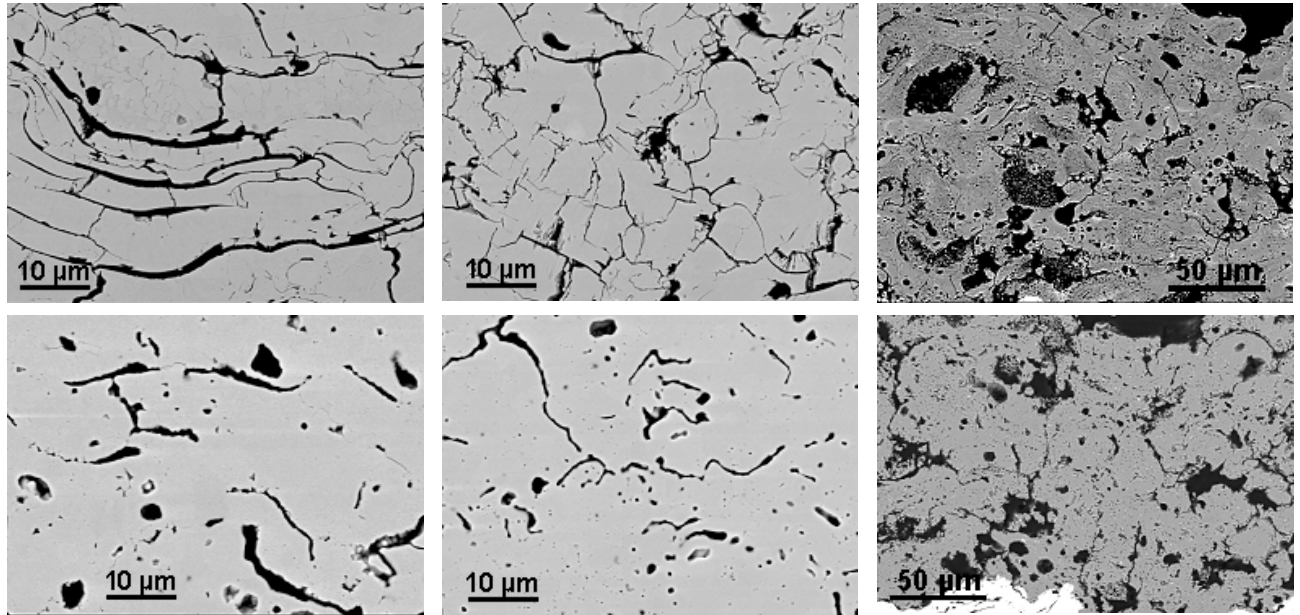


top: 8YPSZ as sprayed
bottom: 8YPSZ aged

top: 14YSZ as sprayed
bottom: 14YSZ aged

top: LaMgAl₁₁O₁₉ as sprayed
bottom: LaMgAl₁₁O₁₉ aged

Fig. 13: Fractography of the single layer TBCs, as sprayed and 1400°C/100h aged



top: 8YPSZ as sprayed
bottom: 8YPSZ aged

top: 14YSZ as sprayed
bottom: 14YSZ aged

top: LaMgAl₁₁O₁₉ as sprayed
bottom: LaMgAl₁₁O₁₉ aged

Fig. 14: Microsections of the single layer TBCs, as sprayed and 1400°C/100h aged

A general observation was the lamellar structure of the zirconia TBCs 8YSZ and 14YSZ compared to a non lamellar amorphous-like structure of the LaMgAl₁₁O₁₉ coating. The main results of the microstructural investigations were summarised in table 15.

	Composition	Morphology evolution with ageing	Porosity evolution with ageing (image analysis)
APS	8YPSZ (ref.)	Original well defined lamellar structure still visible; important grain growth inside the lamellae	19% (virgin) down to 11% (1400°C/100h)
	14YSZ	Lamellar structure no more visible; densification inside the lamellae as soon as 1200°C; very strong grain growth inside the lamellae	16% (virgin) down to 10% (1400°C/100h)
	LaMgAl ₁₁ O ₁₉ (Snecma)	Virgin state: no lamellar structure visible, round closed pores, amorphous-like area; From 1150°C: crystallisation, typical grain size seems unchanged, stable cracked porous structure	22% (virgin) up to 30% (from 1000°C)
	LaMgAl ₁₁ O ₁₉ (LHT)	Virgin state: no lamellar structure visible, round closed pores, no evidence of amorphous phase (stabilisation heat treated)	

Table 15: Microstructure evolution of APS coatings with aging

Amorphous zones could be observed up to 1000°C. These zones crystallised with very small grains from 1150°C to important grain growth at 1400°C (fig. 15). The determination of the amorphous content in LaMgAl₁₁O₁₉ coatings (as sprayed and aged at 1000°C/2 h) had been attempted using electron backscattered diffraction analysis (EBSD) and image analysis.

- as sprayed: 50 – 60% crystalline phase, 40 – 50% amorphous phase
- aged 1000°C/2h: 60 – 70% crystalline phase, 30 – 40% amorphous phase.

As the measurement method was not easy to handle and had not yet been validated, these figures gave only a rough estimation and must be considered with caution.

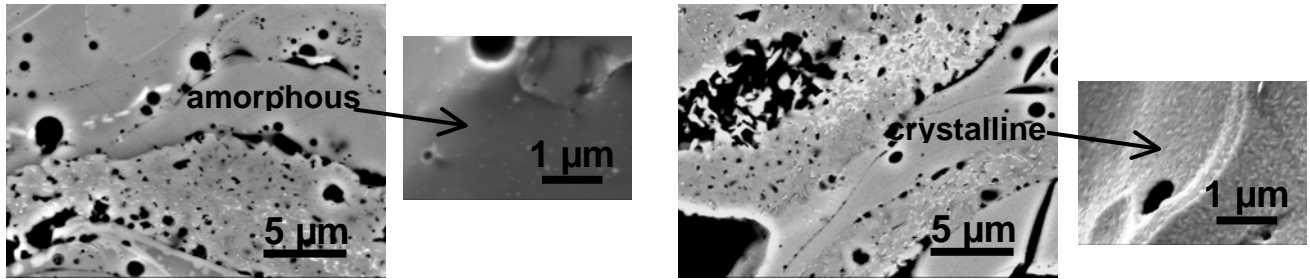


Fig. 15: LaMgAl₁₁O₁₉ Snecma-APS top layer: crystallisation of amorphous zones

EB-PVD coatings on alumina substrate (JRC)

The EB-PVD coatings single layer 8YSZ and double layer 8YSZ/14YSZ on alumina substrate had been aged in air at 1200°C and 1400°C for 100 hours and investigated as the APS coatings. The results were compared with the WP4 investigations (table 16).

Due to the different sintering behaviour of the two layers, the 8YSZ – 14YSZ interface became a preferential path for cracking. This effect was much clearer in the WP6 samples (C-UK production) than in the WP4 samples (DLR production). In the latter case, the 8YSZ did not fully develop and this influenced sintering and morphology aspects. An intergranular phase was found in some areas of both the WP6 coatings, containing Al and hinting to a reaction with the Alumina substrate.

<u>EB-PVD Coating</u>					
		As received	1200°C ageing	1400°C ageing	Comparison with WP4
Single 8YSZ	Morphology	Typical EB-PVD columnar structure	Sintering of the feather-like features, some grain growth near interface	Total recrystallisation of grains in the area near the substrate, inter-columnar sintering	Comparable
	Phase evolution	Tetragonal <2% monoclinic 0% cubic	No evidence of monoclinic Some presence of cubic	No evidence of monoclinic Presence of cubic (≈ 20%)	Comparable
Double 8YSZ/14YSZ	Morphology	Typical EB-PVD columnar structure	Sintering of the feather-like features, some grain growth near interface	Total re-crystallisation of grains in the area near substrate, inter-columnar sintering	Stronger sintering effect, clearer weak interface between bottom and top layer, the sample is bent, with concavity at the coating side.
	Phase evolution	Cubic	Cubic	Cubic	Identical

Table 16: Microstructure of aged EB-PVD coatings (in air, 100 hours, Al₂O₃ substrate)

6.3 Thermophysical properties

As already done in WP4 the main physical properties of the selected coatings were assessed mainly by ONERA:

- thermal expansion
- thermal conductivity / diffusivity
- density and porosity

Generally the investigations had been performed on samples aged at 1200, 1300 and 1400°C (10 hours). In some cases additional heat treatments at 1000 (partially crystallisation) and 1150°C (full crystallisation) for two hours have been performed on hexaaluminate coatings.

APS route

Thermal expansion

Coating shrinkage had been evaluated by dilatometry at 1200, 1300 and 1400°C (10 hours) on the following APS single layer, free standing coatings:

- 8YPSZ reference coating from FZJ which remained from WP4
- 14YSZ and LaMgAl₁₁O₁₉ from Snecma
- LaMgAl₁₁O₁₉ from LHT (stabilisation heat treated 1100°C / 1 hour)

The **14YSZ** coating behaved exactly as the reference. The thermal expansion coefficient between 200 and 1400°C was within the range $(8.7 - 10) \cdot 10^{-6} \text{ [K}^{-1}]$ for both compositions. The APS coating **LaMgAl₁₁O₁₉** from **Snecma** behaved as previously observed in WP4 with FZJ coatings: i.e. it expanded much less than the zirconia based materials (the thermal expansion coefficient was about $5.8 \cdot 10^{-6} \text{ [K}^{-1}]$ between 200 and 800°C) and showed two important shrinking reactions at 875 and 1150°C (fig. 16). These transformations resulted in full crystallisation of the solid phase but their exact role had not been identified so far. After a second dilatometry run on the same sample, thus fully crystallised, the hexaaluminate appeared to sinter much less than the reference. In this case the thermal expansion coefficient was within the range $(6.6 - 8.9) \cdot 10^{-6} \text{ [K}^{-1}]$ between 200 and 1400°C; however, it was still lower than the reference.

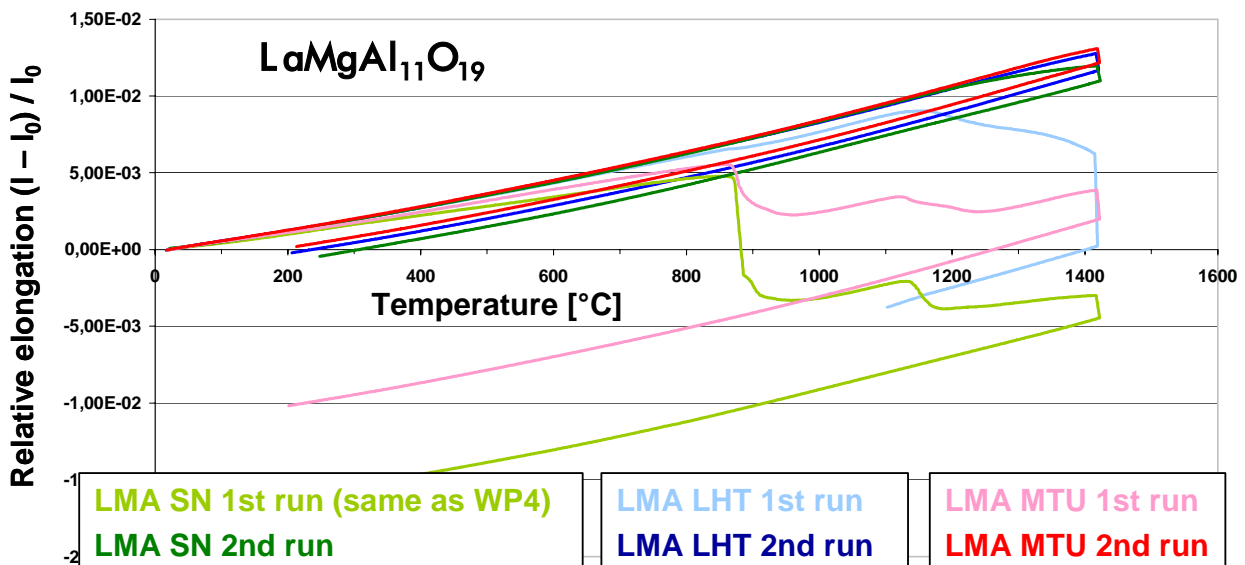


Fig. 16: Dilatometry curves of LaMgAl₁₁O₁₉ composition: relative thermal linear expansion $\Delta l/l_0$ as a function of temperature

The APS coating **LaMgAl₁₁O₁₉** from **Lufthansa** – in the condition as sprayed + stabilisation heat treatment 1100°C / 1h - did not show the shrinking reaction at 875°C anymore and the shrinking at 1150°C was different. However the shrinkage at 1400°C during the 10 hours dwell time was quite important. A second dilatometry experiment performed on the same sample led to the same behaviour as the Snecma LaMgAl₁₁O₁₉ coating (fig. 16).

The APS coating **LaMgAl₁₁O₁₉** from **MTU** (sprayed with a high calcinated DaimlerChrysler powder) showed the most promising results: both transitions at 875 and 1150°C still existed, but they were smoother and less pronounced. Moreover after full crystallisation, the hexaaluminate coating was very stable with regard to sintering at 1400°C (fig. 16).

Conclusions:

The 14YSZ composition behaved exactly as the reference regarding the sintering behaviour and the thermal expansion coefficient.

The LaMgAl₁₁O₁₉ sintered less than the reference provided the coating was subjected to a preliminary heat treatment in order to achieve full crystallisation or structure stabilisation. The coating sprayed with DaimlerChrysler powder showed particularly encouraging sintering behaviour.

Density and porosity

Density had been measured by a water immersion technique for 8YPSZ, 14YSZ and LaMgAl₁₁O₁₉ APS single layer coating, in the virgin and heat treated condition.

For both **zirconia based compositions** density increased continuously with ageing up to a few percents (less than 5%) at 1400°C. Correlatively the total porosity which was mainly composed of open porosity decreased to about 30%. For the **LaMg-Hexaaluminate** the density increased (less than 10%) up to 1400°C. Correlatively the total porosity decreased (to less than 15% for **Snecma APS** and less than 5% for **LHT APS**). Note that for both coating sources the distribution among open and closed porosity was quite different between as-sprayed and aged conditions (50% open-50% closed porosity in virgin state and 80-20 after ageing as low as 1000°C).

Thermal conductivity

Thermal conductivity had been determined from diffusivity measurements by laser flash technique on 8YPSZ, 14YSZ and LaMgAl₁₁O₁₉ free standing, single layer, 0.5 mm thick, APS coatings, in the virgin and heat treated condition.

For both **zirconia based compositions** results were comparable to those in WP4: thermal conductivity increased with ageing (fig. 17). This evolution was mainly related to morphological modifications. As the sintering pores became rounded and partly closed (see microstructure table 15), they were less efficient than the initial lamellar pores for stopping the heat flux. It has to be noted that fully stabilised zirconia had better insulation properties than the reference zirconia at very high temperature (lower thermal conductivity whereas the porosity was lower).

Concerning **hexaaluminates**, notable variations in the thermal conductivity evolution with ageing were observed according to the origin (feedstock powders and spraying conditions) of the coatings (fig. 18). The lowest conductivity on the whole range of ageing temperatures was observed with **LHT coatings** which were the most porous and did not show any amorphous phase in the virgin state due to the stabilisation heat treatment (see microstructure and dilatometry results). These last coatings appeared to be quite competitive regarding to the 8YPSZ reference. However these encouraging results have to be confirmed on more samples and additional ageing temperatures.

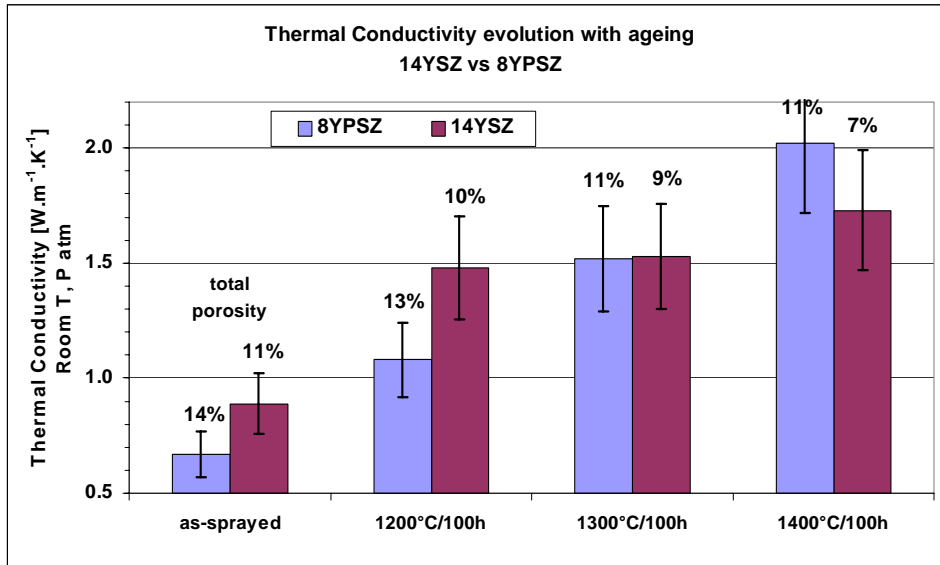


Fig. 17: Thermal conductivity of zirconia based APS coatings and corresponding total porosity determined by water immersion

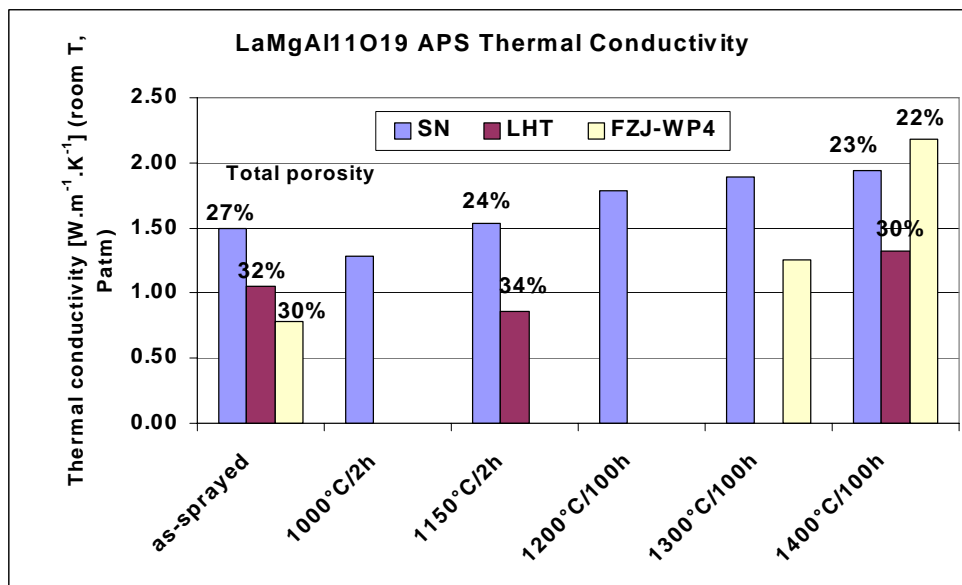


Fig. 18: Thermal conductivity of LaMgAl₁₁O₁₉ APS coatings at room temperature and atmospheric pressure as a function of ageing and corresponding total porosity determined by water immersion

Thermal conductivity had been measured as a function of temperature (fig. 19) up to 1400°C for the three single layer systems **sprayed by S necma** (8YPSZ reference, 14YSZ and LaMgAl₁₁O₁₉), aged at 1200 and 1400°C. As commonly observed, the thermal conductivity slightly decreased with temperature for all compositions.

Thermal conductivity of APS coatings had additionally been measured at room temperature as a function of pressure (fig. 20). This was an indirect way to estimate the effect of sintering on the microstructure, because the thermal conductivity of the gas inside the open pores (and thus the thermal conductivity of the whole coating) depended both on the external pressure and on the pore thickness. Actually 8YPSZ thermal conductivity strongly decreased with decreasing pressure mainly because of the lamellar pores oriented perpendicular to the heat flux. This pressure effect became smaller with increasing ageing temperature due to pore closing and rounding by sintering (fig. 20). On the contrary almost no evolution was

observed for the hexaaluminate, neither in virgin nor in aged states. This confirmed that $\text{LaMgAl}_{11}\text{O}_{19}$ microstructure was very stable provided the solid phase was fully crystallised.

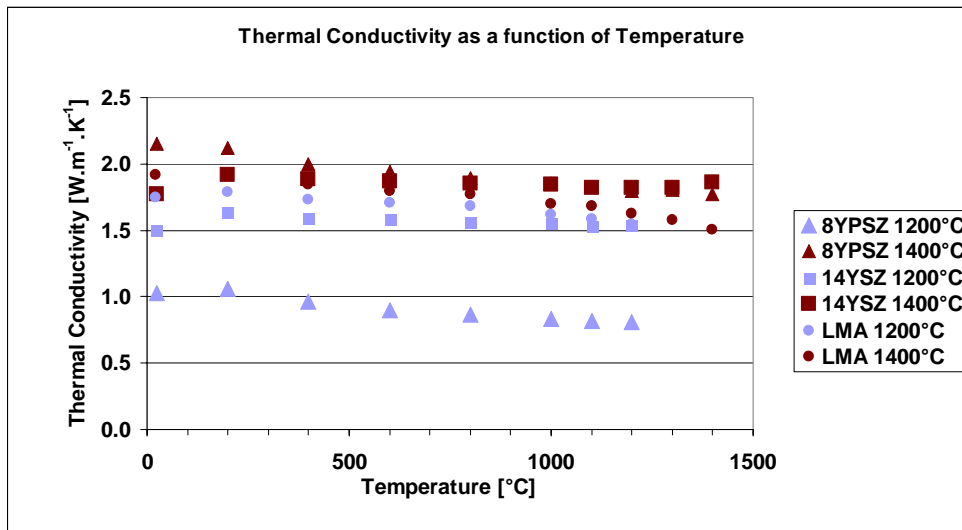


Fig. 19: Thermal conductivity evolution of APS coatings with temperature

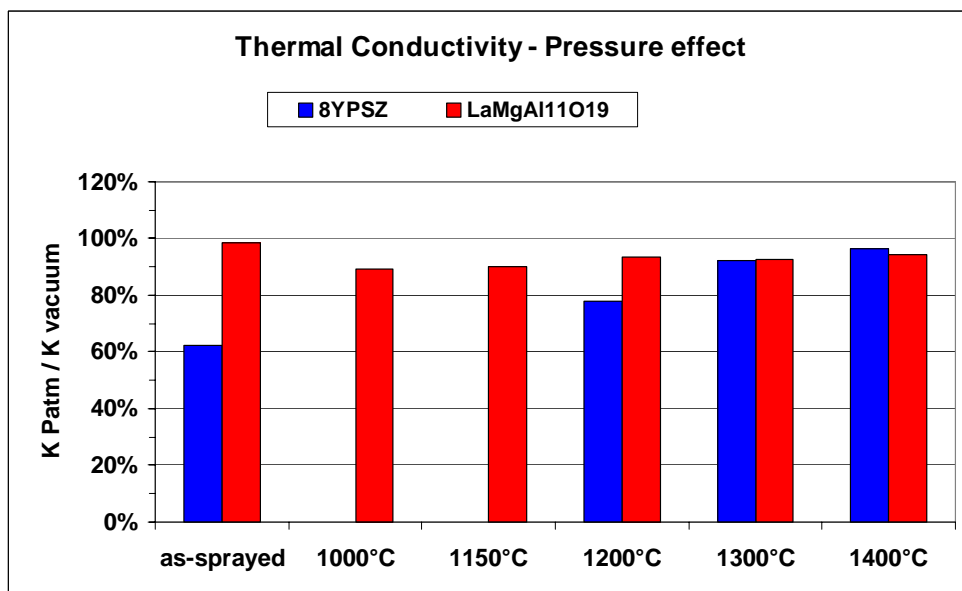


Fig. 20: Pressure effect on APS thermal conductivity as a function of coating ageing

General conclusion on thermal properties of APS coatings

Results obtained in WP6 on the insulation properties of industrial APS coatings (8YPSZ, 14YSZ and $\text{LaMgAl}_{11}\text{O}_{19}$) agreed with those obtained in WP4 on laboratory scale coatings. **14YSZ** thermal conductivity was lower than the reference although both coatings increased with ageing due to sintering (lamellar porosity rounding off).

The evolution of **hexaaluminates** thermal conductivity with ageing depended on the coating source (raw materials and spraying conditions). It appeared that initially highly porous coatings, without any amorphous phase and thus having the most stable porous structure (no cracking due to crystallisation), revealed the lowest thermal conductivity on a wide range of ageing temperatures. These were very encouraging results for this new original composition compared to the 8YPSZ reference.

EB-PVD route

The first samples (duplex 8YPSZ/14YSZ on alumina disks) received for diffusivity measurements were of very poor quality (heterogeneous coating thickness) and gave unreliable results. New samples were water jet cut by Snecma out of coated alumina plates. They were aged at 1200, 1300 and 1400°C for 100 hours and density and thermal diffusivity were measured. Results appeared to be completely meaningless, because the 14YSZ top layer was defect. So no conductivity results were available for EB-PVD coatings in WP6.

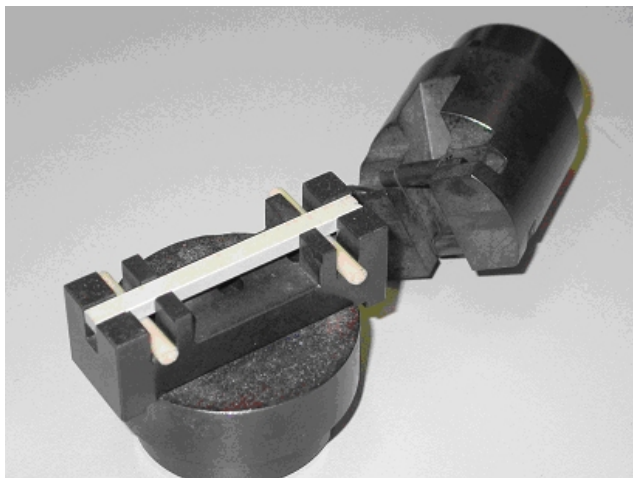
6.4 Mechanical characteristics

With regard to the mechanical properties of the APS and EB-PVD coatings different types of tests were performed.

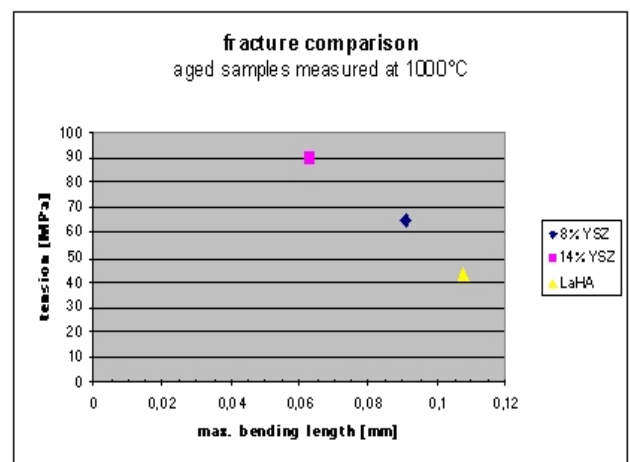
- Bending and creep tests
- Tensile tests for critical strain to cracking
- Micro-indentation on EB-PVD coatings

Bending and creep tests (MTU)

MTU performed 4-point bending tests on plasma-sprayed samples of new thermal barrier coatings: LaMg-Hexaaluminate (LaHA), 14%YSZ and 8%YSZ (reference). Out of the free standing plates, sprayed by SNECMA, 10 samples per material were cut and subsequently grinded. Half of the samples were aged for 240 h at 1200°C. The sample size was 58 mm length, 4.5 mm width and 2.5 to 3.5 mm height – depending on the initial plate thickness (see example in fig. 21).



4-point bending retainer with different sample



Bending strength (tension) and strain (length)

Fig. 21: 4-point bending test facility and test results

To investigate the materials behaviour preliminary 4-point bending tests were performed on virgin and aged samples. Therefore the bending force was increased linearly until fracture of the specimen (fig. 21). Test temperatures were room temperature and 1000°C. The main results of the experiments are depicted in fig. 22:

- Aged samples of all materials showed a higher Young's-modulus than virgin samples. In case of LaHA the change was light. In case of zirconia the increase was dramatic.
- Virgin samples of all materials had a higher bending strain than aged samples.
- At higher test temperatures the bending strain was higher for all materials.
- Order of the measured bending strain (length): **14% YSZ < 8% YSZ < LaHA**
- Order of the measured rupture strength (tension): **LaHA < 8% YSZ < 14% YSZ**

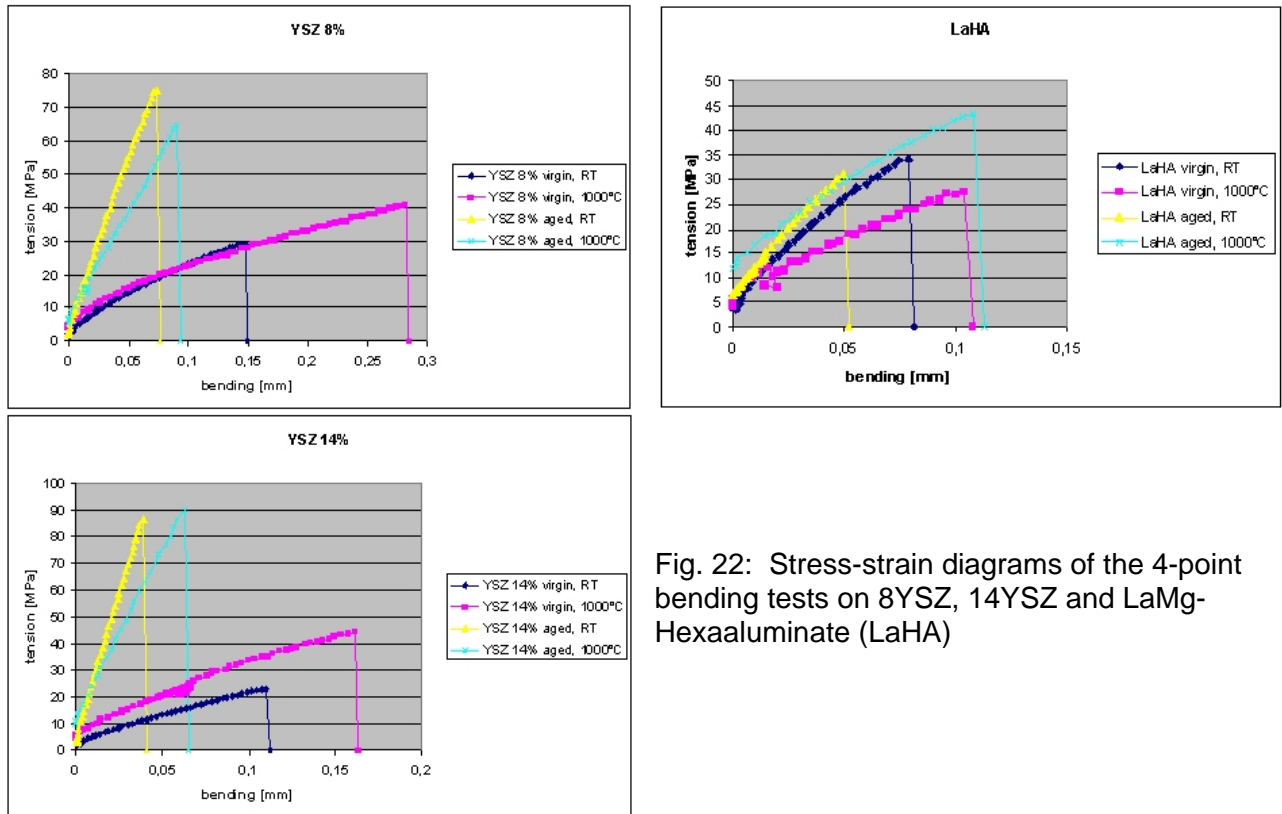


Fig. 22: Stress-strain diagrams of the 4-point bending tests on 8YSZ, 14YSZ and LaMg-Hexaaluminate (LaHA)

The high temperature creep tests were stopped, because the 4-point bending machine (fig. 21) was not adequate to handle brittle ceramic samples. It was designed to operate on metallic specimens with loads up to 10 tons. Using a constant load of 5 N for ceramics measurement noise and fluctuation became so intense that the obtained experimental results were useless. Therefore MTU changed to tests with increasing loads under constant temperature until fracture as shown above. With the remaining fund thermal cycle tests, tension tests and erosion test were performed.

Tension tests for critical strain to cracking (JRC)

In tensile tests on flat specimen the critical strain to cracking was assessed at room temperature, 500°C and 900°C (fig. 23). The results were a bit inconsistent, but for the APS coating systems at 900°C the LaMg-Hexaaluminate revealed the highest strain until the first cracks appeared and for the EB-PVD coatings the 8YSZ coating.

Micro-indentation on EB-PVD coatings (ONERA)

Objective of this task was measuring the "local" Young's modulus along the coating thickness as a function of ageing and at service temperature. The results should partly serve as input data to the modelling task.

The indentation testing had been done on EB-PVD single layer 7YPSZ and duplex 7YPSZ/14YSZ coatings deposited by C-UK on NiAlPt (C-UK) with CMSX4 substrate, in the virgin state and after ageing at 1100°C for 10 hours under air. Measurements were performed on two in-house built, fully instrumented micro-indentation machines working respectively at room temperature and up to 1000°C. Hardness and Young's modulus were measured on sample cross-sections at different positions through the coating thickness, within a single ceramic column (at room temperature and 0.3 [N] load, 10 indentations per value, table 17).

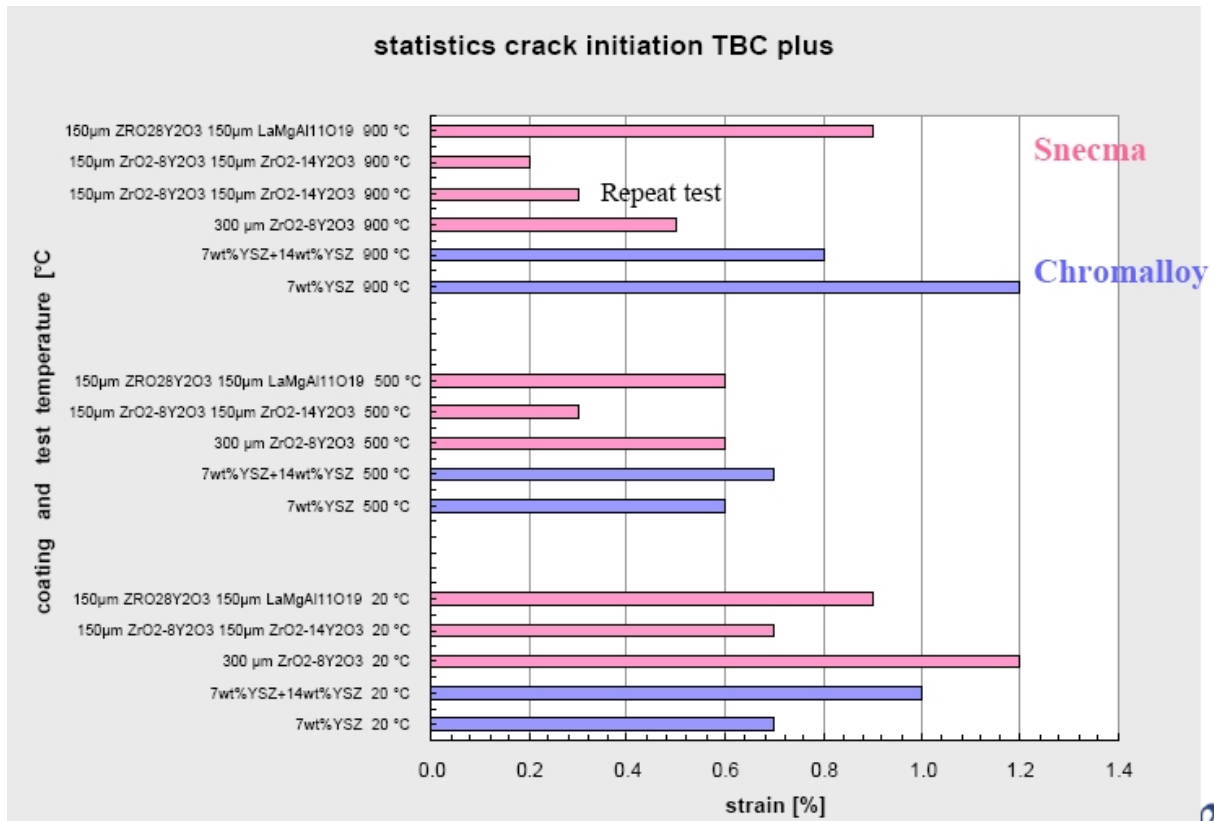


Fig. 23: Critical strain to cracking for APS (SNECMA) ad EB-PVD (Chromalloy) coatings

Sample		Hardness [GPa] ($\pm 10\%$)		Young's modulus [GPa] ($\pm 15\%$)	
		virgin	1100°C/10h	virgin	1100°C/10h
Single layer	7YPSZ top	4.5	8.9	83	77
	7YPSZ bottom	7.8	7.6	132	94
	NiAlPt	4.9	6.2	178	139
Duplex layer	14YSZ top	4.2	7.4	108	-
	14YSZ bottom	4.5	6.4	90	80
	7YPSZ	8.6	7.4	142	88
	NiAlPt	6	6.4	175	133

Table 17: Micro-indentation at room temperature on EB-PVD coatings

The hardness had been measured also up to 900°C on the polished surface of the virgin coating by indentation within a single column. For both 7YPSZ and 14YSZ, it decreased with temperature, remaining almost constant up to 600°C. The local hardness and Young's modulus of the standard zirconia 7YPSZ appeared to be higher than for fully stabilised zirconia. However, it has to be noted that the 14YSZ coating was more porous than the standard. Moreover in both cases the hardness increased with ageing and thus with sintering. Full exploitation of the measurements would require better quality coatings (see problems with thermal conductivity samples).

6.5 Durability and ranking tests

Fatigue and corrosion testing were the main subject of the ranking test for the down selected coating systems and they are described in great detail.

- Thermal shock and thermal cycling tests by SNECMA and Alstom
- Ash corrosion tests by AVIO
- Gas corrosion tests by JRC and FZJ
- Erosion tests by MTU

APS route

Thermal shock and thermal cycling tests (SNECMA)

The thermal cycling test was a sequence of cycles of one hour in a furnace at 1100°C followed by 15 minutes at room temperature with an electric fan assisted air cooling (slow heating and cooling rates). It was stopped when TBC spallation occurred on more than 20% of the coated surface area. The thermal shock test consisted in heating of the topcoat up to 1450-1500°C for one minute by a burner, while the other face was cooled by air (about 950°C in superalloy base material was measured). At the end of the cycle the sample was cooled 1 minute in air (fast heating and cooling rates).



Fig. 24: Standard coating sample after thermal cycling

TBC coating	Thermal cycling cycles	Thermal shock cycles
ZrO ₂ -8%Y ₂ O ₃	404	965 and 1434
ZrO ₂ -8%Y ₂ O ₃ + ZrO ₂ -14%Y ₂ O ₃	404	1659 and 1886
ZrO ₂ -8%Y ₂ O ₃ + LaMgAl ₁₁ O ₁₉	264 and 327	75 and 169

Table 18: Thermal cycling and thermal shock testing results of APS coating systems

The tests were performed on buttons (25mm in diameter and 3mm in thickness) coated by three different APS top coatings (fig. 24, table 18). For all the cases of thermal cycling the spallation occurred at the interface between bond- and top coating (indeed bond coating 8YSZ for all systems) and the ceramic top coating kept its integrity. While the thermal cycling results of the LaMg-Hexaaluminate was in the order of the YSZ coatings, the thermal shock results were clearly worse.

Thermal shock and thermal cycling tests (Alstom)

Three types of tests, thermal shock-, thermal cycling- (cyclic oxidation) and isothermal oxidation tests were carried out on flat samples 60x40x8 mm (substrate IN617) for the 3 coating systems standard (reference) 8YPSZ, duplex 8YSZ/14YSZ and duplex 8YSZ/LaMg-Hexaaluminate.

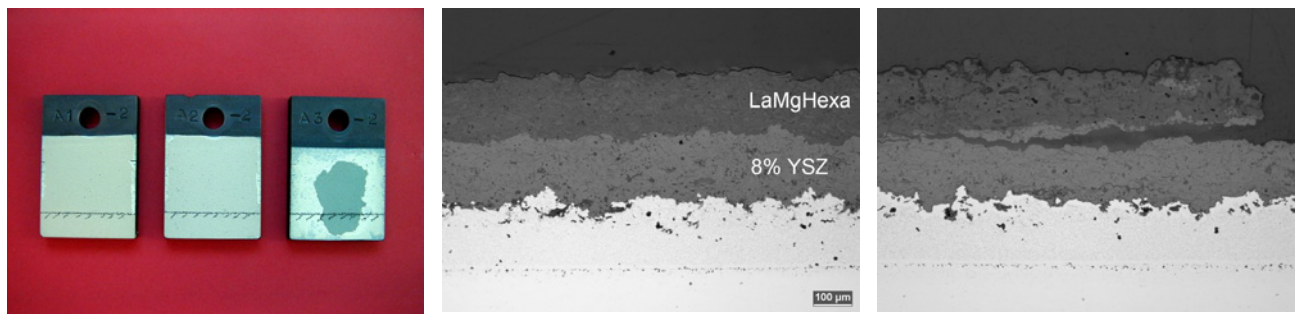
- The thermal shock test was the Alstom standard test consisting of fast heating and cooling rates: heating to 1000°C for 5 min and cooling to room temperature for 5 min, both in a separate fluidised bed test facility; test had passed when 1000 cycles were reached without major coating flake off.
- The Alstom cyclic oxidation test (thermal cycling) consisted of slow heating and cooling rates: heating in a furnace at 1100°C for 23 h and cooling at room temperature for 1h; the test was finished after more than 50% coating flake off occurred.

- The isothermal oxidation test was carried out continuously at 1100°C in a furnace. It was finished after 2000 h (corresponding to failure time of the cyclic oxidation tests); a strip was cut from the samples for metallographic investigations after 165 h, 500 h and 2000 h.

The result of the thermal shock (TS) test was insufficient for the LaMg-Hexaaluminate material (H.C. Starck powder coated by SNECMA).

- The YSZ standard and duplex samples passed the test.
- The duplex 8YSZ/LaMg-Hexaaluminate sample failed by flaking off directly at the interface to the intermediate layer 8YSZ between 600 and 1000 cycles (fig. 25).

For metallographic investigations small strips were cut from the samples prior to testing (initial condition as sprayed) and after the thermal shock test (fig. 25).



Samples after TS test (from. left):
 - 8YPSZ
 - duplex 8YSZ/14YSZ
 - duplex 8YSZ/LaMg-Hexa

Duplex 8YSZ/LaMg-Hexaaluminate in as sprayed condition

Duplex 8YSZ/LaMg-Hexaaluminate after TS test, flake off at interface to 8YSZ

Fig. 25: SNECMA samples after thermal shock test; microstructure of LaMg-Hexaaluminate

In the cyclic oxidation test (fig. 26) 8 coupons were tested for each of the 3 coating systems (one sample was cut into 4 coupons). For all three coatings the TBC flake off was located in the 8YSZ TBC near the interface to the bond coating, but not between the two TBC layers as observed in the thermal shock test. All three coatings achieved comparable life times of about 2200 h or 70 cycles (mean value calculated from all 8 coupons of each coating):

- standard 8YPSZ: 2379 h
- duplex 8YSZ/14YSZ: 2276 h
- duplex 8YSZ/LaMg-Hexaaluminate: 2114 h



Coupons after 1679 h and 53 cycles
 (2-16: Alstom coupons, 1-1 to 1-8: 8YSZ, 2-1 to 2-8: 8/14YSZ, 3-1 to 3-8: 8YSZ/LaMg-Hexa)

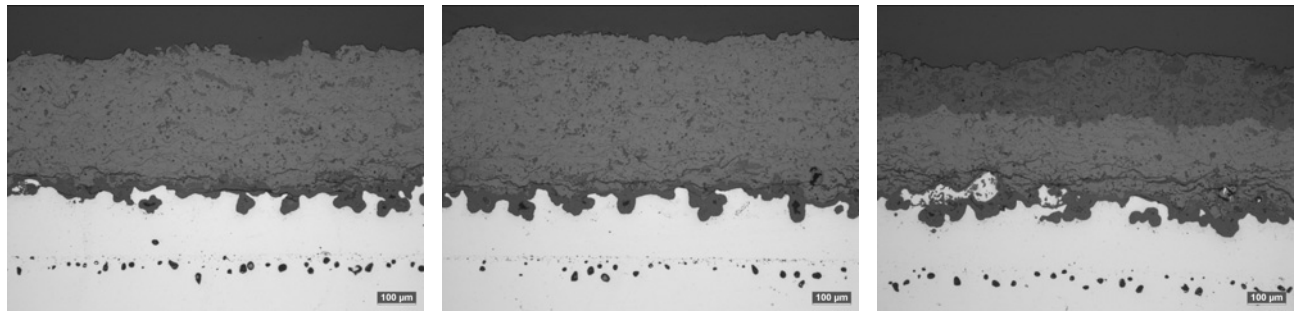


TBCplus coupons after failure in the cyclic oxidation test (top: 8YSZ/LaMg-Hexa, middle: 8/14YSZ, bottom: 8YSZ)

Fig. 26: Coupons during and after cyclic oxidation tests

Microsections after 2000 h isothermal oxidation test presented the microstructure of the 3 coatings, the development of the TGO and the formation of cracks in the TBC (fig. 27).

- The main damage in the isothermal and cyclic oxidation test was observed in the TBC.
- The usual crack path and the spallation of the TBC in the cyclic oxidation was near the interface from the 8YSZ TBC to the bond coating.
- The cracking in the TBC was more pronounced in the 8YSZ/LaMg-Hexaaluminate coating compared to the standard and duplex YSZ coatings.
- At single locations the crack path had partially run through the TGO too.
- The development of the TGO was similar for all three coatings.



8YPSZ (reference)

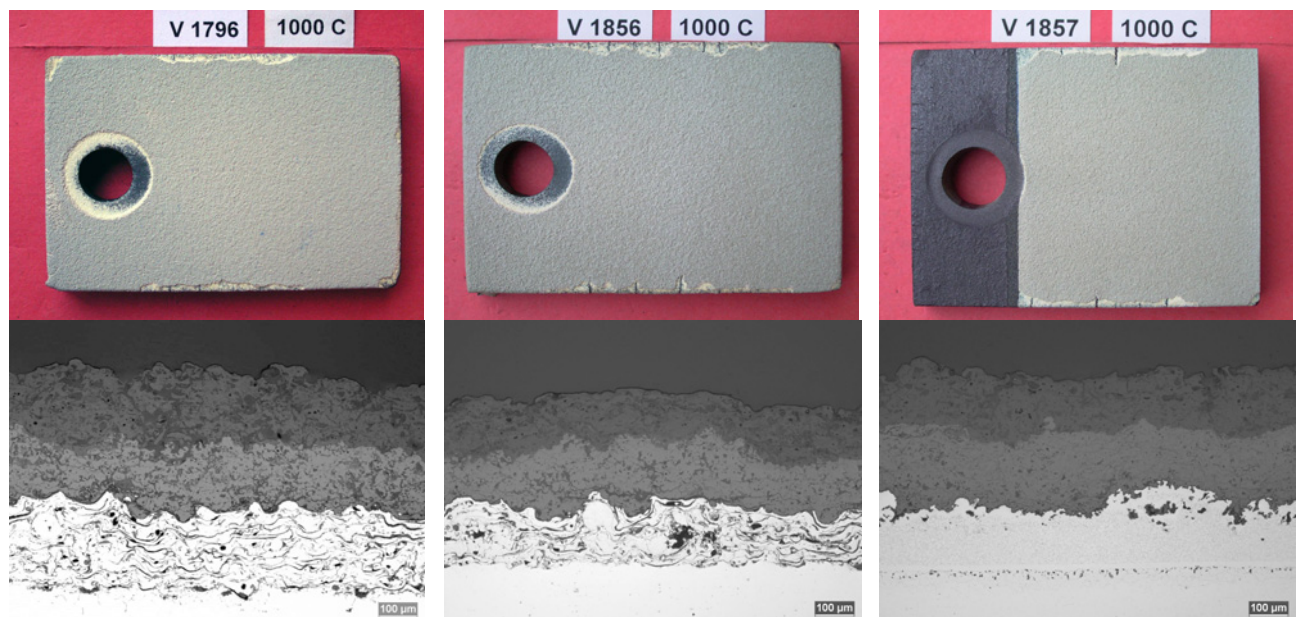
Duplex 8YSZ/14YSZ

Duplex 8YSZ/LaMg-Hexa

Fig. 27: Microsection of samples after 2000 h isothermal oxidation test

The thermal shock and cycling results of the LaMg-Hexaaluminate compared to the standard 8YPSZ and duplex 8YSZ/14YSZ showed a similar tendency as the SNECMA results: thermal cycling results comparable, thermal shock results worse. For that reason further spray trials with LaMg-Hexaaluminate powder were initiated:

- LHT with the H.C. Starck powder from SNECMA; samples stabilisation heat treated 1100°C/1h after spraying
- MTU with DaimlerChrysler Friedrichshafen (DCF) powder; calcinated at 1650°C



LHT
1100°C/1h heat treatment

MTU
as sprayed condition

SNECMA
1100°C/1h heat treatment

Fig. 28: LaMg-Hexaaluminate samples and microstructure after 1000 cycles in the Alstom thermal shock test

Additional thermal shock tests were carried out on those produced samples and on a stabilisation heat treated SNECMA sample too. The results were promising (fig. 28), because all samples only showed minor TBC flake off, passed the test and revealed a quite acceptable microstructure after the test.

Conclusions:

The at higher temperature of 1650°C calcinated LaMg-Hexaaluminate powder produced by DaimlerChrysler Friedrichshafen (DCF) revealed a better cyclic life and a more stabilised microstructure (MTU samples) compared to the H.C. Starck LaMg-Hexaaluminate powder calcinated at 1450°C (SNECMA samples). In the case of the H.C. Starck powder samples from LHT and SNECMA with stabilisation heat treatment of 1h at 1100°C gave rise to an improved cyclic life compared to the as sprayed condition. According to these results and subject to the results of the physical material properties the at higher temperature of 1650°C calcinated LaMg-Hexaaluminate powder was more suitable for industrial application.

Ash corrosion tests (AVIO)

For the corrosion ash test cylindrical specimens (9mm diameter and 50mm length) of single crystal alloy CMSX-4 substrate and three coating systems were used:

- standard (reference) 8YPSZ single layer (APS simplex)
- duplex 8YPSZ / 14YSZ layer (APS duplex)
- duplex 8YPSZ / LaMgAl₁₁O₁₉ (APS Hexa)

The samples were tested in a salty bath (composition: 75% wt Na₂SO₄ and 25% wt NaCl) at the temperatures of 850°C and 950°C. Every 8-20 hours the specimens were taken out for investigation.

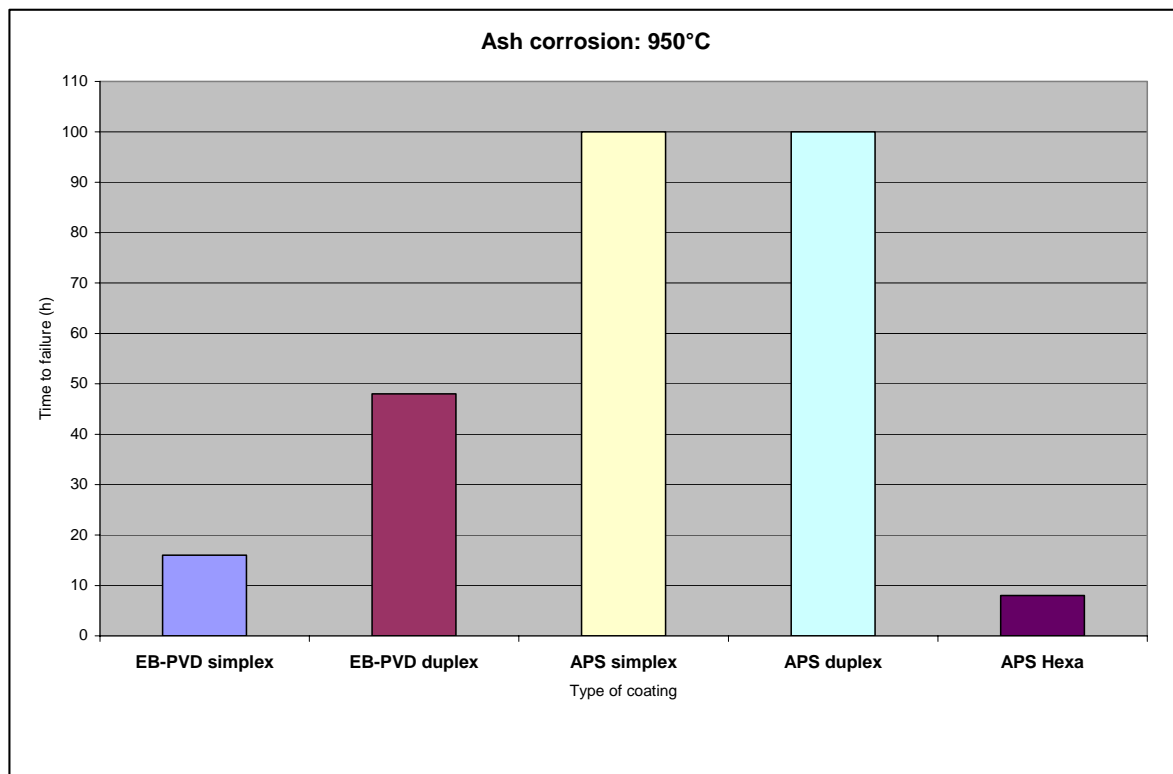


Fig. 29: Time to failure of APS (and EB-PVD) coatings in the ash corrosion test, test temperature 950°C (results at 850°C not shown here)

Generally the life time was lower at 950°C. At both temperatures the APS simplex and the APS duplex coatings showed similar behaviour, while the APS Hexa results were insufficient (see 950°C results in fig. 29). The duplex system of 8YPSZ/LaMgAl₁₁O₁₉ probably flaked off due to the elevated percentage of the amorphous phase present in the deposit and superimposed of a cycling effect. In fact to around 870°C the transition amorphous-crystalline verified, and the phenomenon was accompanied by a strong variation of volume.

Gas corrosion tests (JRC)

Since the samples were not fully coated by the TBCs (uncoated bottom face, for the APS coatings also a lateral surface strip of 20 mm without bond coat), it had been decided to start tests with a lower temperature (1100°C instead of 1200°C) in order to minimise heavy oxidation of the substrate and with shorter cycle time (20 hours instead of 100 hours) in order to allow more frequent monitoring. Cracking (and substrate oxidation for the APS) initiated at a very early stage (first cycle). All the coating failed macroscopically between the second and the eighth cycle, i.e. after 40 to 160 hours. Probable cause of failure was the thermal cycling that took place during loading and unloading of the samples from the burner rig. No conclusion could be drawn on the hot corrosion behaviour of the coating.

Later it was decided in the consortium to carry out additional corrosion tests at FZJ.

Gas corrosion tests (FZJ)

The substrates (IN738 disks, diameter 30mm, thickness 3mm) for the corrosion tests were provided by FZJ and all coatings were applied by LHT. The coatings had been applied to one side of the substrates using an APS Bond coating (about 100µm) and all three down selected coatings:

- Standard (reference) YSZ (about 500 – 700 µm)
- Double layer 8YSZ/14YSZ (total 500 -700 µm)
- Double layer 8YSZ/LaMg-Hexaaluminate (LMAO) (100-150/100-150 µm)

First a brief description of the testing conditions and the main features of the corrosion rig facility is given. The rig operated with a natural gas and an oxygen burner. The samples were heated with the burner from one side and cooled from the other side by compressed air. After 5 min heating the burner was moved from the surface for 2 min and the front additionally cooled by compressed air. The surface temperature was measured by a long-wavelength

Corrosive medium	Description
Reference	This refers to cycling in our corrosion rig without using additional corrosive treatment.
Soaked in salt water	Before cycling samples were soaked in salt water (25 g/l NaCl) for 24 hours, afterwards dried for 2h at 200°C.
NaCl corrosion – 25 g/l NaCl	A solution of 25 g/l NaCl in water was atomized with compressed air and injected through a central nozzle into the gas burner. The feeding rate of the water solution was 1.4 - 1.6 g/min.
Na ₂ SO ₄ corrosion – 10 g / L Na ₂ SO ₄	A solution of 10 g / l Na ₂ SO ₄ in water was atomized with compressed air and injected through a central nozzle into the gas burner. The feeding rate of the water solution was 1.4 - 2.0 g/min.
Coated with silica glued sand	The samples were treated with sand glued with silica. Afterwards samples were dried at 100°C over night.
Kerosene	Kerosene was atomised with compressed air and injected through a central nozzle into the gas burner. The feeding rate was 1.2-1.3 g/min.
Multiple media	Sample were coated with sand and a water solution with 12.5 % NaCl+ 5% Na ₂ SO ₄ was injected into the burner.

Table 19: Corrosive media for the corrosion tests at FZJ

pyrometer, the substrate temperature determined by a thermocouple. The intended substrate and surface temperatures were 1000°C and 1250°C, respectively. All samples had been cycled 200 times.

Corrosive species could be injected into the centre of the flame by an atomising nozzle operating with compressed air. Within this investigation the influence of a pre-treatment of the coatings by corrosive species and of a direct injection of corrosive species into the gas burner was studied (table 19). Due to the extensive results these were summarised in table 20 and only one example for corrosion with Na₂SO₄ is depicted in fig. 31.

System / Corrosive environment	YSZ	YSZ/14YSZ	YSZ/LaMg-Hexaaluminate
None (reference)	good	good	good
Soaked in salt water	good	-	good
NaCl	some attack	damaged	(damaged)*
Na ₂ SO ₄	damaged	damaged	good
Coated with sand	good	good	good
Kerosene	some attack	some attack	good
Multiple media	damaged	damaged	damaged

* only one of two samples damaged

Table 20: Summarised results of the corrosion tests at FZJ

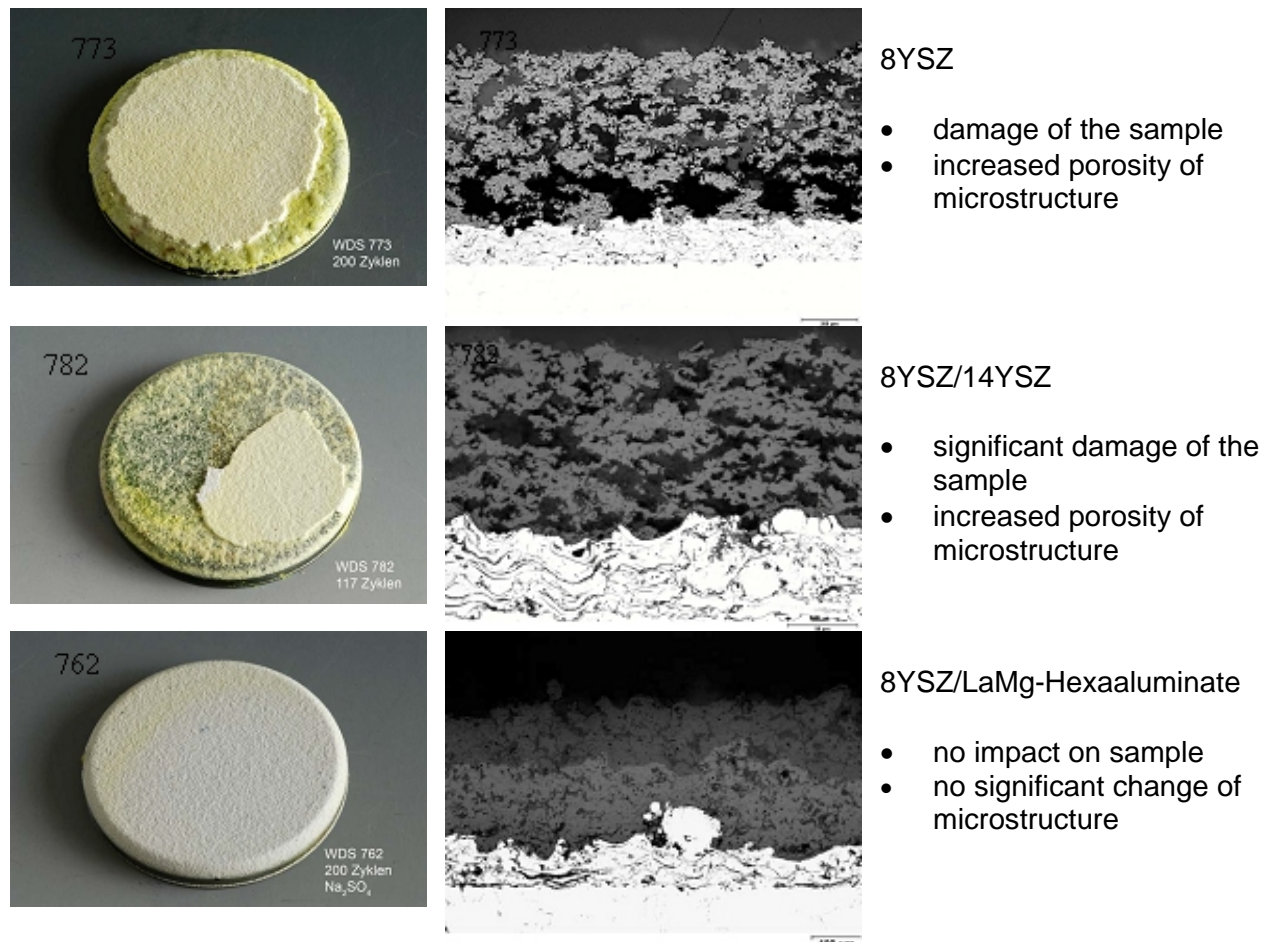


Fig. 30: Corroded samples (left) and corresponding microstructure (right) after Na₂SO₄ corrosion (example of results for one corrosive medium)

Conclusions:

With respect to all corrosive media tested by FZJ the new coating system 8YSZ/LaMg-Hexaaluminate revealed the best performance and the coating 8YSZ/14YSZ revealed the worst. These results were in contrast to the former AVIO and JRC tests, but they were more reliable as they were based on the comparison with a reference without corrosive influence.

Erosion tests (MTU)

MTU investigated the concerned coatings of TBCPLUS but also blends of LaMg-Hexaaluminate in an enlarged programme. With respect to the erosion resistance the following single coatings were tested:

- 8%YPSZ, virgin conditions
- 14%YSZ, virgin conditions
- LaMg-Hexaaluminate (LaHA), aged at 1080°C
- LaMg-Hexaaluminate, aged at 1150°C
- LaMg-Hexaaluminate + 20 wt% (8% YPSZ), aged at 1080°C
- LaMg-Hexaaluminate + 50 wt% (14% YPSZ), aged at 1080°C

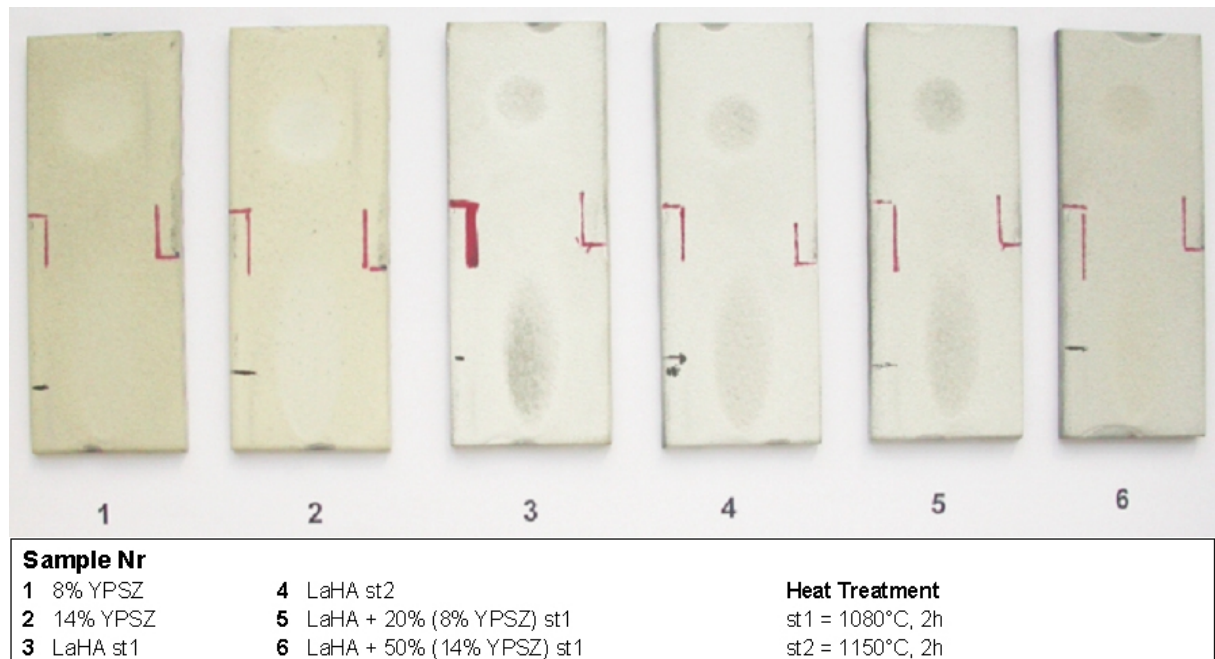


Fig. 31: Erosion test samples after testing with 20° and 90° impact angle

Conclusions:

All new TBCs were more sensitive to erosion than the standard 8YPSZ.

- LaHA aged at higher temperatures (i.e. more crystalline LaHA) was more sensitive due to the formation of an internal micro crack network.
- LaHA / YSZ blends showed better erosion resistance with increasing zirconia content, but were still lower in comparison with standard 8YPSZ.

EB-PVD route

Thermal shock and thermal cycling tests (SNECMA and Alstom)

The two thermal cycling tested coating systems by SNECMA (table 21) showed similar results as the APS coatings (see table 18).

TBC coating	Thermal cycling cycles
ZrO ₂ -8%Y ₂ O ₃	359
ZrO ₂ -8%Y ₂ O ₃ + ZrO ₂ -14%Y ₂ O ₃	359

Table 21: Thermal cycling results of EB-PVD coating systems

In an early stage of the project Alstom subjected two samples with the same YSZ coatings as in table 21 to a thermal shock test. Both samples passed the test. In a later stage the additional produced samples of the **feasibility study with the 8YSZ/LaMn-Hexaaluminate** coating system (see chapter WP3.4) were also tested in different variations for their thermal shock properties (table 22).

- The single layer coatings failed after only 1 and 9 cycles (TBC flake off on sample BS005L already after the stabilisation heat treatment).
- The duplex layer coatings with identical LaMn-Hexaaluminate thickness of 90µm reached 200 and 1025 cycles; the heat treated sample BS001L nearly passed the test (fig. 32).
- The heat treated sample BS002L with thicker LaMn-Hexaaluminate of 120µm failed after only 400 cycles, because the LaMn-Hexaaluminate coating spalled along a porous layer in this coating, while a residue layer of LaMn-Hexaaluminate remained on the surface.

Sample no BS	Alstom sample	Heat treatment	Coating	1. Toplayer 8%YSZ	2. Toplayer LaMn-Hexa	Cycles	Test passed
001 L	V1847	1100°C/1h	duplex	62 µm	90 µm	1025	(yes)
002 L	V1854	1100°C/1h	duplex	54 µm	120 µm	400	no
003 L	V1846	none (as coated)	duplex	60 µm	90 µm	200	no
005 L	V1849	1100°C/1h	single	no	120 µm	1	no
006 L	V1848	none	single	no	100 µm	9	no

Table 22: Thermal shock test results of EB-PVD samples of the DLR feasibility study

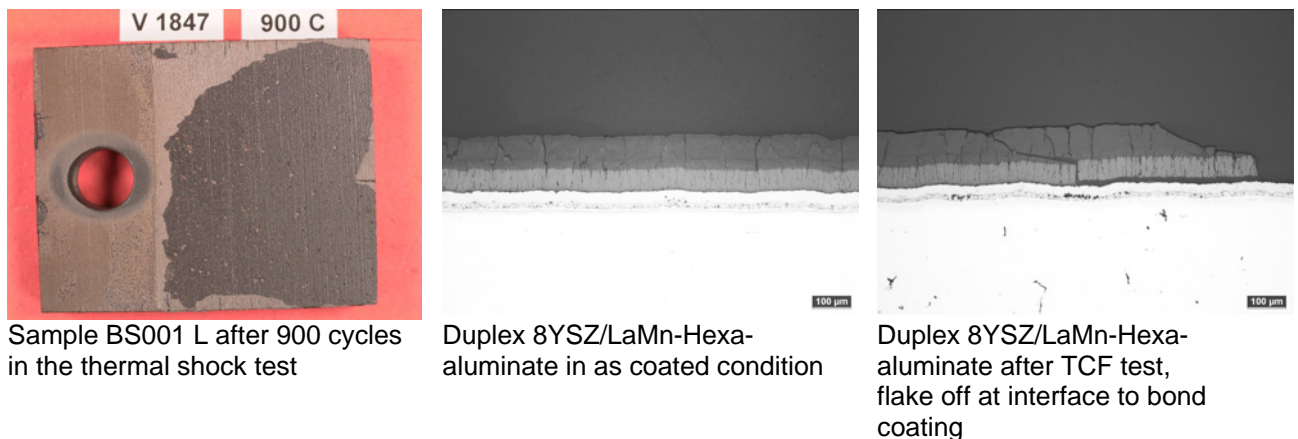


Fig. 32: EB-PVD sample BS001L of DLR feasibility study for ALSTOM SNECMA samples after thermal shock test, microstructure of LaMg-Hexaaluminate as coated and after TCF

Conclusions:

As already experienced with APS coatings single layer EB-PVD coatings of LaMn-Hexaaluminate showed a very low fatigue life, too. A stabilisation heat treatment of 1h at 1100°C on as coated samples already resulted in TBC spallation. Therefore, this coating system was not suitable for industrial application.

Duplex layer TBC coatings of 8%YSZ / LaMn-Hexaaluminate showed a clearly higher fatigue life with the best result for the stabilisation heat treated sample. This heat treatment caused a pre-damage in the LaMn-Hexaaluminate TBC in terms of vertical and horizontal cracks. But these cracks didn't affect the spallation in the thermal shock test. The spallation area of both duplex samples was directly between the intermediate 8YSZ TBC and the TGO (on the bond coating) nearly without any TBC residues on the spalled surface (fig. 32).

Ash corrosion tests (AVIO)

The corrosion testing conditions and the evaluation of the investigated TBC systems

- standard 8YPSZ single layer (EB-PVD simplex)
- duplex 8YPSZ/14YSZ layer (EB-PVD duplex)

were described in the "APS route" (see above). The EB-PVD results were already depicted in fig. 29. The duplex coating revealed a higher life time at 950°C, while at 850°C both coatings were comparable.

EB-PVD specimens had shown the presence of compounds rich in O, Al, Cr and Z at the separation interface between bond coat and top coat. In contrast to the APS specimens any phenomenon of chemical attack of the bond coat interface was never observed.

6.6 Modelling

A model aimed at predicting TBCs lifetime has been developed throughout the project by using FE method. It was structured in a modular way, so that every module took into account a different factor influencing TBC behaviour and all modules strictly interacted.

- bond coating (BC) oxidation process
- thermal expansion misfit stresses
- thermally grown oxide (TGO) growth strain
- morphology of the oxidised interface BC/TGO
- sintering of ceramic coating
- creep processes

It must be pointed out that among all the phenomena participating in the system the main stresses to which a TBC was subjected were two:

- stresses due to thermal expansion misfit and
- stresses due to the TGO growth because of different specific volume between the substrate (BC) and the originated oxide (TGO).

Some simplifying hypotheses have been introduced in order to simplify the model:

- linear elastic materials
- constant TGO thickness
- planar interfaces
- plain strain.

BC oxidation model for thermal cycling

The first step in the implementation of the computational model dealt with the correct description of the growth rate of TGO, because BC's oxidation at high temperatures greatly reduced TBC's efficiency. A fraction x of the TGO actual thickness increase (Δx) in a specimen subjected to a number n of thermal cycles was due to damaging phenomena and the remaining fraction $1-x$ was due to diffusion phenomena:

$$\Delta s = \Delta s_d (1 - x) + x \Delta s_c$$

with the fractions for the TGO thickness increase:

- Δs_d is the thickness increase resulting from diffusion phenomena
- Δs_c is that due only to cracking phenomena; computed multiplying the TGO thickness grown for diffusion phenomena in the first thermal cycle by the number of thermal cycles.

The reaction rate, given by the increase of thickness of oxide layer per unit time, should be inversely proportional to the instantaneous thickness Δx at time t :

$$\frac{d(\Delta x)}{dt} = \frac{k'}{\Delta x}$$

where k' is a constant. Upon integration:

$$\Delta x = (2k't)^{1/2} = (k_p t)^{1/2}$$

where k_p is the parabolic rate constant.

Stress analysis

In the analysis of stress distribution in TBC (top coating, TC), BC had been assigned an elastic perfectly plastic behaviour. In the case of planar interfaces and high temperatures, the TGO layer underwent a tension residual stress heavily dependent on BC yield stress; the worst case was for high BC yield stress. At room temperature TGO underwent high compression stress, especially for thin thickness, when oxidation started. A compressed thin layer motivated instability and cracking of TGO at the beginning of the oxidation process. Introduction of a yield stress for the BC of 400 MPa mitigated the TGO stress.

The effect of non-planarity of TGO-TC interface had been introduced in the model: the TGO undulation had been assigned a representative S-shape and a typical thickness. The model was parametric and a wide range of undulation amplitude (A) and TGO thickness (h_{TGO}) could be performed. Materials properties were temperature independent. Behaviour of TGO and TC was considered elastic while BC was elastic-perfectly plastic with temperature dependent yield strength (example in fig. 33).

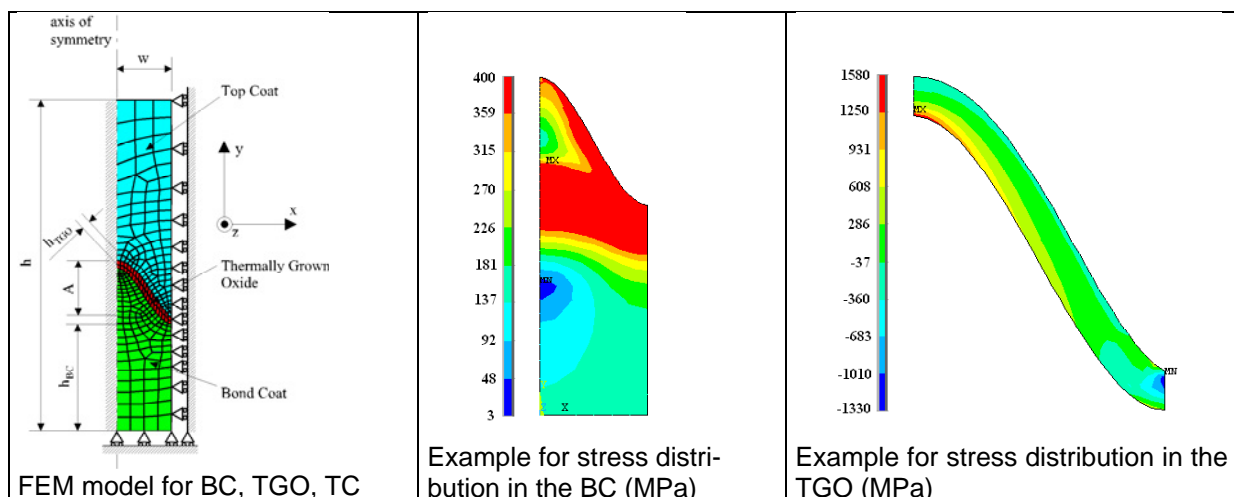


Fig. 33: Examples for stress analysis calculated with the FEM model for the bond coating (BC), TGO and top coating (TC),

The simulations done with this model had been performed for both a 2D axisymmetric and a 3D FEM calculation. It could be identified four possible simulations: isothermal 2D and 3D, cyclic 2D and 3D.

Validation of the numerical analyses

The validation of the established model was carried out on basis of the presumptions and conditions described above (example in fig. 34), but additional improvements were done.

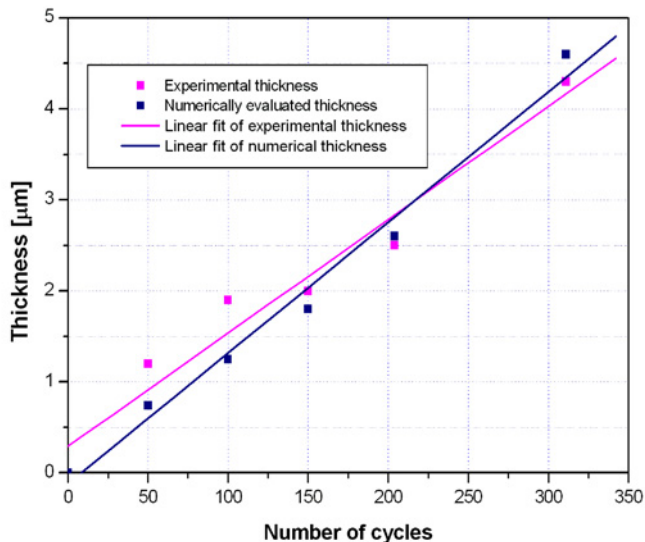


Fig. 34:

Validation of numerical and experimental data for TGO thickness grown in a specimen thermally cycled between 300°C and 1070 °C

A parabolic law could describe the growth kinetic of the scale, so growth rate decreased with increasing oxidation time. The oxidation constant could be calculated from Wagner's theory. The FE model, subsequently built to analyse stresses in the TBC, was constituted by a unit that periodically repeated represents in a way as realistic as possible the real system. Materials had been assigned temperature dependent properties taken from literature and elastic behaviour, apart from BC (elastic perfectly plastic).

A rough creep behaviour had been simulated in the case of TGO, imposing a limit to the oxide stresses. Analysis of the stress distribution in the TBC revealed that the stress events in the barrier as a function of the different factors appeared to be highly dependent on the applied growth strains of TGO, which on the contrary were object of high uncertainty. The executed parametric analysis reported that literature values were probably too high to be applied in this situation and lower values probably furnished results that were more reliable.

Other important sources of stress in TBC system lay in the creep characteristics of both the BC and the TGO and in the sintering effects occurring in the TC, that could multiply the stress levels in the course of time. At the moment the model takes into account some of these material characteristics only at a rough estimate because no accurate data were available on this side, neither coming from scientific literature, nor from experimental activity.

At the present level of knowledge of the TBC, the real stress levels in the system were substantially unknown so that further experimental evidences would have been necessary to validate or not the analysis. The original purpose was to obtain the interfacial adhesive strength of the coatings and its evolution with exposure time at high temperature by means of adhesion tests and to compare the obtained values with the maximum stress computed at TC/TGO interface in direction perpendicular to the interface. The validation by adhesive tests on coated samples did not behave as expected on the basis of the previous ageing tests. Therefore the validation of the model and the statement of a failure criterion of TBC system has been compromised.

WP7 Production of coated industrial scale components

In this work package the specification, preparation and production of the component coatings was documented.

- Antle vanes for burner rig testing
- APS coating for stationary gas turbine component
- EB-PVD coatings for aero-engine components

7.1 Process development and coating application for burner rig test vane

EB-PVD coating process (C-UK)

Avio sent 4 off scrap unmachined antle vanes to C-UK for initial coating trials (standard and duplex thermal barrier coating systems) to assess coating microstructure and thickness profile around the part. Initial discussions took place between Avio and C-UK to produce a coating specification for Antle vane drawing. Following application of platinum aluminide bond coating two parts were coated with duplex (7wt. % +14wt. % YSZ) and the other two were coated with standard 7 wt. % YPSZ.

Once the 4 off thermal barrier coated scrap parts had been metallographically assessed for the bond- and thermal barrier coating and the process capability established, a further 2 machined vanes for burner rig testing were sent to C-UK for coating:

- 1 off with standard 7 wt.% YPSZ coating (datum)
- 1 off with duplex (7wt.% +14wt.%) YSZ

C-UK test pieces were used as part of process control for both the parts (table 23). Both the standard and duplex coated vanes were returned to AVIO for burner rig testing.

	7wt% YSZ EB-PVD	7+ 14wt% YSZ EB-PVD
Bond coating (µm)	55	58
Composition (wt%)	Al 18.4 Pt 20.1	Al 17.6 Pt 19.8
EB-PVD thickness (µm)	204	211

Table 23: Coating results of AVIO antle vane coating

APS coating process (SNECMA)

A similar procedure was done by SNECMA for the antle vanes with APS coating systems, but a documentation was not provided.

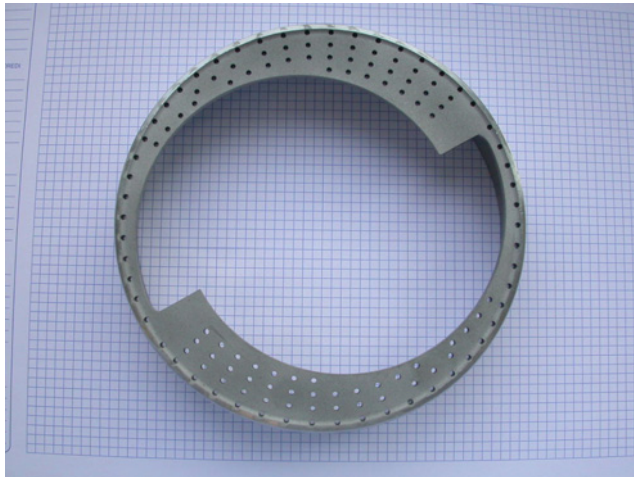
7.2 Process development and coating application for stationary gas turbine

As a suitable component for a field test a burner ring of the Alstom gas turbine GT26 was identified (fig. 35). Two burner rings already coated with YSZ were provided by Alstom to MTU for stripping and recoating with the APS TBC system 8YSZ/LaMg-Hexaaluminate applying the preferred DCF powder:

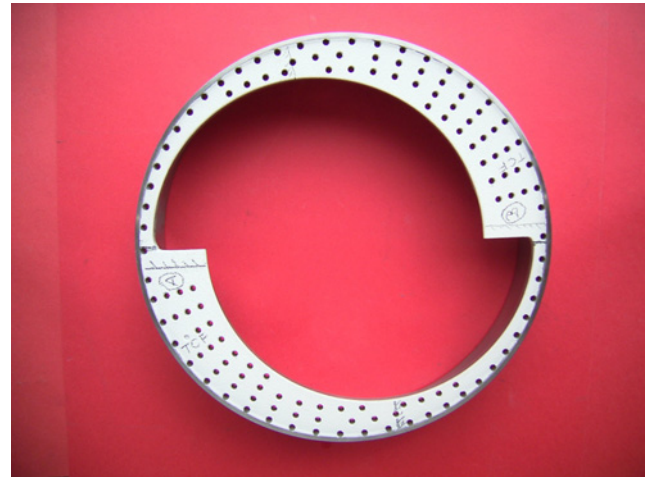
- bond coating APS NiCrAlY (Amdry 962), thickness about 100µm
- intermediate TBC layer of 8YSZ (H.C.Starck powder), thickness about 200µm
- top coating TBC layer of LaMg-Hexaaluminate (DCF powder) thickness about 600µm

One of the rings was cut in samples A and B representing the two conditions:

- sample A as sprayed
- sample B additionally subjected to a stabilisation heat treatment of 1h at 1100°C



Burner ring stripped by MTU



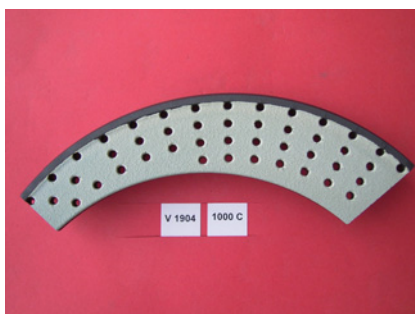
Burner ring coated by MTU with 8YSZ/LaMg-Hexaaluminate, samples A and B marked

Fig. 35: Burner ring of the Alstom GT26 gas turbine

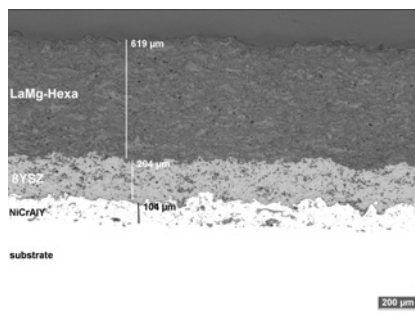
Both samples A and B passed the 1000 cycles in the thermal shock test according to the Alstom specifications.

- The heat treated sample B (V1904) did not show any spallation (fig. 36).
- The as sprayed sample A (V1903) revealed some TBC spallation of the LaMg-Hexaaluminate coating starting after 600 cycles, but still acceptable.

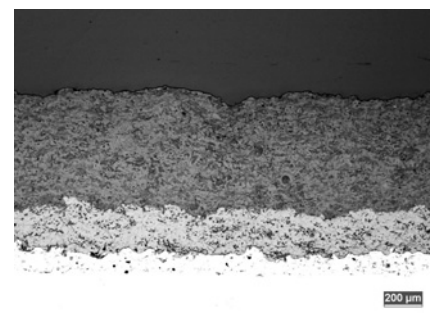
In initial condition there were no vertical or horizontal cracks in the LaMg-Hexaaluminate microstructure in as sprayed and heat treated condition (fig. 36). After the thermal shock test some small horizontal cracks were observed in the intermediate 8YSZ TBC layer but no cracks were found in the bulk area of the LaMg-Hexaaluminate coating – for both conditions with (fig. 36) and without heat treatment. But at the outer edge large horizontal cracks were detected in the LaMg-Hexaaluminate layer near the interface to the intermediate 8YSZ layer. These cracks were more pronounced in the as sprayed condition and resulted in a partially spallation of the LaMg-Hexaaluminate coating.



Burner ring sample B after thermal shock test



Duplex 8YSZ/LaMg-Hexaaluminate in as sprayed condition



Duplex 8YSZ/LaMg-Hexaaluminate after TS test,

Fig. 36: Thermal shock test on burner ring of the Alstom GT26 gas turbine; microstructure of LaMg-Hexaaluminate

Conclusions:

The LaMg-Hexaaluminate powder from DCF seems to be suitable for industrial application even for thicker TBC coating requirements. The stabilisation heat treatment resulted in better fatigue properties and should be a standard application for this coating.

7.3 Process development and coating application for aero-engine

The down-selection process within the materials matrix investigated by the TBCplus consortium had revealed three candidates to date. Agreed coating systems inclusive LHT additional work on APS for thermal spray coatings comprise:

1. APS Two – Layer TBC 8YSZ / 14YSZ (fig. 37)
2. APS Two – Layer TBC 8YSZ / $\text{LaMgAl}_{11}\text{O}_{19}$ (fig. 38)
3. EB-PVD Two – Layer TBC 7YSZ / 14YSZ (fig. 39)

APS coating systems (LHT)

Based on the industrialisation process deposition trials had been performed according to double TBC layer TBCplus specifications. The different TBCplus specifications were discussed and agreed by the consortium based on the results from WP6. Effort was used to obtain the required porous $\text{LaMgAl}_{11}\text{O}_{19}$ and 14% YSZ APS top layer. Based on successful coating production, according test samples have been prepared and provided to achieve and to confirm sufficient thermal cycle fatigue strength. The applicable specifications for the 8%/14% YSZ double layer (fig. 37) and for the $\text{LaMgAl}_{11}\text{O}_{19}$ / YSZ APS double layer (fig. 38) were set up for the industrial coating process.

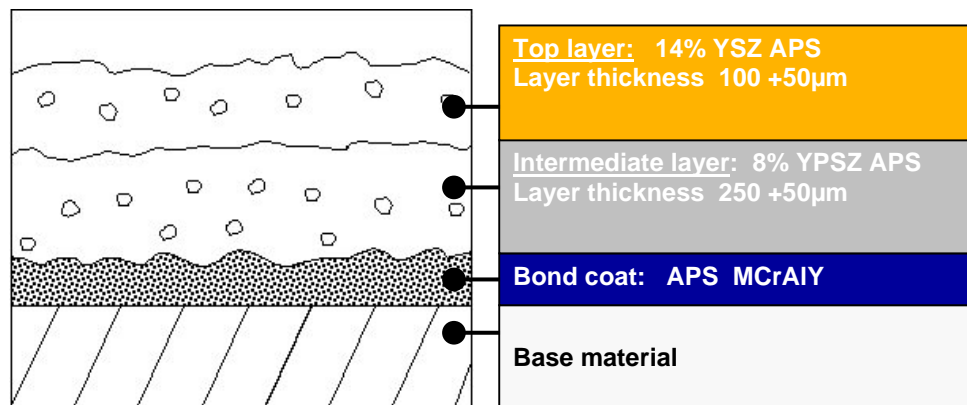


Fig. 37: Double TBC layer for APS 8% YPSZ / 14% YSZ industrialisation process

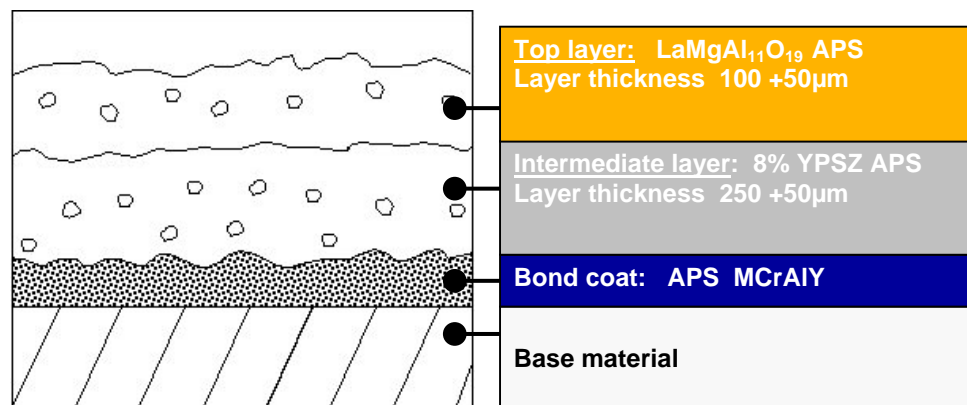


Fig. 38: Double TBC layer for APS 8% YPSZ / $\text{LaMgAl}_{11}\text{O}_{19}$ industrialisation process

EB-PVD coating system (LHT)

Beside preparation on TBC coatings by thermal spray equipment, progress had been made also on the EB-PVD process route. Two options were under investigation for industrialisation: lanthan hexaaluminate type and a 7%+14% YPSZ type were considered within the TBCplus project. Evaluation of actual data profile of lanthan hexaaluminate type was completed by a task force lead by DLR (feasibility study). Data profile of the coating system consisting of a 7%+14% YSZ type had already reached promising and comprehensive level. Therefore it

had been agreed to proceed to development stage of component trials. The applicable TBCplus coating specification for the EB-PVD 7% YPSZ / 14% YSZ is depicted in fig. 39.

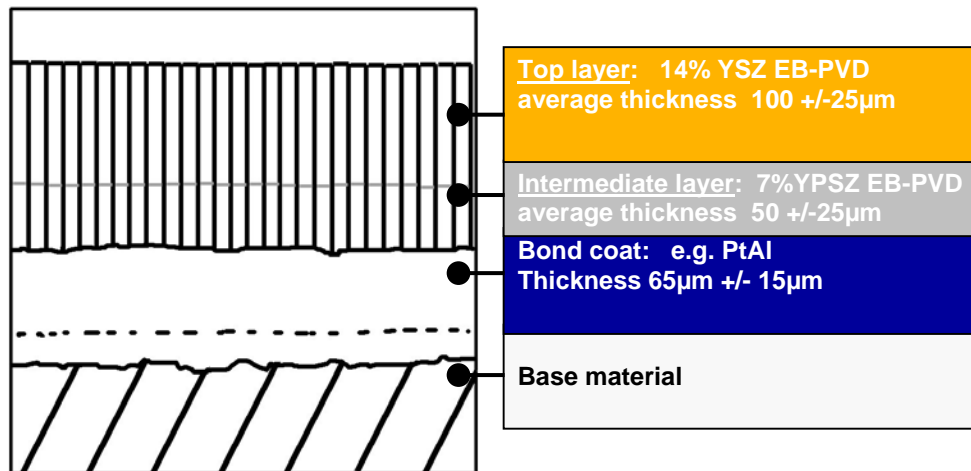


Fig. 39: Double TBC layer for EB-PVD 7% YPSZ / 14% YSZ for industrialisation process

Within the industrialisation process airfoil components had been prepared by LHT with bond coatings and provided to the TBCplus partner Chromalloy UK (C-UK) for deposition with EB-PVD coating according to the double TBC layer TBCplus specification (fig. 40).



Fig. 40: Turbine blades (test samples / scrap) provided by LHT and coated by C-UK with the double EB-PVD TBC layer 7% YPSZ / 14% YSZ as coated for industrialisation process

An according qualification plan had been derived for the required approval processes prior to service evaluation. Subsequently 16 serviceable components for the on-wing service evaluation had been provided for EB-PVD coating to C-UK in December 2005. Meanwhile the components have been coated and forwarded into in the LHT facilities to continue preparation for the on-wing evaluation (see WP 8.3).

EB-PVD coating at C-UK

As part of coating CF6-80C2 HP turbine blades for engine testing by LHT, initial discussions took place between LHT and C-UK to develop and produce a coating specification for the EB-PVD duplex layer thermal barrier coating system. The initial draft specification (LHTS-P009) comprised platinum aluminide bond coat + duplex ceramic layer thermal barrier coating (7wt% YPSZ +14 wt% YSZ). LHT sent 16 off engine test blades plus a further 4 off scrap blades, for process control, to C-UK for coating with the duplex ceramic system. Test

pieces were measured to LHTS – P009 and had an average standard thickness of 45µm and 120µm duplex thickness.

Area	EB-PVD Thickness in µm	
	7wt % YSZ EB-PVD	7wt% + 14wt% YSZ EB-PVD
Concave	52	163
Convex	54	165
Leading Edge	49	158
Trailing Edge	54	167

Table 24: Results from CF6 blade cut up

The scrap CF6-80C2 HP turbine blades from LHT in the fully repaired and platinum aluminised condition were coated with 50µm thick standard 7wt%. YPSZ plus 100µm thick top coat of 14 wt% YSZ. Representative blades were sectioned and the ceramic coating thickness was measured (table 24). The weight gain window was between 1.55 – 1.76g.

C-UK had provided details of the EB-PVD process (i.e. ingot usage, coating specification, equipment set-up, etc,) to LHT as part of obtaining approval for new thermal barrier coating prior to the engine test. In order to approve C-UK for coating “live” production parts, C-UK provided the following certifying documents to LHT:

- C-UK EASA Part 145 certificate
- FAA form 8110-3 for DER No. N045

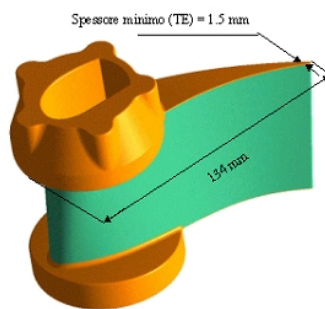
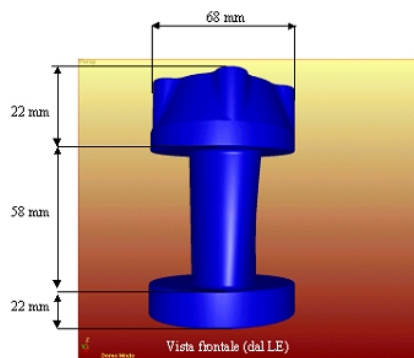
WP8 Rig and engine tests

The final part of the project included the testing of components and has exceeded the end of the project. Only half the burner rig tests could be completed within the project duration and the remaining test were still running. The component test in a stationary gas turbine and the aero-engine on-wing test will be further pursued after the project end.

8.1 High temperature burner rig test

Preliminarily to the realisation of the antle vanes (fig. 41) to be tested in the burner rig, a long design activity was necessary, in order to adapt the antle vanes to the burner rig geometry by issuing the following official drawings:

- Overall of burner rig chamber, modified to receive the Antle vanes;
- Overall of assembly;
- Machined vane;
- Instrumented vane;
- Coated vanes (2 drawings, one for the APS vanes and one for the EB-PVD vanes).



Model of antle vane

Machined and instrumented vane

Fig. 41: Antle vane for burner rig test

The instrumentation of the vanes was a challenging process, that required more than one month of activity: each vane was drilled in 8 points through E.D.M. and then in each quarry one thermocouple of 0.5 mm diameter was inserted. After the application of the thermocouples, the aerodynamic profile of the vanes was restored through the application of Ni-171 powder with a Metco gun.

The setting of the burner rig chamber was realised by performing some tests on an uncoated vane (example of thermal cycle in fig. 42). This activity included a complete analysis of the thermal behaviour of that vane in different conditions of external gas temperature and internal cooling and providing of the reference data which were useful to compare the different performances of the coated vanes to understand more deeply the real performances of the tested TBCs. The results were the assessment of the hottest location at the trailing edge (M108 in fig. 42), a well performing cooling system while the gas temperature was about 1300°C and a temperature stabilisation time of less than 10 seconds.

After having fixed the parameters of the cycle, the test procedure was applied. The thermal fatigue tests was started by performing the first 50 cycles. If no problems were found during the test the burner rig was switched off after steps of 100-200 cycles and a visual inspection of the vane was performed by means of a boroscope. The boroscope inspection was

necessary to verify the condition of the ceramic barrier, even in zones far from the thermocouples.

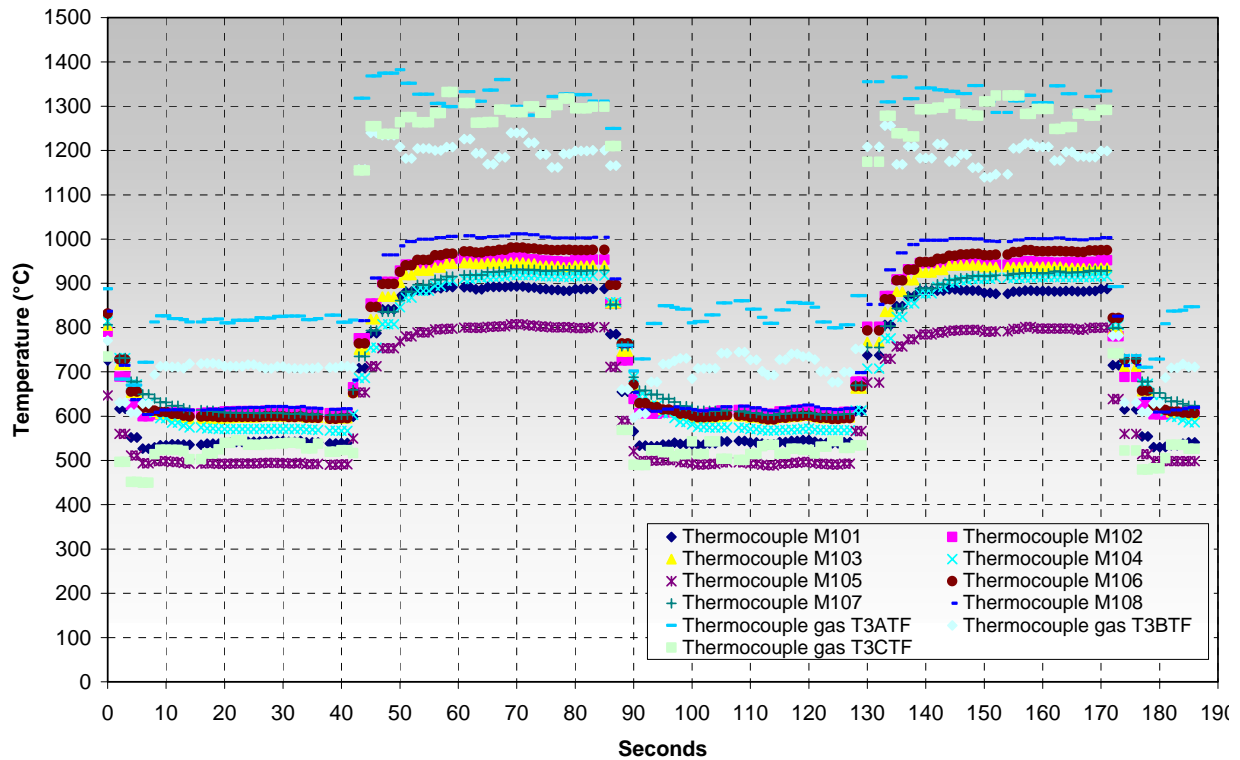


Fig. 42: Example of record of 2 thermal cycles in the burner rig test for an uncoated vane

The test results of the first tested EB-PVD coated vanes were summarised in table 25. The EB-PVD simplex vane was inspected after 50, 150, 300 and 500 cycles, revealing a TBC spallation at the leading edge pressure side after 500 cycles (fig. 43). Therefore this damage could have occurred anytime between the 300th and 500th cycle.

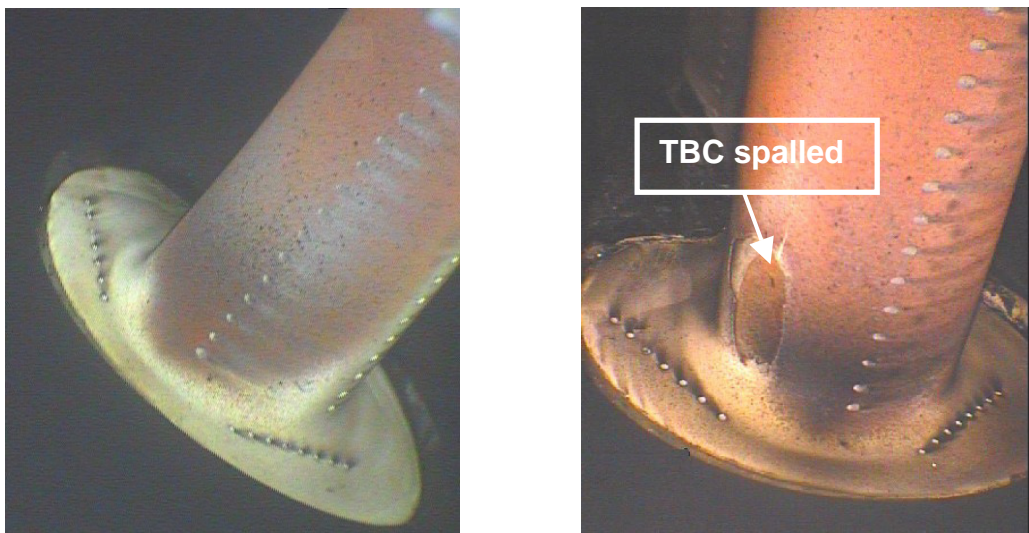


Fig. 43: Boroscope photos of the vane with EB-PVD simplex TBC (leading edge zone)
 - after 50 cycles
 - after 500 cycles

The EB-PVD duplex vane was inspected in the same manner, but taking into account the experience with the first tested vane the checks were set after 200 and 400 cycles. An elliptical spallation was observed after 400 cycles at the same location (fig. 44). However, the **life time of both vanes was considered as the same** (anytime between 300 and 500 cycles).

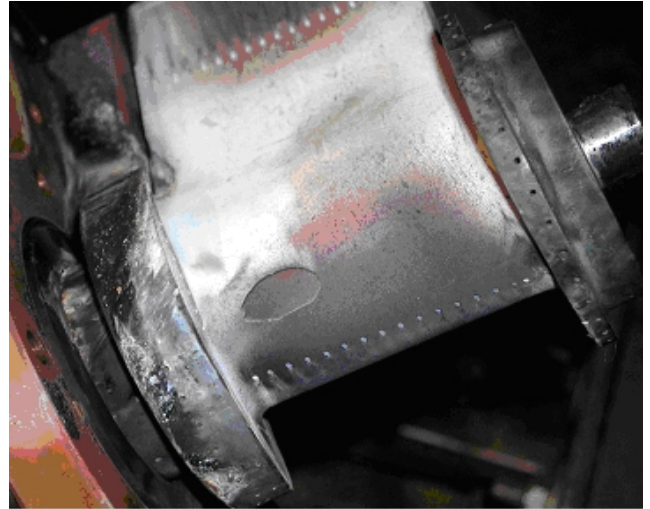
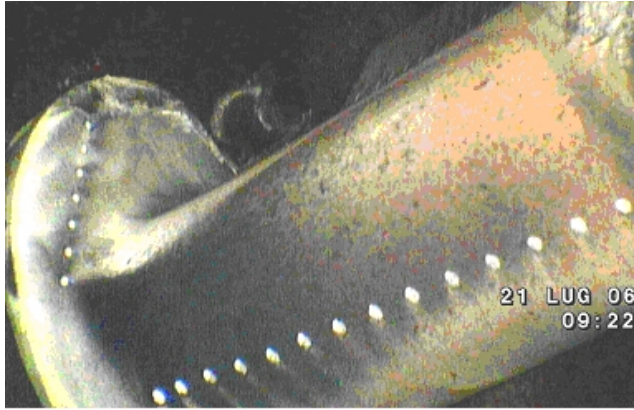


Fig. 44: Boroscope photos of the vane with EB-PVD duplex TBC (leading edge zone)
 - after 200 cycles
 - after 400 cycles

The results on the both EB-PVD coated antle vanes were summarised in table 25. The test on the 3 APS coated vanes were still running, when this report was completed. The results will be provided to the EC and the consortium partners in terms of a separate AVIO report after the tests will be finished.

TBC	Setting phase	50 th cycle	150 th cycle	300 th cycle	500 th cycle
EB-PVD simplex p/n 40-35093	TBC unbroken Broken thermocouples M103, M105	TBC unbroken Broken thermocouple M104	TBC unbroken	TBC unbroken	TBC delamination in the leading edge (pressure side) and exposure of the base metal. <u>LIFETIME of simplex EB-PVD TBC</u>
TBC	Setting phase			200 th cycle	400 th cycle
EB-PVD duplex p/n 40-35094	TBC unbroken Broken thermocouples M102, M104, M106, M107			TBC unbroken Broken Thermocouple M108	TBC delamination in the leading edge (pressure side) and exposure of the base metal. <u>LIFETIME of duplex EB-PVD TBC</u>

Table 25: Results of the burner rig test for EB-PVD coatings

8.2 Component testing in stationary gas turbine

The component test of the selected GT26 burner ring as part of the EV combustion chamber (fig. 45) is planned to be carried out in the Alstom test turbine GT26 in Birr / Switzerland. The first steps for the qualification of this component had been already achieved by the successful metallographical examination and thermal shock testing of the

- test samples in WP6.5 to qualify the APS LaMg-Hexaaluminate coating system with the DCF powder and
- the subsequent component testing of the GT26 burner ring in WP7.2.

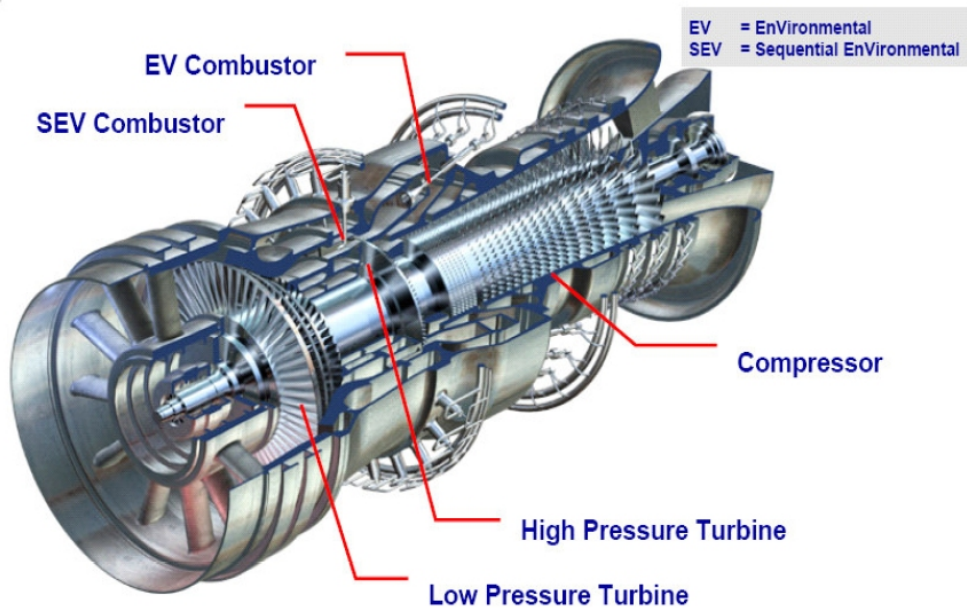


Fig. 45: Alstom gas turbine GT26

However, further qualification steps have to be taken in an comprehensive Alstom internal review programme in order to get the status of a test component.

8.3 Field test on wing

Subsequent to the component preparation and testing prior to any installation of the TBCplus coating system an extensive qualification was required. The documentation for the airworthiness authorities had to be compiled and comprised test results of the project partners. Applicable tests performed within the TBCplus consortium had been selected, agreed and confirmed meanwhile. Appropriate format of required report documentation (specific test results excerpts) had been confirmed by the TBCplus partners during the progress meetings.

For the engine on-wing evaluation one promising coating system had been selected to proof stability also under long term loading conditions. The down-selected coating system was the EB-PVD 7%/14% YSZ. As component for this on-wing evaluation the high pressure turbine 1st STG blade of the CF6-80 engine was chosen that powers the aircraft MD11 of Lufthansa Cargo AG (fig. 46).

This engine version did not necessarily require TBC protection of the turbine blades. Therefore the full thermal capability at increased temperature load of subject novel TBC was not focussed within this comparative evaluation, but the long time behaviour under the standard harsh environmental condition of an jet engine was the main focus.



Fig. 46: Jet aircraft engine CF6-80 (left) which powers the aircraft MD11 Turbine (right)

Prior to application a comprehensive FAA and EASA qualification program was required and was in process executed in cooperation with the Aviation Authorities. Two engines were selected to be equipped with TBCplus (EB-PVD 7%/14% YSZ) coated blades.

During the preparation for the EB-PVD route several documentation issues were covered together with the project partner C-UK (see WP7.3). Several component tests were performed to check the requirements of the TBCplus specification for this coating system. For the on-wing evaluation a number of 16 parts were TBC coated at C-UK according to the TBCplus specification. After final repair steps and inspections, the parts had been released to service. The first engine with the TBCplus coated components will be assembled during mid of 2006. A second engine will follow in the 3rd quarter of 2006.

For the on-wing evaluation during aircraft operation an additional inspection-schedule has been developed to monitor the on-wing performance of the TBCplus coating system. In a defined time interval the turbine blades will be inspected by borescope inspection during the service life of the engine. Due to the fact that the engines are operated "on engine condition" there is no defined time schedule for the next shop visit. Within the next shop visit of these two engines the TBCplus coated turbine blades will be comprehensively inspected. Two blades of each engine will be scrapped for a detailed metallographic investigation. Subsequently a comprehensive report of the on-wing performance of the TBCplus coating will be distributed to all partners of the TBCplus consortium.

5. List of deliverables

The reporting deliverables D1 to D9 were all done, while D9 was a 48 month progress report due to the prolongation of the project to 62 months in all.

- Additional deliverable D10a is the actual 62 month final report
- Deliverable D10: 62 month technological implementation plan will be delivered later in agreement with the EC officer due to access problems with the eTIP

Additionally a feasibility study about the coating systems EB-PVD LaMn-Hexaaluminate was carried out by partner DLR, which was not intended in the deliverable list.

Del. No	Nature of deliverable and brief description	Due date (month)	Status
D11	Range of TBC compositions to protect	2	done
D12	Material specification and quality standards	2	done
D13	Bond coated specimens for screening tests	11	done in WP6
D14	Bond coated specimens for full characterisation tests	20	done in WP6
D15	Bond coated components for rig/engine testing	36	done in WP7
D16	Report on manufacturing procedure	10	done
D17	Final delivery of spray powders and ingots o	10	done
D18	Process optimisation finished for zirconia TBC systems	10	done
D19	Process optimisation finished for new TBC systems	12	done
D20	Coated test specimens for WP4	14	done
D21	Data for down-selection	16	done
D22	Down-selection	16	done
D23	Reference data of selected coatings for WP6	18	done for 3 of 4
D24	Transfer to industrial equipment	21	done for 3 of 4
D25	Procurement of new powders and ingots	21	done for 3 of 4
D26	Delivery of coated test pieces for full characterisation	30	done for 3 of 4
D27	Microstructure defect maps	34	done for 3 of 4
D28	Sintering kinetics	34	done for 3 of 4
D29	Thermo physical and mechanical properties	36	done for 3 of 4
D30	Structure-property thermal history correlations	36	done for 3 of 4
D31	Life prediction model and ranking tests	38	done for 3 of 4
D32	Pre-standardisation of TBC testing	38	done for 3 of 4
D33	Coating of engine components	41	done for 3 of 4
D34	Quality reports	41	done for 3 of 4
D35	Performance data of new TBC systems (burner rig)	46	running
D36	Field test results from boroscope inspection	46	running
D37	Validation of life prediction model	48	running
<u>3 of 4 means:</u> 3 of 4 down selected coating systems except EB-PVD LaMn-Hexaaluminate, which was subject of the feasibility study in WP3.4			

Table 26: List of deliverables

Milestone M5 (demonstrate existence of stable processing window for industrial scale applications) was achieved for the APS coatings and for the EB-PVD 14% YSZ coating. The milestones M6 to M9 referring to the properties of the material were done for 3 of 4 down selected coating systems except EB-PVD LaMn-Hexaaluminate, which was subjected to the feasibility study in WP3.4.

Milst. No	Brief description of milestone objective	Due date (month)	Status
M1	Demonstration that new TBC's can be plasma sprayed and evaporated	9	achieved
M2	Demonstrate stable processing window for laboratory scale coating application	14	achieved
M3	Decision to proceed to industrial processing	18	decision made
M4	Midterm assessment review	25	done
M5	Demonstrate stable processing window for industrial-scale applications	30	achieved for 3 of 4 materials
M6	Approve industrial processing of coatings	34	achieved 3 of 4
M7	Acceptable phase stability characteristics	34	achieved 3 of 4
M8	Approved thermal conductivity properties	36	achieved 3 of 4
M9	Coatings with better thermal cycling resistance at elevated temperatures	36	achieved 3 of 4
M10	Selection of coatings for rig and engine testing	36	done
M11	Property database of new coatings	38	done
M12	Release of coated engine components	41	done
M13	Decision to install best TBC system on wing	46	done
M14	In service ranking of new TBC systems	48	running
M15	Realisation of techno-economic performance	48	running

Table 27: List of milestones

6. Comparison of initially planned activities and work actually accomplished

As already documented in the deliverable list some changes were made in the course of the project. The main changes were:

- The EB-PVD process development of the new coating material LaMn-Hexaaluminate was set back to development state. A feasibility study about this coating systems was carried out by partner DLR.
- The powder of the new coating material APS LaMg-Hexaaluminate delivered by H.C. Starck was of bad quality, which could not be completely improved. Higher calcinated powder from DCF provided by partner MTU was of much better quality and showed a better performance with regard to the fatigue ranking tests.

EB-PVD LaMn-Hexaaluminate

Due to the described problems with the EB-PVD LaMn-Hexaaluminate coating process a re-evaluation of the process was agreed in the consortium by carrying out a feasibility study at DLR (implemented as sub task WP3.4) with the objective to establish a stable process which can produce samples with correct coating composition and structure as well as providing a suitable efficiency for industrial processing requirements.

This study comprised the two parts optimisation and reproducibility and included the production of test samples. The tests on these samples were partially successful that showed the potential of this EB-PVD LaMn-Hexaaluminate process and set up a basis for further developments. But the remaining time was too short to establish an industrial production process. Therefore, the second down-selected coating system - double layer zircon oxide – was taken for the planned tests on components in the burner rig test facility and in the on-wing tests.

APS LaMg-Hexaaluminate

The procurement of a suitable powder for the industrial application turned out to be difficult as already described above in this reports. In the end the fatigue test results of the employed H. C. Starck powder were unsatisfactory compared to the standard coatings. The accompanying metallurgical investigations revealed an amorphous-crystalline transition of the LaMg-Hexaaluminate at a temperature of about 1000°C. This effect involved a volume change causing an early flake off of the coating during the fatigue tests.

The best quality was found with the powder of company DaimlerChrysler Friedrichshafen (DCF) - calcinated at 1650°C instead of the usual 1450°C - provided by partner MTU. The amorphous-crystalline transition was found too, but in a less pronounced degree. Additional samples for fatigue tests and material property investigations had been coated by MTU, which showed a clearly better performance in the thermal shock tests carried out at Alstom. For that reason it was decided to take that powder for the planned component test in the stationary gas turbine.

These additional actions as well as the coating problems with the burner rig components for partner AVIO resulted in a strong time delay and required an extension of duration of the project of 14 months in all. However, even including this additional time the task WP8.1 (burner rig tests) could not be finished completely as originally planned and will be completed after the project end. The field test tasks WP8.2 and WP8.3 were originally planned to run even after the project end, but they were also delayed.

7. Management and co-ordination aspects

7.1 Performance of the consortium

Consortium

The motivation and dedication of the participants towards achieving the preset goals were very high. The cooperation was close among the partners - by phone calls and e-mails – and decisions were made always in consensus after discussions. The exchange of special information between the partners was organised via e-mail, details discussed via phone or in bilateral meetings or even in special task meetings. Some partners took over tasks from other partners to achieve a better progress.

The supply of deliverables was in time and of high quality. The reporting and documentation was mostly complete but not always in time. However, some tasks remained incomplete due to delayed or incomplete contributions.

Project coordination

During the course of the project 3 coordinators were acting, but due to an organised transition no interruption had been occurred in the performance of the project.

- A. Kranzmann from start until Jan. 2002, now director at BAM
- R. Knödler from Feb. 2002 to Dec. 2003, now in retirement
- R. Hartfiel since Jan. 2004

Participants

The business area Alstom Industrial Turbines was taken over by Siemens in April 2004. Some partners of consortium didn't accept Siemens as partner in the project. Therefore, Siemens was excluded from the project.

The company names for following partners changed during the project, which was laid down in amendments to the contract:

- Fiat AVIO to AVIO
- Alstom Power Support GmbH to Alstom Power Generation AG
- Snecma Moteurs to Snecma S.A.

Changes in the project

Three extension of durations were applied and approved resulting in a total project duration of 5 years and 2 months (62 months instead of originally 48 months).

Two budget redistributions were agreed between the partners to finance

- the feasibility study at partner DLR with 62.000 EUR and
- additional corrosion tests at partner FZJ with 20.000 EUR.

Meetings

In all 18 meetings were held in the course of the project: 1 kick off meeting, 10 regular meetings and 7 special task meetings. Minutes of meetings were issued in all cases.

- Kick-off in Mannheim May 2001
- Special task meeting, Limoges July 2001
- 6-month meeting, Cologne Sep. 2001
- 12-month meeting, Jülich Febr. 2002
- Meeting in Munich July 2002
- Special task meeting, Cologne Sep. 2002
- 18-month meeting, Chatillon Nov. 2002
- 24-month midterm meeting, Brussels April 2003
- Special task meeting, Paris airport July 2003
- 30-month meeting, Torino Oct. 2003
- 36-month meeting, Nottingham Mar. 2004
- Special task meeting, Paris airport May 2004
- 42-month meeting, Corbeil Oct. 2004
- Special task meeting, Cologne Jan. 2005
- 48-month meeting, Hamburg Mar. 2005
- Special task meeting, Cologne Jun. 2005
- 54-month meeting, Mannheim Sep. 2005
- 60-month final meeting, Brussels Mar. 2006

Problems during project

However, considering the harmonic atmosphere there were also problems between the partners to be solved. One subject was the disagreement about the down-selected new EB-PVD coating material magnetoplumbite (pyrochlore instead of magnetoplumbite was an alternative suggestion of one partner):

- Two special meetings about this subject
- Several months of stagnation due to that subject
- Differences were settled by a voting within the consortium

The re-evaluation of the EB-PVD LaMn-Hexaaluminate process after the industrial application failed was intensively discussed in the consortium, if the feasibility study should

be carried out by a partner or an external company. At least it was decided on the basis of the submitted orders of the two candidates to choose DLR and to finance the study by a budget redistribution.

Publications and presentations

The following publications and/or presentations were performed during the project:

- DLR and FZ:J: “EVALUATION OF TWO NEW THERMAL BARRIER COATING MATERIALS BY APS AND EB-PVD”, conference contribution for the Cocoa Beach conference in Florida USA presented in January 2004. The presentation were held by B. Saruhan (DLR) for the EB-PVD part and by R. Vaßen (FZJ) for the APS part.
- AVIO in collaboration with the polytechnic school of Torino (Politecnico di Torino): “Modelling of TBC failure: stress distribution as a function of TGO thickness and thermal expansion mismatch”, conference contribution for the ICEFA congress in Lisbon at 12th July 2004.
- Alstom: “Development and Investigation of Advanced Thermal Barrier Coatings for Higher Temperature Applications – Results of the EC/FP5 Project TBCPLUS”, presentation on the ASME Turbo Expo 2006, 8th to 11th May 2006, Barcelona. The presentation was held by the coordinator Ralph Hartfiel.

7.2 Name and contact details of follow-up persons

Comp.	Name	Adress	Phone	e-mail
JRC	Peter Hähner	Institute for Energy JRC, NL-1755 ZG Petten, The Netherlands	0031 (0) 224 565 217	peter.haehner@jrc.nl
LHT	Christian Siry	Lufthansa Technik HAM WR 124, Weg beim Jäger 193, 22335 Hamburg	040 5070 4299	christian.siry@lht.dlh.de
FZJ	Robert Vaßen	Inst. Für Werkstoffe und Verfahren der Energietechnik, IWV1, Forschungszentrum Jülich 52425 Jülich	02461 61 6108/ Frau Groten: 3599, Frau Bosch: 4236	r.vassen@fz-juelich
DLR	Uwe Schulz	Inst. Für Werkstofforschung, DLR, Linder Höhe, 51147 Köln	02203 601 2543	uwe.schulz@dlr.de
ON	Odile Lavigne	Dept. of metallic materials, ONERA, DMMP BP72-29 av. De la Division Leclerc, F-92322 Chatillon CEDEX, France	0033 146 73 4511	odile.lavigne@onera.fr
SN	Florent Bourlier	Material and process Dept., SNECMA S.A. Centre de Villaroche, 77550 Moissy-Cramayel, France	0033 1 60 59 78 05	florent.bourlier@sneema.fr
AV	Silvia Sabbadini	Avio SpA , Via I Maggio 99, I-10040 Rivalta di Torino, Italy	0039 (0) 11 0082862	silvia.sabbadini@aviogroup.com
MTU	Roland Schmier	MTU Aero Engines, Dachauerstrasse 665, 80995 München	089 1489 7409	roland.schmier@muc.mtu.de
CUK	Rodney Wing	Chromalloy UK Linkmel Road 1 Eastwood, NG16 3RZ Nottingham, England	0044 1773 521522	rwing@chromalloy.com
ALS	Ralph Hartfiel	Alstom Power Generation, Boveristrasse 22, D-68309 Mannheim, Germany	+049 (0) 621 329 7183	ralph.hartfiel@power.alstom.com

Table 28: Contact persons and contact data for TBCPLUS project

8. Results and Conclusions

Summarising the main results achieved in this project the tasks prior to and after the midterm meeting have to be considered separately.

1. WP1 to WP4 (until midterm meeting)

Spray powders and ingots of different compositions and morphologies were prepared and coating processes developed. Also test specimens were manufactured, either as free-standing bodies or on alumina substrates. After detailed characterisation of the physical properties, two systems showing promising physical material properties were selected to be applied both by APS and EB-PVD.

- APS double layer coating: 8YPSZ / 14YSZ and 8YPSZ / LaMg-Hexaaluminate.
- EB-PVD double layer coating: 8YPSZ / 14YSZ and 8YPSZ / LaMn-Hexaaluminate.
- A patent of the double layer coating 8YPSZ / 14YSZ was filed by Forschungszentrum Juelich prior to this project. A patent of the double layer coating 8YPSZ / LaMg/Mn-Hexaaluminate was filed by MTU during this project.

2. WP5 to WP8 (after midterm meeting)

The coating parameters developed in the laboratory were transferred to industrial scale (WP5). The results were different for both coating types and coating materials.

- The coating processes for the 8YPSZ / 14YSZ coatings were successful for APS and EB-PVD.
- APS coating LaMg-Hexaaluminate: problems with the powder quality, which could be overcome by a subsequent stabilisation heat treatment after coating or even by applying a better powder from DCF.
- EB-PVD coating LaMn-Hexaaluminate: coating process problems using only one ingot. This coating process was re-evaluated in terms of a feasibility study carried through by the partner DLR showing promising results for the established coating process.

The most comprehensive task WP6, the investigation of the physical and mechanical properties, mainly resulted in two summarising findings:

- The characterisation of the microstructure and the determination of the physical properties revealed advantages of the new coating LaMg-Hexaaluminate compared to the zirconia coatings.
- The fatigue properties of the zirconia coatings 8YPSZ and 14YSZ were comparable, while the LaMg-Hexaaluminate revealed worse results; but an improvement was achieved by applying a stabilisation heat treatment or even better a different APS powder of better quality from DCF.

Due to the achievements conclusions were drawn with regard to the application of the suitable coating systems in the component tests. The selected components were coated successfully (WP7) and the component testing (WP8) has been started, but only achieved different status.

- The burner rig tests were completed for the EB-PVD coating systems resulting in comparable results, while the APS coating systems will be completed after project end.
- The component testing in a gas turbine on APS 8YPSZ / LaMg-Hexaaluminate coating system requires comprehensive Alstom internal review programme in order to get the status of a test component, which will be further pursued.
- On-wing tests were started on EB-PVD 7YPSZ / 14YSZ coating system applied on high pressure turbine 1st STG blades of the CF6-80 engine for evaluation under long term loading conditions.

About the progress of the component tests will be further informed by separate reports.